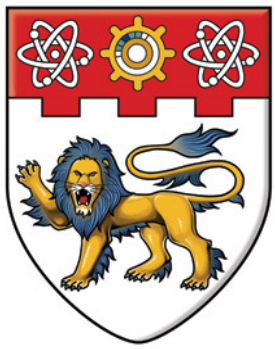

NANYANG TECHNOLOGICAL UNIVERSITY

TIGHTENING AND LOOSENING OF BOLTED JOINT

IVAN TANRA
SCHOOL OF MECHANICAL AND AEROSPACE ENGINEERING
2013

Tightening and Loosening of Bolted Joint
Ivan Tanra
2013

TIGHTENING AND LOOSENING OF BOLTED JOINT

Ivan Tanra

Ivan Tanra

School of Mechanical and Aerospace Engineering

A thesis submitted to the Nanyang Technological University in partial fulfilment of the requirement for the degree of Doctor of Philosophy

2013

ABSTRACT

A bolted joint is a common joint encountered in mechanical structures or machine design. Its tightness is important in order to secure the structure or machine it is attached to. A proper tightness is installed at a bolted joint to resist static and dynamic loading it is subjected to. When tightness is not sufficient, it can cause failure such as loosening and in extreme cases, joint separation.

In this project, a bolted joint and its tightness are objects being studied. The purpose of this project is to understand the factors affecting tightness of a bolted joint and causes of its loosening under dynamic loading (vibration). A DC motor with known transduction matrix was used as a device to measure mechanical condition of a bolted joint. By obtaining the 2x2 transduction matrix, mechanical output of a DC motor can be related with its electrical input. With this relation, a DC motor was used to tighten a bolted joint and measure its mechanical condition by controlling and measuring its electrical input. Based on this mechanical condition, tightness and dynamic condition of a bolted joint were obtained.

The project is divided into 2 parts. In the first part, the tightening process of a bolted joint is studied. The experiment results show that torque is not sufficient in indicating tightness of a bolted joint. Under different friction conditions, tightness that is achieved by the same value of torque differs significantly. Thus, energy is used as a tightening indicator. With simultaneously measurement of torque and rotation speed, energy applied to a bolted joint can be measured. The experiment results show that energy is a better tightening indicator as compared to torque.

In the second part, dynamic behavior of a bolted joint under dynamic loading is studied. First, mechanical impedance of a bolted joint is measured with usage of Hilbert Transform. The Hilbert Transform helps to obtain mechanical impedance in time domain. With this, change of mechanical impedance over a period of time can be monitored. By obtaining mechanical impedance, system properties can be

derived from their relation. The results show that system properties of a bolted joint are affected by tightness of a bolted joint (preload), its surface condition and frequency of applied excitation. After obtaining system properties of a bolted joint, response of a bolted joint to a vibration, especially transverse vibration, can be calculated. The results show that a transverse vibration given to a bolted joint can cause loosening due to thread geometry and system properties of a bolted joint.

ACKNOWLEDGMENT

I would like to praise my thanks to the God for the completion of this thesis report. I also would also like to thank my supervisor, Professor Ling Shih Fu, for his ideas, guidance and support in this research. Even in his busiest schedule, he still spends his time in discussing this research.

Secondly, I would like to thanks my fellow friends, Lian Kar Foong, Wong Yoke Rong, Felicia Rezanda, Hossein Mousavi and Peng Xin for their care and support. Their thoughts and ideas contribute and help me in the progress of the project. I would also like to thanks the fellow technician in the Mechanics of Machines and Mechantronics lab, Mr Poon, Mrs, Yap, Mr Soh and others for their support in providing equipment and space for me to conduct the research.

Lastly, I would like to thank my family and my undergraduate friends for their support and encouragement during the research.

TABLE OF CONTENT

LIST OF FIGURES

LIST OF TABLES

NOMENCLATURE

α	:	Thread profile angle at bolt thread (°)
β	:	Lead angle at bolt thread (°)
θ_{bh}	:	Angle at bolt head (rad)
θ_{bt}	:	Angle at bolt thread (rad)
θ_{bolt}	:	Turning angle of the bolted joint (rad)
ζ	:	Damping ratio
μ_{bt}	:	Coefficient of friction at surface of bolt thread
μ_{bn}	:	Coefficient of friction at surface of bolt head
ω_d	:	Damped natural frequency (rad/s)
ω_f	:	Force frequency/excitation frequency given to bolted joint (rad/s)
Ω_m	:	Rotation speed of electric motor (rad/s)
a_{ij}	:	Element matrix of row i and column j
c	:	Damping (Ns/m)
dF_{bh}	:	Total force per radian acting at bolt head (N/rad)
$dF_{bh\text{-}P}$	:	Force per radian at bolt head due to preload (N/rad)
$dF_{bh\text{-}Fs}$	:	Force per radian at bolt head due to transverse force (N/rad)
$dF_{bh\text{-}Mb}$	:	Force per radian at bolt head due to bending moment (N/rad)
$dF_{bh\text{-}fric}$	:	Force per radian at bolt head due to friction force (N/rad)
dF_{bt}	:	Total force per radian acting at bolt thread (N/rad)
$dF_{bt\text{-}P}$	:	Force per radian at bolt thread due to preload (N/rad)
$dF_{bt\text{-}Fs}$	:	Force per radian at bolt thread due to transverse force (N/rad)
$dF_{bt\text{-}Mb}$	:	Force per radian at bolt thread due to bending moment (N/rad)
$dF_{bt\text{-}fric}$	:	Force per radian at bolt thread due to friction force (N/rad)

$dF_{bt\text{-}sum}$: Summation of $dF_{bt\text{-}P}$, $dF_{bt\text{-}Fs}$, and $dF_{bt\text{-}Mb}$ (N/rad)

dT_{bh} : Differential torque generated at bolt head (Nm/rad)

dT_{bt} : Differential torque generated at bolt thread (Nm/rad)

e_{in} : Input effort

e_{out} : Output effort

f_{screw} : Coefficient of friction of power screw

f_{in} : Input flow

f_{out} : Output flow

$g(t)$: Impulse response of the system (rad)

$h(\tau)$: Weighting function

i : Current of electric motor (A)

k : Spring constant (N/m)

k_E : Rotation speed constant at electric motor (Vs/rad)

k_T : Torque constant at electric motor (Nm/A)

k_{spring} : Spring stiffness (N/m)

m : Mass (kg)

n_t : Number of thread engagement

p : Pitch of the bolt (m)

r_{bho} : Outer radius of bolt head (m)

r_{bhi} : Inner radius of bolt head (m)

r_{hole} : Radius of hole for bolt to pass thru (m)

r_{btm} : Median radius of bolt thread (m)

r_{bti} : inner radius of bolt thread (m)

r_{bto} : outer radius of bolt thread (m)

t_{ij} : Element matrix of tranducstion matrix at row i and column j

$x(t)$: input function

$y(t)$: output function

A_{bh} : Area at bolt head (m^2)

C_{bolt} : Damping of bolted joint (Nms/rad)

D_p : Diameter of power screw (m)

E : Voltage of electric motor (V)

E_{bolt} : Total energy input to a bolted joint (Joule)

E_{emf} : Emf voltage generated at electric motor (V)

F_{axial} : Axial force generated due to bending moment (Nm/rad)

F_s : Transverse force applied to bolted joint (N)

$H(f)$: Frequency response function of a system

I_{ring} : Second moment of area of a ring (m^4)

I_{bolt} : Effective mass moment inertia of the bolted system (kgm^2/radian)

J_{motor} : Moment inertia of electric motor (kgm^2/radian)

K_{bolt} : Stiffness of bolted joint (Nm/radian)

L : Motor inductance (H)

L_{bolt} : Grip length at bolted joint (m)

L_{screw} : Grip length of power screw (m)

M_b : Bending moment applied to bolted joint (Nm)

N : Number of section divided bolt head or bolt thread

P : Preload of bolted joint (N)

R : Resistance of the motor (Ω)

$\left[T_{x,u}\right]$: Transformation matrix from x,y,z coordinate system into u,v,w coordinate system

$\left[T_{u,u_1}\right]$: Transformation matrix from u,v,w coordinate system into u_1,v_1,w_1 coordinate system

$\left[T_{u_1,u_2}\right]$: Transformation matrix from u_1,v_1,w_1 coordinate system into u_2,v_2,w_2 coordinate system

T_{bh} : Torque generated at bolt head (Nm)

T_{bt} : Torque generated at bolt thread for 1 thread engagement (Nm)

T_{btn} : Torque generated at bolt thread for n thread engagement (Nm)

T_{bolt} : Total torque generated at bolted joint (Nm)

T_{exc} : Excitation torque (Nm)

T_f : Friction torque at electric motor (Nm)

T_L : Load torque apply to electric motor (Nm)

T_m : Torque generated by electric motor (Nm)

$X(\omega)$: Fourier Transform of function $x(t)$

$Y(\omega)$: Fourier Transform of function $y(t)$

Z_e : Electrical Impedance of the motor (Ω)

Z_m : Mechanical Impedance of the motor (Nms/rad)

CHAPTER 1
INTRODUCTION

This chapter presents the motivation behind the study of tightening and loosening mechanism of a bolted joint. The objective and the scope of this study are presented. An outline of the entire thesis will be provided at the end of the chapter.

1.1. Background

The structure of machinery consists of various mechanical components fastened with different types of fasteners such as bolts, rivets, pins, and adhesives. By joining the components, loads can be transferred from one component to another. The joints are designed to withstand the loads and limit the component's movement during the transfer of forces. The three main types of joints that may be used are mechanically fastened joints, adhesive bonded joints and welding. Mechanically fastened joints involves the use of, for example, bolts, rivets, or pins to join the mechanical components. Adhesive bonded joints uses chemical substances such as epoxies. Welding joints uses heat to melt and join the parts together. The scope of this thesis is limited to bolted joints, which is usually the fastener of choice in machinery structures because of their strength in sustaining loads, reliability, and ease of disassembly.

A bolted joint uses a bolt and a nut to fasten two structural elements together. A bolt is inserted through a hole in both elements and mated with a nut. To tighten the bolted joint, the nut is turned relative to the bolt and moves along the bolt's threads. Further tightening after the nut makes contact with the elements stretches the bolt and causes the elements to be compressed together (Figure 1-1). The stretching generates a preload at the bolt to secure and clamp the structural elements together. To loosen the bolted joint, the nut is turned in the opposite direction. This causes the nut to release the tension and reduces the preload to zero.

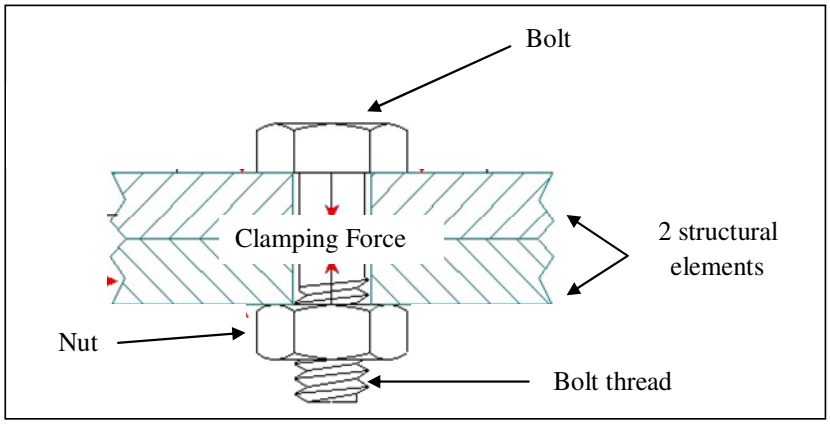

Figure 1-1 A bolted joint [1]

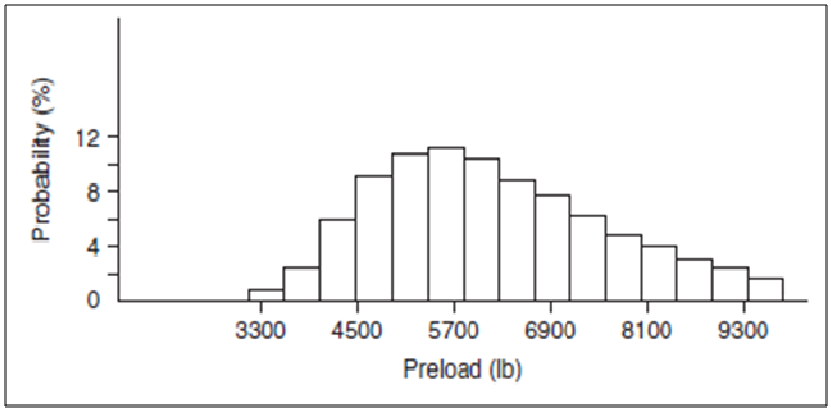

Figure 1-2 Histogram of preload achieved from a uniform torque level [2]

A properly tightened bolted joint is important for the structural element. An over-tightened joint may stress the element and lead to element breakage. An under-tightened joint might loosen the connection between the elements and may lead to structure separation or fatigue. Thus, a good tightness indicator is needed to indicate that the joint is tightened enough.

Preload as the result of bolt stretching is the most accurate tightness indicator. A non-zero preload value indicates that the elements are in contact with each other and the joint is intact. A load cell is installed between the elements to measure the

preload directly. This method provides a highly accurate preload measurement but at the cost of additional weight at and interference with the joint structure.

In common practice, the tightening torque is used as an indicator of the tightness of the bolted joint. Tightening torque is measured directly from a torque wrench without introducing additional weight to the joint structure. The tightening torque is assumed to be linearly proportional to the bolt preload generated at the joint [3]. However, this is not true in reality. It was stated by Bickford that the preload generated under a single value of torque varies with friction [2]. Figure 1-2 illustrate how the use of tightening torque to measure preload may be inaccurate. Thus, a tightening indicator to indicate the tightness accurately is desired. The indicator must be able to measure tightness without introducing additional sensors and weight to the joint's structure.

During the tightening of a bolted joint, energy is built up inside the joint. This energy is the potential energy generated from the stretching of the bolt. The bolt threads are designed such that there is sufficient friction to retain this potential energy inside the joints. However, under external excitation from the vibrations of the joined structures, this friction may change and cause the potential energy to dissipate. This phenomenon is known as the self-loosening of the bolted joints.

Several theories of vibration loosening have been proposed. The most known amongst the theories is Gerhard Junker's [4]. Junker simulated the self-loosening of bolted joints under transverse vibration with his "Junker Machine". His experiments showed that the self-loosening occurs due to slippage between the mechanical components. This slippage overcomes friction at the bolted joints and permits relative motion between the threads. The motion causes the bolt to rotate in the loosening direction. The amount of loosening depends on the initial tightness, the surface friction of bolted joint, the thread pitch of the bolt, and hole clearance [5-8].

R.A Ibrahim further explained in his review that under dynamic loading or vibration, the bolted joints may slide and result in energy dissipation [9]. Due to the energy dissipation from the sliding, the bolt loosens. To describe the mechanism sliding of and dissipation of energy from the bolted joints, they calculated stiffness and damping of the bolted joint theoretically. This stiffness and damping of bolted joint are used to describe loosening mechanism of bolted joints under vibration.

In this research, the tightening and loosening of a bolted joint are studied to provide the design engineer greater insight in designing a secure and reliable bolted joint. The dynamic behaviour of a bolted joint under vibration is also observed to understand mechanism of self-loosening of bolted joint. An electric motor is employed in this study as the tightening and measurement device for bolted joints.

Electric motors is chosen because of its characteristic. Electric motor, as an electromechanical device, transducs input electrical power into mechanical power in the form of torque and shaft rotation. This transduction process can be described with a transduction matrix. The idea of using a transduction matrix was proposed by Ling et al in a piezo transducer [10]. In their experiments, a transduction matrix was used to measure the output mechanical power of piezo transducer indirectly from the transducer's input electrical power. The concept of a transduction matrix is adopted in this thesis for the development of a method to measure the tightness of bolted joints. Based on this tightening method, a new tightening indicator will be introduced

The measurement device which is developed in this thesis for measuring the tightness of the bolted joint can also be used to obtain the dynamic model of the bolted joint. The electric motor has sensing and actuating capabilities and simultaneously measure the response of bolted joint due to the actuation as it provides excitation to the bolted joint. The dynamic model of the bolted joint can

be constructed from the excitation and response measured by the electric motor. This model will be used to describe the behaviour of bolted joint under vibration. The loosening mechanism of bolted joint will be also described based on this model.

1.2. Objective and Scope

The overall aim of this thesis's research is to investigate the tightening and loosening mechanism of bolted joints. An in-situ measurement method based on the transduction matrix of the tightening motor will be developed for the investigation. The mechanical outputs from this sensor-less method are further utilized to develop a new tightening indicator that is more accurate than torque. Based on this investigation, factors that affect the tightness and looseness of bolted joints are identified and defined. The detailed objectives of the research are as follows:

1. To develop a measurement method to simultaneously tighten bolted joints and measure their mechanical conditions based on the concept of the transduction matrix.

2. To determine a novel and more appropriate tightness indicator with the use of a motor as the tightening tool.

3. To develop a dynamic model of the bolted joints in order to analyze the behaviour of bolted joints under dynamic loadings such as transverse vibration.

To achieve these objectives, the following tasks will have to be performed:

1. Literature review on bolted joints. The literature review will focus, in particular, on the tightness indicators commonly used for bolted joints, the

method to measure the indicators, and the cause of self-loosening of the bolted joints.

2. Development of techniques to identify or calibrate the transduction matrix of a given DC motor for use as a self-sensing actuator of the tightness the of bolted joint. With a transduction matrix, the mechanical output of the motor can be indirectly ascertained from the motor's electrical input.
3. In-process measurement of the tightness of bolted joint during the tightening process with the calibrated motor. The tightening mechanism of the bolted joint can be investigated from the measurements taken and a better tightness indicator will be suggested.
4. Formation of the bolted joint's dynamic model from the input and output measurements from the dynamic measurement method developed in chapter 3. The motor will be used as an actuating device to perturb the bolted joints. The responses are measured indirectly from the electrical input of motor. A dynamic model of bolted joints can be thereby identified and their components obtained.
5. Investigation of loosening mechanism of bolted joints. Transverse vibration, a common cause of self-loosening of bolted joints, will be studied. The vibration will be regarded as an input excitation to the identified dynamic model of bolted joints to calculate its response. Based on the response, factors causing the loosening of the joints can be investigated.

1.3. Organization of the report

This report is divided into 6 chapters as follows:

- Chapter 1 sets out the introduction, objective, research plan and organization of the thesis.
- Chapter 2 presents an overview of the bolted joint, its tightness indicators, the existing methods and tools used to measure these indicators and the weaknesses of each indicator. Recent research on the effect of vibration on

the loosening of bolted joints, and the dynamic modelling of bolted joints are also presented.

- Chapter 3 discusses the characteristics of electric motors, the transduction matrix used to model their transduction behaviour, the various approaches that may be used to identify the transduction matrix. A typical DC motor is chosen and its transduction matrix is calibrated to develop a self-sensing actuator. The actuator will be used in the investigation of the tightening and loosening mechanism of bolted joints.
- Chapter 4 explains how the tightness of bolted joints are measured from the motor's input electrical with help of transduction matrix. Based on the measurements, a new tightening indicator is proposed.
- Chapter 5 describes system identification of bolted joints with the motor. System properties of bolted joints are obtained by perturbing the bolted joints with the motor. Dynamic model of bolted joints is constructed and the loosening mechanism is investigated from this model.
- Chapter 6 summarizes the research work undertaken, concludes the findings made, and makes recommendations for future project on the basis of those findings.

CHAPTER 2
TIGHTNESS OF THE BOLTED JOINT

Tightness of bolted joint is the main concern in its design. The joint should be tight enough to support the external load applied on it from the joined structures. Improper tightness may cause the joint to loosen or put the structure under stress and result in joint failures. However, a proper tightened bolted joint under vibration might be loosen itself, which normally called as self-loosening. Research in tightening and loosening of bolted joint is needed to give the designer a better insight in designing a proper tightened bolted joint.

In this chapter, literature on the bolted joints will be reviewed. Tightness indicators that are used in bolted joint will be introduced. Their relationship with tightness of bolted joint is discussed and their measurement method and accuracy are discussed. Self-loosening of bolted joint as one of common problem in bolted joint is also explained. Theory that discussed about self-loosening is discussed to understand cause and condition of this loosening. Lastly, dynamic model of bolted joint is reviewed to understand dynamic behaviour of bolted joint under dynamic condition such as vibration.

Section 2.1 discusses about common tightness indicators of bolted joint, their measurement methods and accuracy. Section 2.2 discuss about mechanism loosening of the bolted joint due to vibration based on several theories. Section 2.3 discusses about literature on dynamic model of a bolted joint

2.1. Tightness Indicator of the Bolted Joint

The tightness of the bolted joints is crucial in keeping the joint intact. Improper tightness in the joint may lead to joint failure. Under-tightening may cause joint separation while over-tightening may cause joint breakage. To properly install bolted joints, a good tightness indicator is essential. In this section, a few

commonly utilized indicators are presented, and their working functions and measurement methods are explained.

2.1.1. Clamping force of bolted joints

The clamping force is the force generated by the bolt and nut to fasten two parts together. A force with same magnitude is generated at the interface of the two jointed parts. This interface force indicates that the joint is still intact. A load cell can be installed at a bolted joint to measure the interface force. The donut load cell, a cell with a hole in the centre (Figure 2-1), is commonly used for this purpose. It is usually placed in between the fastened parts and the bolt is inserted through its hole. The load cell has a high measurement accuracy (around 1%-2%error) [11, 12]. However, this method introduces additional weight because the load cell needs to remain at the joint.

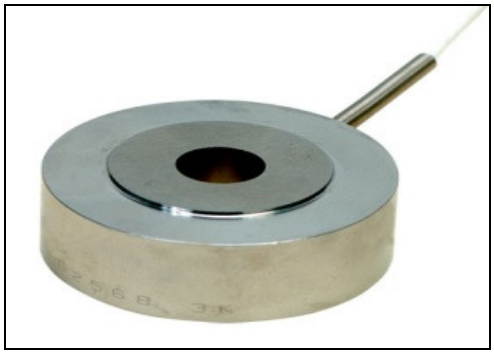

Figure 2-1 Donut load cell

2.1.2. Preload of bolted joints

Preload is the tension force generated at the bolt due to its stretching. The stretching occurs as a result of the compression of the jointed parts by the nut and the pull on the bolt. In most cases, the preload is equal to the clamping force. However, there are several cases where the two forces differ as follows:

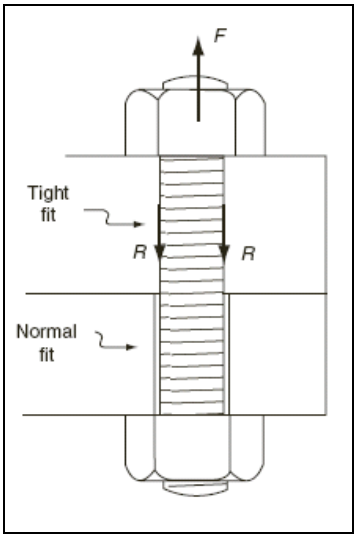

Figure 2-2 Hole interface in a bolted joint [2]

a) Bolted joint with tight hole interference

Figure 2-2 shows a bolt tightened through an undersized hole. The bolt will have a tight fit in the hole and additional preload is generated. This additional preload is used to overcome the frictional and embedment constraints between the sides of bolts and the walls of the hole, but is not used to generate clamping force at a bolted joint. Hence, the amount of preload is higher than clamping force.

b) Bolted joint with hanged weight

Figure 2-3 shows a bolted joint with a weight hanging on its bottom part and with a fixed top part. Due to gravity, the weight pulls down the bolt and an additional preload is generated. This additional preload does not reflect through the clamping force of the joint. Hence, the preload force has a higher value than the clamping force.

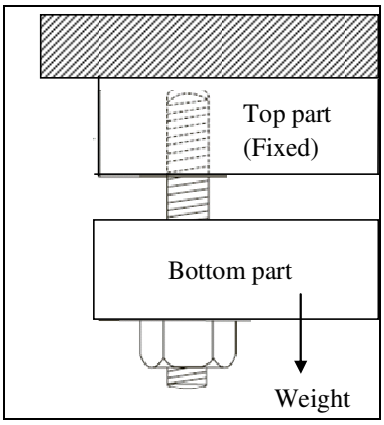

Figure 2-3 A bolted joint with a hanged weight

There are 3 common methods to measure the bolt preload. They are as follows:

a) **Direct measurement of preload**.

The preload is measured directly using a special washer installed at the bottom surface of bolt head or nut. The bolt preload is calculated from the strain undergone by the washer. An example of such a washer is the direct tension indicator washer (DTI washer) as shown in Figure 2-4. The DTI washer is a modified washer with bumps to indicate the bolt preload. As the nut is tightened, the bump is compressed and the gap between the nut and surface is reduced. The preload is determined based from the amount of gap generated. This method produces accurate measurements of the preload with error around 10% [13]. However, each washer has its range of preload and introduces additional weight to the joint.

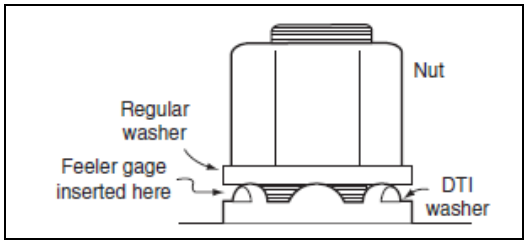

Figure 2-4 Direct Tension Indicator Washer (DTI) Washer

b) The elongation of a bolt/ bolt stretching

As aforementioned, the bolt preload (P) is generated from the stretching/elongation (ΔL_b) of the bolt. The relationship between the bolt preload and the bolt stretching is written as follows:

$$P = k_b \Delta L_b \tag{2-1}$$

where, k_b is bolt stiffness and is calculated as follows:

$$k_b = \frac{EA_b}{L_b} \tag{2-2}$$

where E is Young Modulus of the bolt, A_b is surface area of the bolt, and L_b is the initial bolt length.

With this relationship, the preload can be calculated from the bolt elongation. In practice, the bolt elongation is obtained by measuring the bolt's length before and after the bolt is tightened. Examples of the measurement tools used include the C-micrometer (Figure 2-5) and ultrasound measurement.

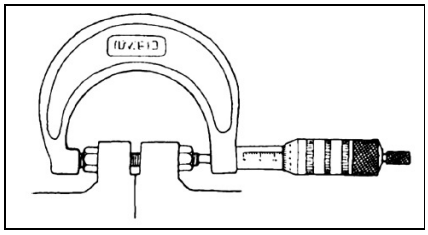

Figure 2-5 C-micrometer to measure the bolt lenght

However, there are several problems with using the bolt elongation to measure preload. They are as follows:

a) Dimensional variation in the body part and thread part of bolts which causes variation in stiffness for each part [14]
b) Temperature change which affects the bolt length
c) Tightening of the bolts near to the plastic region

d) Bending of the bolt and non-perpendicular surfaces may lead to dimension errors

c) Turning angle of the bolts

When a nut is turned for a full circle (360°), it will advance or retract in a linear displacement equals to one thread pitch (p). The bolt is assumed to stretch by the same length as the nut's linear displacement. The amount of the bolt's stretch may be expressed in term of turning angle (θ_r) as follows:

$$\Delta L_b = p\frac{\theta_r}{360°} \tag{2-3}$$

Thus, the bolt preload can be calculated from the turning angle as follows:

$$P = k_b \times \Delta L_b = k_b \times p\frac{\theta_r}{360°} \tag{2-4}$$

The difficulty with using turning angle to calculate preload is that no or little preload is produced for the first few turns as the bolt has not been stretched yet. In addition, the relationship between the turning angle and the bolt preload is not linear at the beginning of the stretch as shown at Figure 2-6**.** These will lead to inaccuracies in the calculated value of the preload.

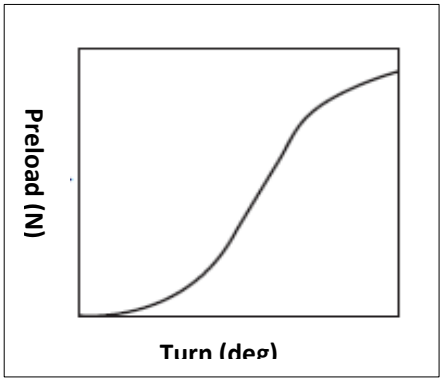

Figure 2-6 The preload vs Angle of turn graph [2]

2.1.3. Torque applied to a bolted joint

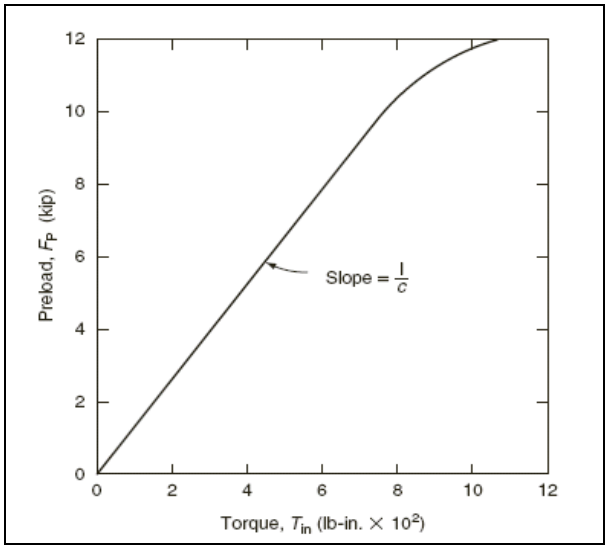

Figure 2-7 Relationship between applied torque and achieved preload [2]

Torque is the commonly used as a tightness indicator for a bolted joint due its ease of measurement. Torque is applied to the bolted joint and causes the bolt to turn relative to the nut. Initially, torque is used to overcome friction. When the bolt starts to stretch (generating preload), additional torque is needed. This additional torque is needed to turn the bolt further and to produce a higher preload. According to Bickford[2], the additional torque and the bolt preload are linearly related. The slope between them is constant (Figure 2-7).At higher values, the slope is not constant because the bolt is tightened near to its plastic region.

In deriving this relationship, there are two equations which can be used as follows:

a) Torque vs. preload: the short form equation

   The short-form equation relates the slope of the graph with the diameter of the bolt (D) multiplied by the nut factor (K) as follows:

$$T_{in} = K \times D \times P \tag{2-5}$$

The nut factor (K) in this equation is determined experimentally. The advantage of this equation lies in the use of a single constant to summarize the relationship of the preload with torque. However, the constant has to be determined for each new application.

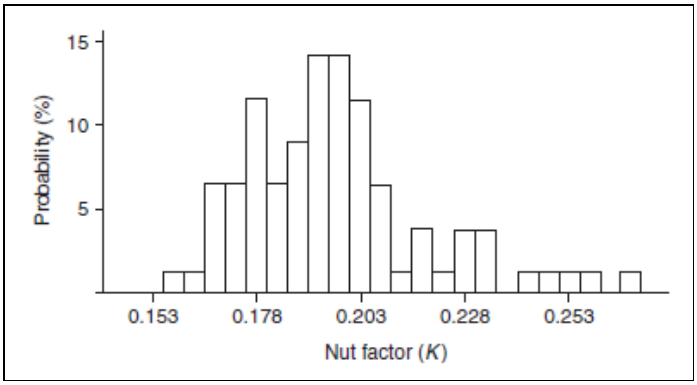

Figure 2-8 Histogram of K values reported for steel bolts from a large number of sources [2]

Equation (2-5) assumes that bolts with the same material, surface friction and thread angle share a similar value of nut factor (K). In fact, the value of the nut factor (K) can vary for bolt of the same material. Figure 2-8 shows the histogram of K values for steel bolts from various sources that are gathered by Bickford [4]. From the graph shown, the K value for a steel bolts varies from 0.15 to a maximum value of 0.25. This variation value of K causes same value of tightening torque for bolts of the same material generate the variation of preload. Figure 2-9 shows that the bolt preload generated can be scattered for ±50% for a single value of tightening torque. Thus, we can conclude that there are inaccuracies from using torque to indicate the bolt preload.

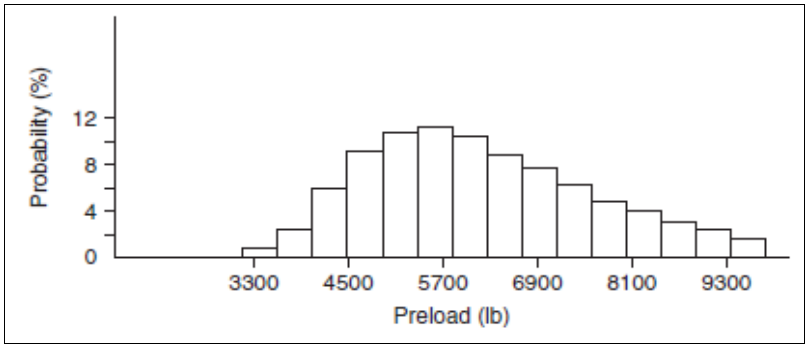

Figure 2-9 Histogram of the preload achieved from a single value of torque [6]

b) Torque vs. preload: the long-form equation

The long-form equation is proposed by Motosh [3]. According to Motosh, the input torque applied to tighten a bolt is resisted by three reaction torques as follows:

a. Torque from the stretching of the bolt
b. Torque from the surface friction at the threads of the bolt and nut
c. Torque from the surface friction between the face of a bolt or nut and the washer or the joined part.

Mathematically the equation for the input torque is written as follows [3, 15-17]:

$$T_{in} = P\left(\frac{p}{2\pi} + \frac{\mu_t r_t}{\cos\alpha} + \mu_n r_n\right) \tag{2-6}$$

where:

a. $P\frac{p}{2\pi}$ is the torque from the stretching of the bolt and p is thread pitch.

b. $P\frac{\mu_t r_t}{\cos\alpha}$ is the torque from the surface friction at the threads of the bolt and nut, μ_t is coefficient friction at the threads of the bolt and nut, r_t is the effective contact radius of the thread, and α is the thread angle.

c. $P\mu_n r_n$ is the torque from the surface friction between the face of a bolt or nut and the washer or the joined part, μ_n is coefficient friction between the face of the nut and the joint, and r_n is the effective contact radius between the nut and joint surface.

By assuming the value of the coefficient of friction and the bolt size and substituting them into the equation, the distribution of each reaction torque relative to the input torque can be found as shown in Figure 2-10. Figure 2-10 shows that most of the input torque is used to overcome the friction at bolt head and bolt thread, and only small portion (10%) of the input torque is used to stretch the bolt.

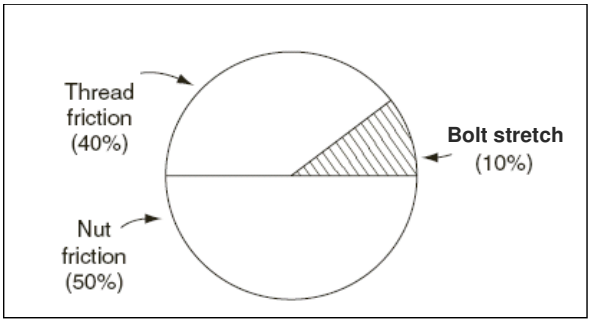

Figure 2-10 Relative magnitude of the three reaction torques oppose the input torque [2]

Equations (2-5) and (2-6) suggest that the torque and preload at a bolted joint is linearly related. However this relationship is highly affected by friction of a bolted joint. This is confirmed by Nassar, S. A. et al. in their experiments [18-22], which identified several factors affecting the relationship between input torque and preload generate at the bolt. They are the surface finish, tightening speed, coefficient friction of the bolt [21], and the lubricant used [22]. These factors affect the friction condition of a bolted joint.

An example of a tool used to measure torque is a beam type torque wrench (Figure 2-11). The wrench consists of a long lever arm between the handle and the wrench head. The arm is made of a material which bends elastically in response to

applied torque. The other example is strain gauge torque wrench. The strain gauge measures torsional deflection of the torque wrench's shaft. The result is converted into electrical display at the torque wrench. Normally, torque wrenches are designed to have accuracies range between ±2 to 10%.

Figure 2-11 The torque wrench

Beside tools for measuring torque, there are different types of bolt designs, which indicate the applied torque. One example is the twist-off bolts. The bolts have a neck that will break apart when the desired torque is reached (Figure 2-12). The disadvantages of this bolt are that the torque value is required beforehand and a special tool is needed to tighten the bolt and break the neck.

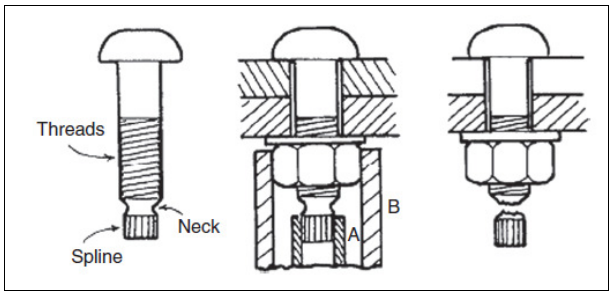

Figure 2-12 A twist-off bolt

2.1.4. Electrical impedance measurement

Along with advancements in the development of smart materials, a piezoelectric material was developed to measure the tightness of a bolted joint. The concept originates from Park et al, who used piezo transducer patches to assess the damage of a bolted joint in his experiments [23-25]. His method is known as the impedance-based monitoring technique. The principle behind his method is the measurement of the dynamic properties of a bolted joint that is reflected in electrical impedance of PZT.

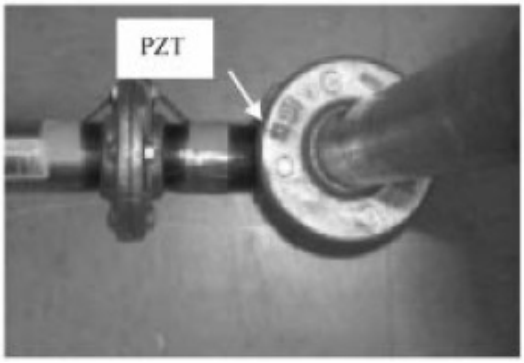

Figure 2-13 Location of PZT patched at a bolted joint [23]

In his experiment, a piezo transducer (PZT) is patched near to the bolted joint at a pipeline to assess the damage (Figure 2-13). When the joint is damaged (loosening, corrosion, thermal cycling), its impedance changes. This change will be manifested in the PZT's electrical impedance. The relationship between the electrical impedance, which is the ratio of the input voltage to current, is related and the impedance of a bolted joint is as follows[26]:

$$Y(\omega) = \frac{I}{E} = i\omega a\left(\bar{\varepsilon}_{33}^{\ T} - \frac{Z_s(\omega)}{Z_s(\omega) + Z_a(\omega)} d_{3x}^2 \hat{Y}_{xx}^{\ E} \right) \tag{2-7}$$

where:

- E is the input voltage to the PZT actuator,
- I is the output current from the PZT,
- a is the geometry constant,
- d_{3x}^2 is the piezoelectric coupling constant,
- $\hat{Y}_{xx}^{\ E}$ is the Young's modulus,
- $\bar{\varepsilon}_{33}^{\ T}$ is the complex dielectric constant of the PZT at zero stress,
- $Z_s(\omega)$ is the Impedance of a bolted joint, and
- $Z_a(\omega)$ is the Impedance of the PZT

As most of the variables in the equation are determined by the properties of the PZT, the change in the electrical impedance of a PZT is only affected by the change of the impedance of the bolted joint. The results of his experiments show that it is possible to distinguish between the loosening and tightening of bolts from impedance.

Following this concept, Mascarenas used a PZT enhanced washer to measure the bolt preload as shown in Figure 2-14 [27].The washer was attached to each bolt to measure the bolt's impedance. A ½-13 bolt was used and tightened to different torque levels. The impedance's magnitude at the resonant frequency is measured. The results are plotted in Figure 2-15 where the impedance of the PZT varies under different torque levels. The change in impedance is inversely proportional to the torque level However, for higher levels of torque, the change in impedance is less significant.

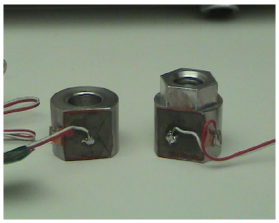

Figure 2-14 A nut and washer equipped with PZT wafer [27]

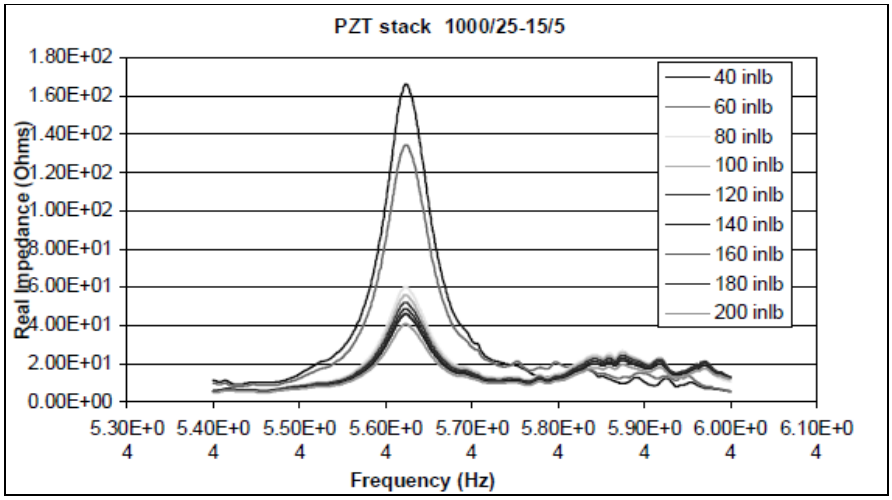

Figure 2-15 Impedance value from PZT washer [27]

Ritdumrongkul also used the PZT to identify the damage at a bolted joint [28].However, instead of measuring the impedance's amplitude, he observed a shift of resonance frequency at the PZT. His observation was concluded from a set of experiments with different torque levels. The shifting of the resonance frequency and the reduction of the impedance's peak height were observed in his

experiments. However, similarly to Mascarenas, the change was quite small to observe at a higher torque level. We can conclude that impedance measurement with PZT is only applicable at small tightening torque value.

2.2. Self- loosening of bolted joints

The common cause of bolted joints loosening by themselves is vibration. Under severe vibration, the jointed parts may experience slip and rotation which may lead to self-loosening of the joint. In this section, published works on the self-loosening of bolted joint under vibration, mechanism of self-loosening and factors to resist the self-loosening are summarized.

2.2.1. Vibration on a bolted joint

Bickford believes that when a bolt is tightened, energy is stored inside it as potential energy [29]. After the tightening is completed, the energy is held by friction constraints in both the bolt threads and in between the contact surfaces of the nut and the joint. If there is an external disturbance, such as vibration, to overcome these frictions, the potential energy will be released. The bolt is rotated back and the joint is loosened.

Several researchers have investigated the cause of bolts loosening under vibration [4, 30, 31]. They all agree that loosening occurs if the frictional force is overcome. They investigated two types of vibration applied to a bolted joint based on its direction, as follows:

1. Axial vibration

   Normally, a bolted joint has a high resistance to axial load as it is designed to sustain load in that direction. Based on Hess, the vibration in the axial direction affects the preload of a bolted joint but does not loosen the joint completely [32-34]. He proves this hypothesis with an experimental study of bolted joint under axial loading. From the experiment, he found that a bolt can be tightened or loosened in the presence of axial vibration. He also observed

that the loosening occurred at the vibration frequencies of 730-1130 Hz, while tightening occurred at the frequencies of 370-690 Hz. Based on the different axial vibration levels and initial preloads, he found that the clamping force would remain steady, decrease, or increase depending on the preload and vibration levels as shown in Tables 2-1 and 2-2. Based on these results, he concluded that a bolted joint can be tightened or loosened under axial vibration and the maximum loosening is only 52.9% of the original tightness. There is no complete loosening during the experiment.

Pre-load (N)	Steady state clamping force (N)	Change in clamping force (%)	Cycles to steady state	Time to steady state (s)
12	21·014 ± 0·068	+75·1	15050	30·1
15	22·525 ± 0·075	+50·3	12500	25·0
17	23·490 ± 0·030	+38·2	1700	3·4
20	25·009 ± 0·007	+25·1	2000	4·0
25	27·479 ± 0·031	+11·0	2050	4·1
30	29·975 ± 0·025	0·0	0	0·0
35	34·760 ± 0·520	−0·7	150	0·3
40	39·640 ± 0·000	−1·0	200	0·4
45	42·135 ± 0·005	−6·4	1850	3·7
55	47·135 ± 0·005	−14·4	6800	13·6
75	57·135 ± 0·005	−23·9	15500	31·0
100	69·633 ± 0·004	−30·4	26650	53·3

Table 2-1 Change in clamping force for different preload with constant vibration level [35]

Vibration level (m/s^2)	Steady state clamping force (N)	Change in clamping force (%)	Cycles to steady state	Time to steady state (s)
10	10·827 ± 0·001	−45·9	31250	62·5
80	9·423 ± 0·030	−52·9	12800	25·6
100	9·507 ± 0·573	−52·5	11350	22·7
250	16·868 ± 0·004	−15·7	5900	11·8
500	20·861 ± 0·861	+4·3	1250	2·5
600	23·306 ± 0·052	+16·5	2600	5·2
750	25·009 ± 0·007	+25·1	2000	4·0
1000	28·430 ± 0·007	+42·2	2150	4·3
2000	36·680 ± 0·009	+83·4	4350	8·7

Table 2-2 Change in clamping force for different vibration levels with constant preload [35]

2. Transverse vibration

Transverse vibration is vibration of a bolted joint perpendicular to the axis of the bolt. In a bolted joint, the transverse force due to vibration is resisted by friction. Usually, the resistance of a bolted joint in the transverse loading is

lower than that in the axial loading because the frictional force is product of preload and coefficient of friction. The value of coefficient of friction is normally less than one. Hence, the frictional force is smaller than the preload.

In 1960, Junker confirmed that a common cause of the total loosening of a bolted joint is transverse vibration [4]. His conclusion was verified with his "Junker Machine" (Figure 2-16). The machine consisted of an eccentric cam, a bolted joint and a load cell to measure the bolt's preload. In the interface between the plates, rollers are attached to allow the plates to slide relative to each other. The eccentric cam is driven by an electric motor and causes the bolted joint to vibrate with a small displacement. After a few thousand cycles of vibration, total loosening occurs if tightness is insufficient. The nut is loosened and the load cell shows a zero preload reading.

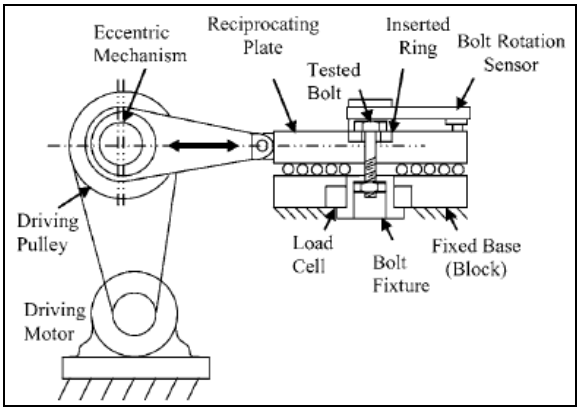

Figure 2-16 Junker Machine [2]

Other transverse vibration experiments have also been carried out by several other researchers [30, 36-39], who applied continuous transverse force to a bolted joint. Their results show a total loosening of the bolted joint as well. From these experiments, we can conclude that transverse vibration can lead to a total loosening of a bolted joint.

2.2.2. Mechanism of self loosening of a bolted joint

As mentioned previously, transverse vibration may cause self-loosening of a bolted joint. The mechanisms of transverse vibration in loosening a bolted joint are as follows:

a) Due to the previous cycle of vibration, the bolted joint is in the position as shown in Figure 2-17a.The top plate is moving to the left as the transverse vibration applies force to the left of the plate.

b) As the transverse force changes its direction, the top plate slides to the opposite direction (right). This causes the bolt to bend towards the right because the bolt head is fixed with the bottom plate (Figure 2-17b).

c) When the bending force overcomes the friction force at the thread and nut surfaces, the nut moves to the left and rotates slightly. The bolt is straightened and the top plate continues to slide to the right (Figure 2-17c).

d) When the top plate continues to slide further, the hole at the plate touches the bolt shank and the bolt is stuck. At this point, there is no further preload loss and the whole process is reversed where the force is applied back to the left (Figure 2-17d).

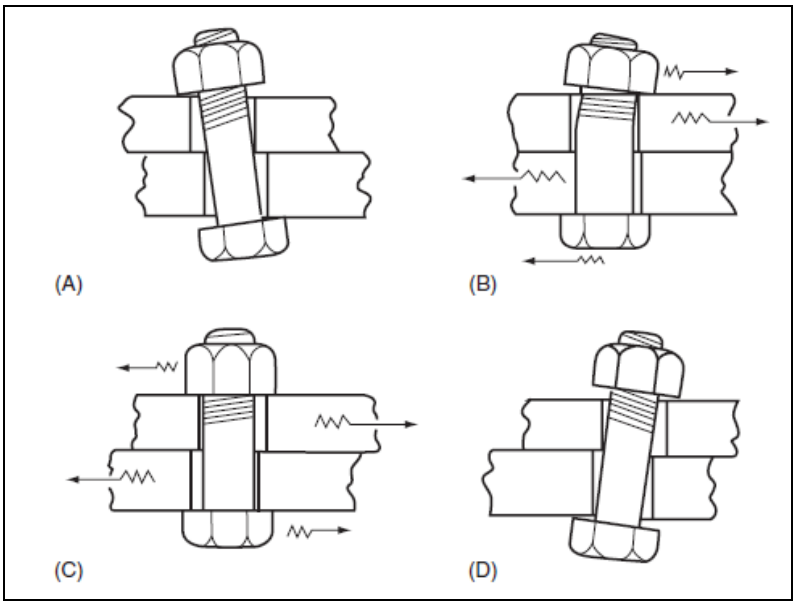

Figure 2-17 Mechanism of loosening of bolted joint due to transerse force [2]

Based on the explanation above, the loosening happens due to the relative motion at bolt thread. According to the Bolt Science website, the common causes of this motion are as follows [40]:

1. Bolt bending results in the induction of forces at the friction surface. If slip occurs, the head and threads of the bolts will slip, which may lead to loosening.
2. Differential thermal effects caused by differences in temperature or differences in the bolted joint's materials.
3. Applied forces on the joint that lead to the sliding of the joint parts and the eventual loosening of the bolt.

In order to verify the mechanism of self loosening of bolted joint, Yokoyama make a FEM analysis of bolted joint under transverse loading [12]. They analysis the load-displacement behaviour of bolt before slip happens at bolt head. Based on their analysis, they formulated reaction moment on the bolt head and thread due to applied transverse force. They found out that the reaction moment is depends on stiffness of bolt joint and the stiffness is affected by slip happen at bolted joint.

2.2.3. The factors influencing self loosening of a bolted joint

There are several factors which influence the self-loosening of bolted joints from vibration, such the thread pitch of the bolt, the initial tightness of the joint [7], the coefficient of friction of the bolt surface[5, 6], the hole clearance and the fitting between the threads [38]. A detailed discussion on each factor is as follows:

a) Thread pitch of the bolted joints

The threads of the bolt are a helical structure used to convert a given rotational movement into linear movement. The linear distance travelled by a bolt for one rotation is called the thread pitch. According to the Unified Thread Standard (UTS), there are 3 types of threads: "coarse",

"fine", and "extra fine". A coarse thread has the largest pitch whereas an extra fine thread has the smallest pitch. The effect of difference in pitch sizes on the self-loosening of a bolted joint is shown in Figure 2-18. Figure 2-18 shows that the finer the bolt thread, the more cycles that are needed to loosen a bolt. This is because a finer thread has a small lead angle due to its small pitch. The small lead angle reduces the loosening force.

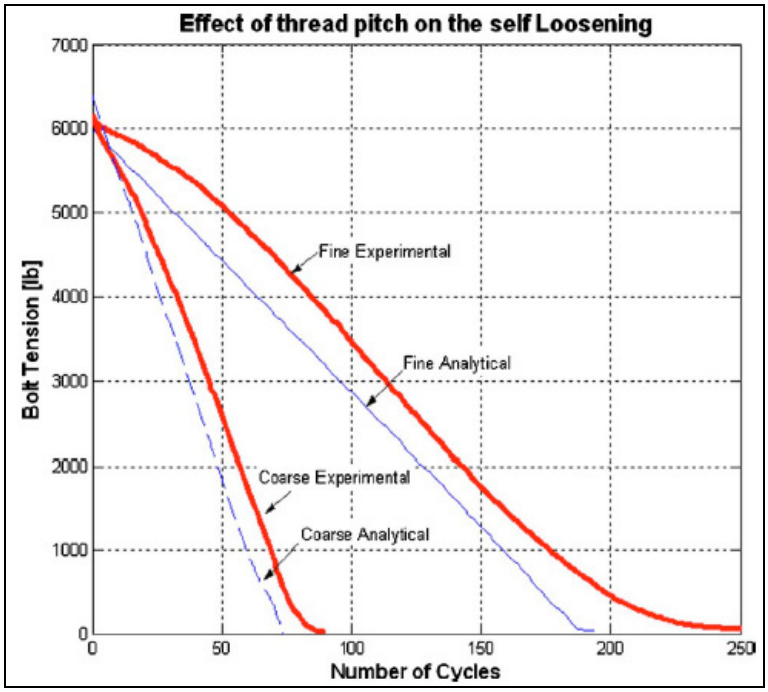

Figure 2-18 Effect of thread pitch on the self loosening [7]

b) Initial tightening of a bolted joint

c) Normally, a bolted joint is tightened to a certain value of preload. The value of the preload is decided by considering the load applied to the joint. This preload helps to resisting vibration as shown in Figure 2-19. The results show that the higher the preload, the greater the number of cycles that are needed to loosen a bolted joint. However, there is a point where loosening will not occur. If the bolted joint is tightened above this point, the vibration applied will not reduce the bolt preload. This point is defined based on applied vibration's amplitude. Figure 2-20 shows that for lower levels of vibrational amplitudes (0.03 inch excitation), a bolted joint needs

to be tightened to above 4,000 lb. to prevent loosening. For higher levels of vibration amplitude (0.05 inch excitation), a bolted joint needs to be tightened to above 9,000 lb.

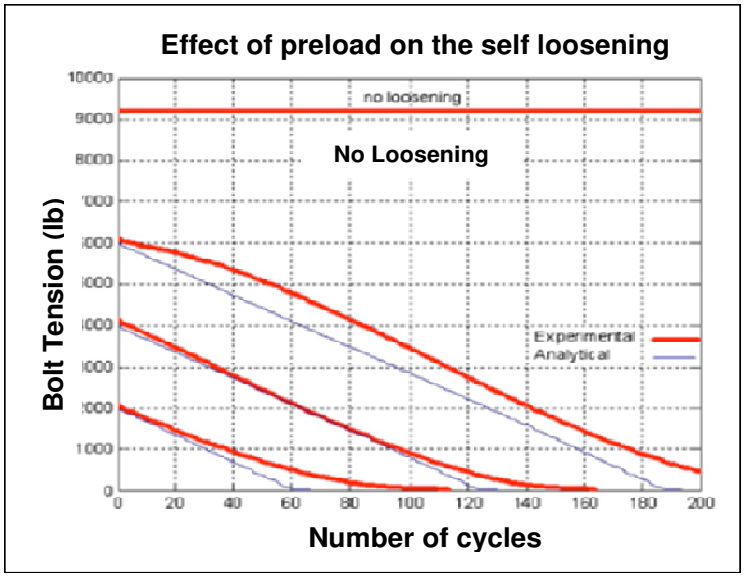

Figure 2-19 Effect of initial bolt tension on the self loosening [7]

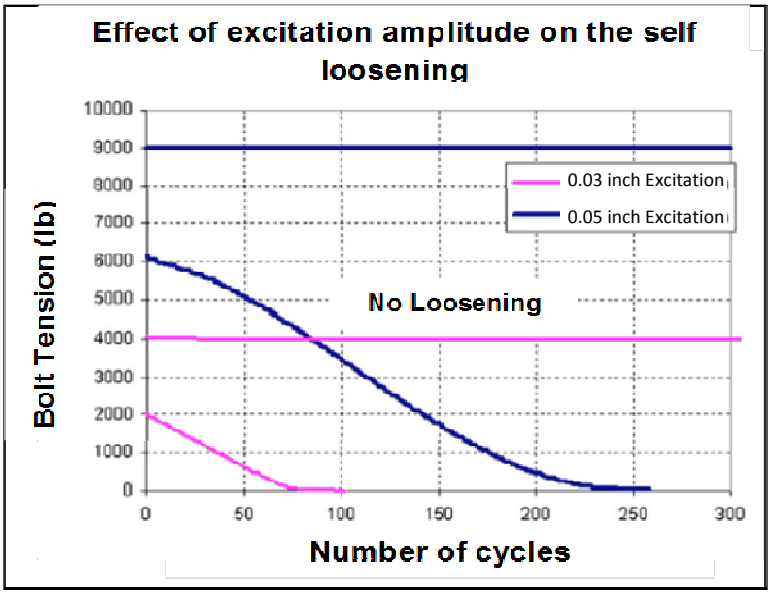

Figure 2-20 Effect of excitation amplitude on the self loosening [8]

d) Coefficient of friction of the bolt surface

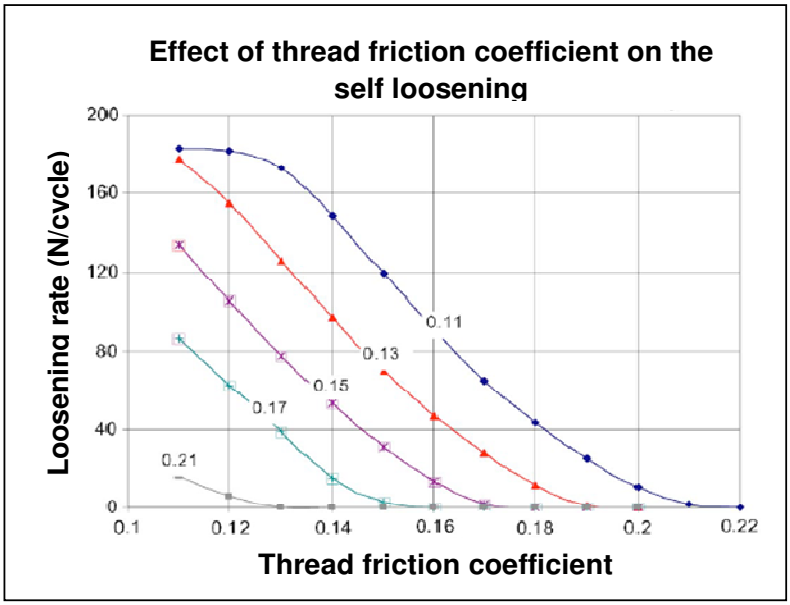

Figure 2-21 Effect of thread friction coefficient on self loosening [6]

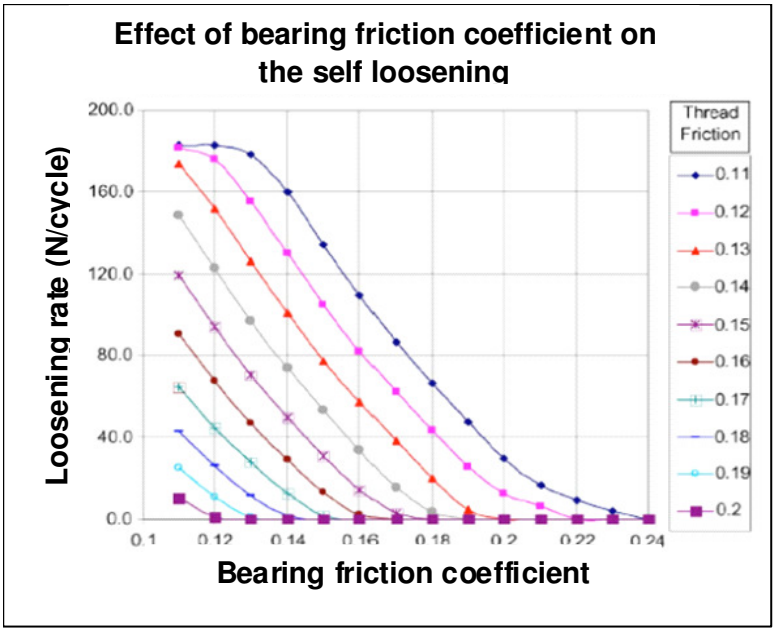

Figure 2-22 Effect of bearing friction coeeficient on self loosening [6]

The coefficient of friction is a scalar value that describes the ratio of frictional force between the two bodies and the normal force acting on them. Its value

depends on surface condition of the bodies and their material. The rougher the surface, the higher is the value of the coefficient of friction. There are two friction coefficients at the bolted joint, the thread friction coefficient and bearing friction coefficient. The thread friction coefficient describes the friction between thread of the bolt and nut. The bearing friction coefficient describes the friction between surface of bolt head and joined part. Both frictions help to prevent bolt loosening as shown in Figures 2-21 and 2-22. Less preload is lost for one cycle of vibration due to a higher coefficient of friction.

e) Hole clearance

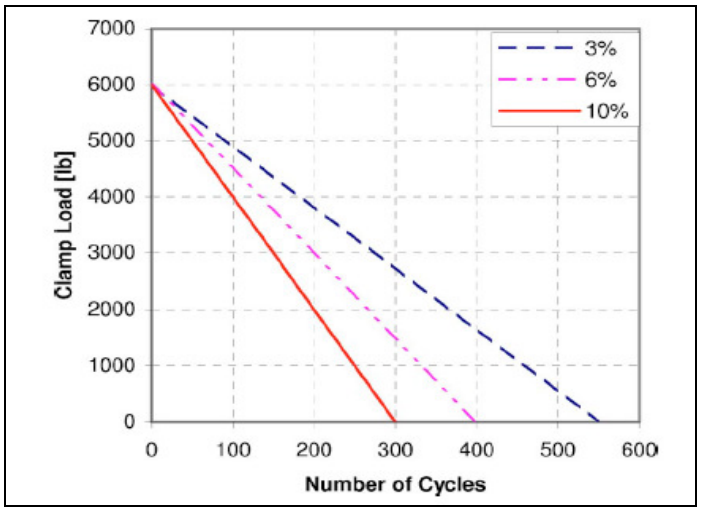

Figure 2-23 Effect of hole clearance on self loosening [8]

Before tightening a bolted joint, a bolt is inserted through a hole in two joined parts. To prevent the bolt from being jammed and to generate additional preload, the hole should be bigger than the bolt diameter (the hole clearance).The clearance affects the contact area between the joint and the bolt head. A larger clearance leads to smaller contact area. Hence, the resistance of bolted joint against the vibration is lower (Figure 2-23). This has been experimentally proven by Basil Housari [8]. His results show that with a larger hole clearance, less cycles

are required to loosen a bolted joint. This is because the larger hole clearance allows the bolt to be loosened more before it is stuck.

f) The fitting/ matching between the threads

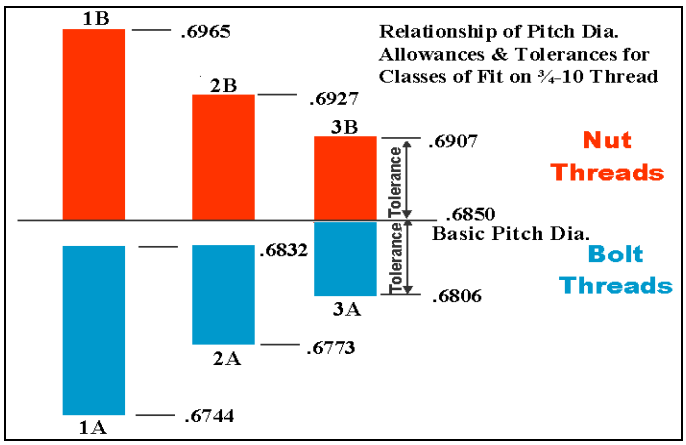

Figure 2-24 Difference between class of fit at bolted joint

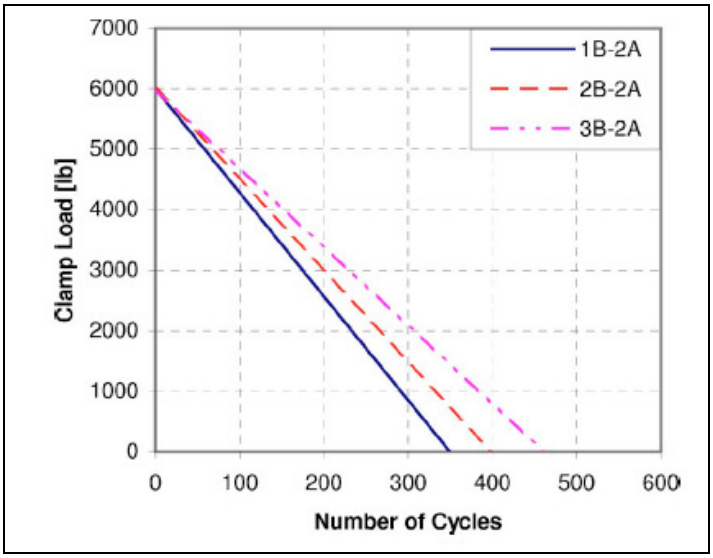

Figure 2-25 Effect of fitting on self loosening [38]

Based on the UTS, there are three classes of fit by which the external and internal threads of a bolted joint mates together. They are classes 1, 2, and 3, in ascending order of tightness. A (external) and B (internal) are used to indicate the types of

thread. The difference between each class is the tolerance for the pitch diameter as shown in Figure 2-24. Class 3 has a smaller tolerance compared to Class 1. This tolerance affects the resistance of a bolted joint to loosening (Figure 2-25). A smaller tolerance leads to a slower rate of loosening.

2.3. Dynamic modeling of a bolted joint

In the previous section, the loosening mechanism of bolted joints due to vibration was examined by a review of the experimental studies. Vibration is an external excitation given to the bolted joint. Under this excitation, the joint gives out a response in form small displacement and dissipate some of the energy. Several researchers try to model this dynamic behaviour of bolted joint by model this dynamic behaviour. This section reviews existing dynamic models of bolted joints.

2.3.1. Bolted joint based on a spring and a damper

In his modelling of the bolted joint, Tsai used the receptance method proposed by Bishop[41, 42]. He assumed that two structures, structure I (region a) and structure II (region c), were assembled on an interface b (a bolted joint) as shown in Figure 2-26. When a transverse force is applied to the structures, a small displacement occurs at the interface. This displacement is explained with the following matrix formula:

$$U_b^{(2)} - U_b^{(1)} = H_j f_b^{(1)} \tag{2-8}$$

where $U_b^{(n)}$ is transverse displacement of structure n, H_j is the receptance matrix and f_b is transverse force applied to the system.

This receptance matrix (H_j) is related with the system properties of the interface. Based on the model, Tsai assumed that the matrix relates with the stiffness (K) and damping coefficients (C) of the interface with negligible mass. Mathematically, it is written as follows:

$$H_j = \left(K + j\omega C\right)^{-1} \tag{2-9}$$

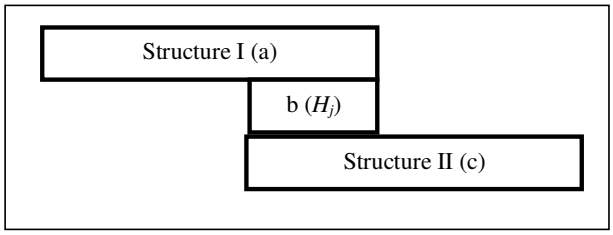

Figure 2-26 Model for a bolted joint according to Tsai [41]

Another example of a bolted joint model with spring and damper is Hanss' model (Figure 2-27). Hanss assumed that damping (*d*) and stiffness (*k*) of bolted joints are related with the geometry and material properties of two joined rods. The damping and stiffness are calculated as shown below [43-48].*E, ρ, l* are Young modulus, density and length of rod 1 and 2.

$$k = \mathrm{Re}\left(-\frac{s\beta_1\beta_2}{\beta_1 \coth\left(s\alpha_2\right) + \beta_2 \coth\left(s\alpha_1\right)}\right) - d\,\mathrm{Re}\left(s\right) \tag{2-10}$$

$$d = \frac{1}{\mathrm{Im}\left(s\right)}\mathrm{Im}\left(-\frac{s\beta_1\beta_2}{\beta_1 \coth\left(s\alpha_2\right) + \beta_2 \coth\left(s\alpha_1\right)}\right) \tag{2-11}$$

Where:

$$\alpha_1 = \sqrt{\frac{\rho_1}{E_1}}l_1, \qquad \alpha_2 = \sqrt{\frac{\rho_2}{E_2}}l_2, \qquad \beta_1 = A_1\sqrt{E_1\rho_1}, \qquad \beta_2 = A_2\sqrt{E_2\rho_2}$$

The results were obtained with a fuzzy arithmetic method and shows a variation in the damping and stiffness obtained (Figure 2-28). This variation is caused by the variability of the material's properties and geometries, frequency of excitation, and other uncertain parameters in the bolted joint.

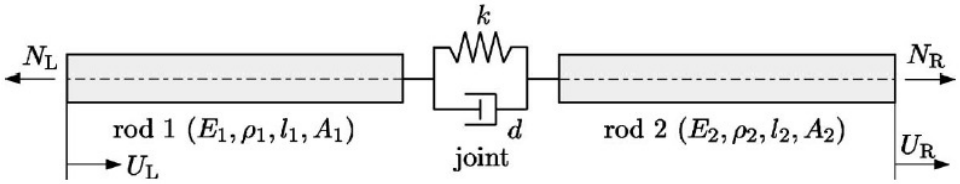

Figure 2-27 Two rod connected by a bolted joint (Hanss' model) [43]

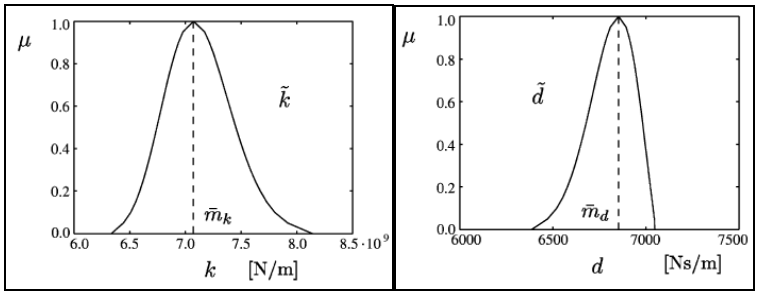

Figure 2-28 Uncertain stiffness parameter and damping parameter of model joint [43]

2.3.2. Bolted joint modelling based on Jenkins element

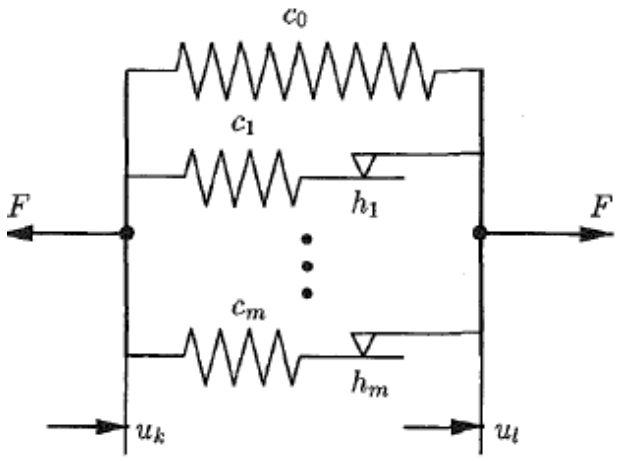

Figure 2-29 Jenkins element model [49]

Another example of a bolted joint's model is the Jenkins element model. Oldfield used Jenkins element to model friction at the bolted joint[49, 50]. In Jenkins'

element model, the friction is modelled as an ideal coulomb element with a threshold value (h),and connected in series with a spring element (c_i)[51, 52]. The spring element is used to show the deformation phenomenon that occurs prior to the interfacial slip and before the static force is fully overcome.

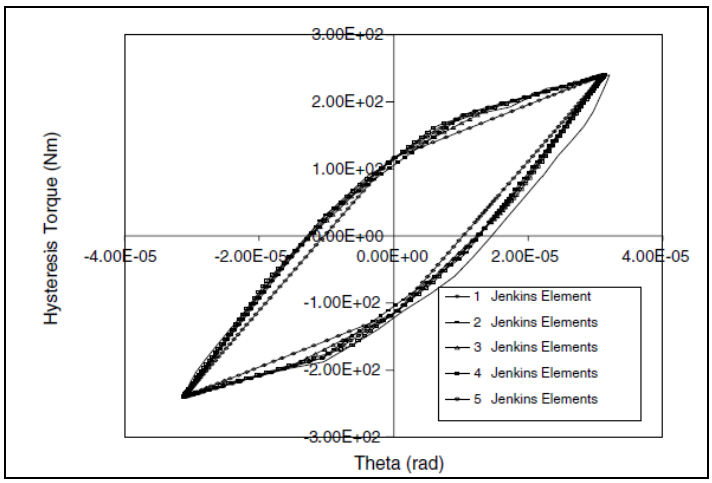

Figure 2-30 Hysteresis loop of bolted joint under different number of Jenkins elements [49]

Under harmonic excitation, the Jenkins element produces an ideal elastic/perfectly-plastic hysteresis curve. With a single element, the bolted joint has two states, the sticking and slipping states. However, a single element of Jenkins element is not sufficient to model the micro slip happening in a bolted joint. The micro slip is a state in the joint where some regions are sticking while others have exceeded the threshold of friction force and are slipping. N-numbers of Jenkins-Elements are needed to model this micro slip. Those n-numbers of Jenkins-Elements are arranged in parallel (Figure 2-29).The equation below describes the relationship of the elements with the contact force (F) [51] :

$$F\left(u,\dot{u}\right)=c_0u+\sum_{i=1}^{m}\begin{cases} r_i\left(t\right) & \left|r_i\left(t\right)\right|<h_i \\ h_i\,\mathrm{sgn}\,\dot{u} & \end{cases} \tag{2-12}$$

where:

$$u = u_k - u_l, \tag{2-13}$$

$$\left|r_i\right| = \left|c_i\left(u - u^+\right) - h_i \operatorname{sgn} \dot{u}^+\right| \tag{2-14}$$

By increasing the number of elements, the hysteresis curve becomes smoother (Figure 2-30). However, the challenge lies in determining the spring elements and threshold value.

2.3.3. Bolted joint modeling based on Bouc-Wen model

The Bouc-Wen model combines a hysteresis function with a non-hysteretic function to describe the restoring force of a system that has yielded to some degree[53, 54]. Mathematically, it is written as follows:

$$Q\left(x, \dot{x}\right) = g\left(x, \dot{x}\right) + z\left(x, \dot{x}, t\right) \tag{2-15}$$

where g is a non-hysteretic component and z is the hysteretic function dependent on displacement history of the model.

The z function is defined by a nonlinear first order differential equation as follows:

$$\dot{z} = -\alpha\left|\dot{x}\right|\left|z\right|^{m-1} z - \beta\dot{x}\left|z\right|^m + A\dot{x} \tag{2-16}$$

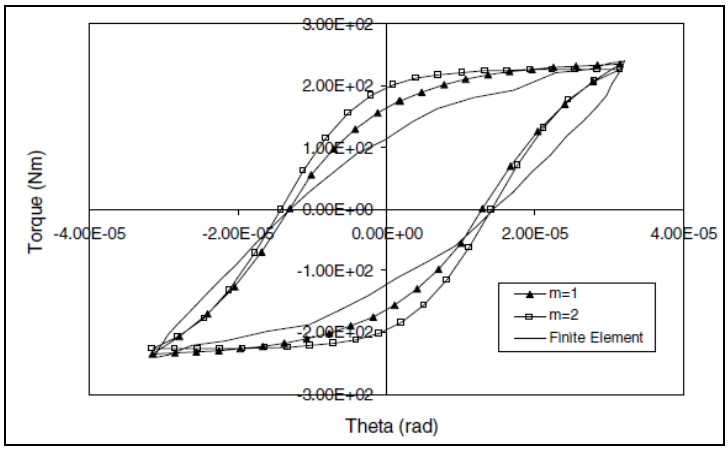

Figure 2-31 Hysteres loops using Bouc-Wen model [49]

The versatility of this model arises from the ability to tune the parameters, α, β, A, and integer m. α and β define the shape of the hysteresis loop, while A defines the initial stiffness, and m is used to manipulate the smoothness of the loop. When $m = 1$, the response deviates from a pure elasticity. $m = \infty$ describes a bilinear restoring force. The graph produced by Bouc-Wen model is a smooth graph (Figure 2-31). However, the parameters α and β do not have any obvious physical meaning. Thus it is difficult to associate them with the stick-slip behaviour at the joint's interface.

Those mentioned models are based on Finite Element Method, with no experimental to confirm their results. Thus, an experimental method to measure system properties of bolted joints and verify the model is needed. With the model, dynamic cases of bolted joint, such as bolted joint under loosening, can be simulate. The phenomenon or the response of bolted joint can be investigated from the simulation.

CHAPTER 3
DC MOTOR AS A TIGHTNESS MEASUREMENT TOOL FOR BOLTED JOINTS

Bolted joints are normally tightened with a torque wrench equipped with a dial indicator. The dial indicator shows the resistance torque exerted by the bolted joint on the wrench. It allows the operator to see when the desired torque is achieved so that he can stop tightening. However, the bolt's conditions may cause the torque to be misread by the indicator. For instance, damage to the bolt's coating or threads may cause the torque's reading to increase. This may lead the operator to stop tightening when further tightening is in fact necessary to achieve his desired tightness. To avoid such a problem, a real time tightness measurement system, which is able to monitor the tightening process from start to end in real time, is required. Any change in tightness during the tightening process can then be perceived by the operator right away.

In this project, a brushed DC motor is developed into a real time sensing and actuating device to monitor the tightening process of bolted joints. The motor applies mechanical output (torque and rotational speed) to the bolted joints transduced from the motor's electrical input (voltage and current) to tighten the bolt joint. The transduction relationship between the mechanical outputs and electrical inputs can be described by a 2x2 matrix called the transduction matrix. Each element in the transduction matrix represents a transfer function between a variable of the mechanical output and a variable of the electrical input under certain boundary conditions in frequency domain. The transduction matrix allows the motor's mechanical output variables to be calculated from the motor's electrical input variables. This allows the motor to be developed into a simultaneous sensing and actuating device for real time monitoring of the tightening process of bolted joints. This chapter presents the theory behind and method of this development.

Section 3.1 introduces the theoretical background of the transduction matrix in the modelling transduction process of brushed DC motors and outlines the assumptions involved. Section 3.2 introduces the methods to identify the transduction matrix. Section 3.3 presents the measurement results of a calibrated brushed DC motor to assess the accuracy of the transduction matrix. Section 3.4 summarizes of the chapter.

3.1. Mechanism and Characteristic of Brushed DC Motors

In this thesis, a brushed DC motor is chosen as the tightness measurement tool for bolted joints due to its portability, and the linear relationship between torque and rotation speed. The motor transduces the supplied electrical power into mechanical power. This transduction process can be modelled with the transduction matrix, which enables the mechanical output of motor to be calculated from its electrical input. This obviates the need to install bulky force and motion sensors to measure the mechanical output of the motor. The DC motor's transduction mechanism, linear characteristic and how the transduction mechanism is modelled by the transduction matrix will be explained in this section.

3.1.1. Mechanism of brushed DC motors

A brushed DC motor is an internally commutated electric motor powered by a DC power source (Figure 3-1). The voltage applied to the motor energizes the motor and generates a current. The voltage and current is transformed into mechanical power by the rotation of the shaft. The transduction process is based on the electromagnetic interaction between two main components of the motor, the stator and rotor.

a) The **Stator is** a stationary part of motor located under the motor housing. In brushed DC motors, the stator acts as the field magnet and provides magnetic flux to interact with the armature. The stator is usually made of a permanent magnet to generate the magnetic flux.

b) The **Rotor** is a rotating part of motor. It is located at the centre of the motor and connected to the motor shaft. In brushed DC motors, the rotor acts as the armature that carries the current and interacts with the magnetic flux generated from the field magnet. The rotor is usually made of a conductor or conductive winding.

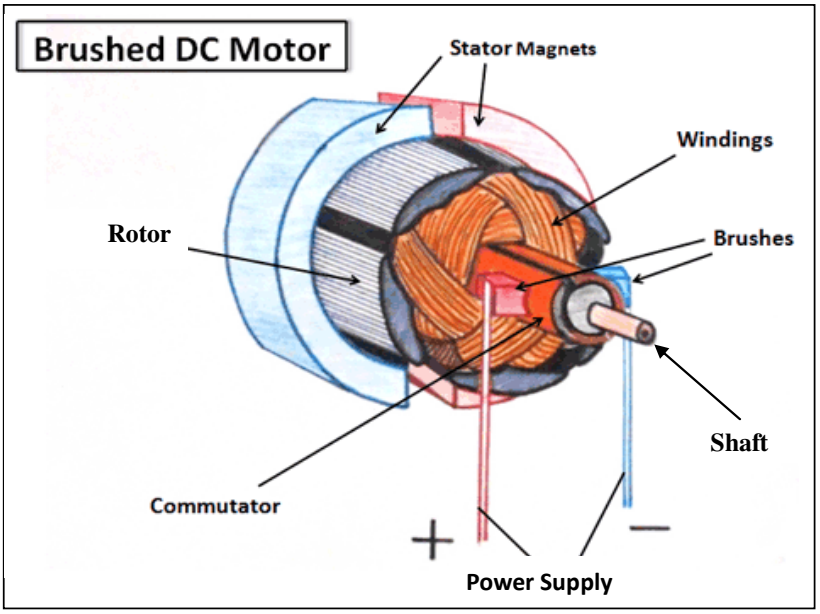

Figure 3-1 Schematic diagram of brushed DC motor [55]

For simplicity, it is assumed here that the two components have two magnetic poles (see Figure 3-2). The stator is made up of a permanent magnet and the rotor is made up of coil windings. When voltage is applied by the power supply, current flows to the rotor windings which generate electromagnetic flux. The commutators connect the power supply to the rotor windings and control its polarity. The rotor that is connected to the positive terminal of the power supply becomes the north pole and thus has the same polarity as the stator. The repulsion between the rotor and stator causes the motor shaft rotates for half a circle. After this rotation, the current is reversed to change the polarity of rotor. The rotor connected with the positive port of power supply becomes the north pole. The repulsion between the rotor and stator causes the motor shaft rotates for a further

half circle. This process repeats continuously as long as there is electrical power supplied to the motor.

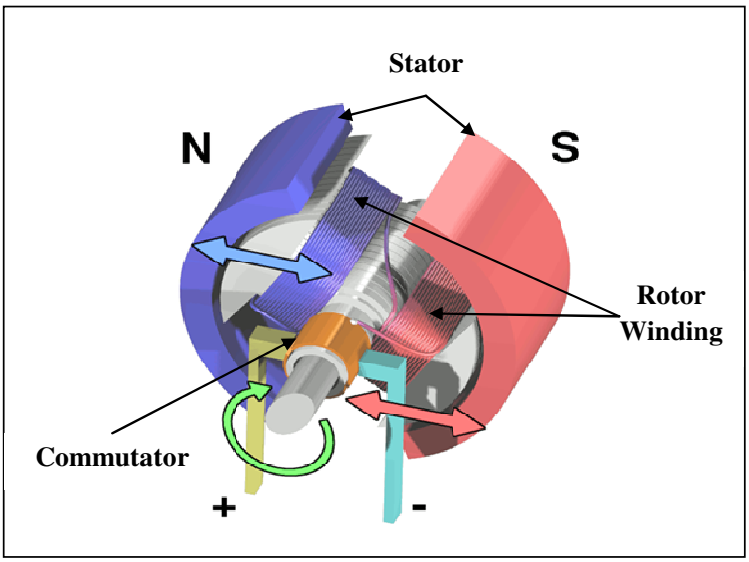

Figure 3-2 Operating process of a brushed DC motor

Due to the rotation of the shaft, the rotor experiences a time varying magnetic field. Following Faraday's law, the time varying magnetic field induces a back-electromotive force (back-EMF) voltage inside the motor. The magnitude of this voltage (E_{emf}) is proportional to the motor speed (Ω_m) and its polarity is the reverse of the applied voltage. The motor constant (k_E) defines the relationship between the back-EMF voltage and the motor speed. Mathematically, the relationship is written as follows:

$$E_{emf} = k_E \Omega_m \tag{3-1}$$

The k_E is a function of the motor's parameters such as the dimension of the magnet, the generated magnetic field and the number of rotor windings. Usually, the k_E value is specified by the motor's manufacturers.

Besides k_E, there is also another motor constant (k_T), which governs the relationship between the motor's torque (T_m) and the applied current (i).

According to Lorentz force law, a current-carrying conductor placed within an external magnetic field will experience a force or torque. This relationship can be simplified with k_T, which is also a function of the motor's parameters such as the dimension of the magnet, the generated magnetic field and the number of rotor windings. The relationship is written as follows:

$$T_m = k_T i \tag{3-2}$$

The next section shows how the relationship between the electrical power and mechanical power of the motor can be defined with k_E and k_T,

3.1.2. Linear characteristic of brushed DC motors

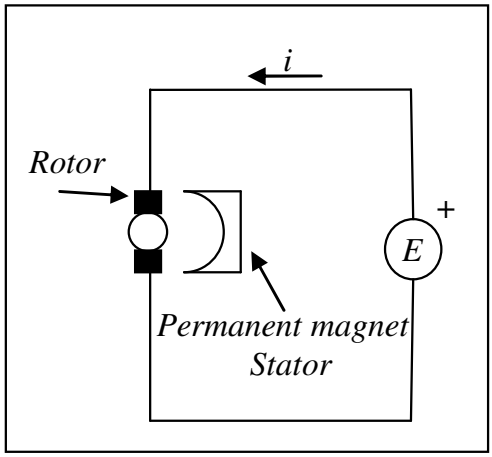

Figure 3-3 Schematic diagram of permanent magnet DC motor

Figure 3-3 is a schematic diagram of the permanent magnet of a DC motor. As the stator is made of a permanent magnet, the voltage is only supplied to the rotor through the commutator to energize the coil winding. The torque and rotational speed of the permanent magnet DC motor are linearly related with the voltage and current supplied. Thus, the permanent magnet DC motor has a more linear torque-speed characteristic than other motors which has a stator made of coil winding. In a motor with a stator made of coil winding, the stator and rotor share the same electrical supply. The current supplied to the motor flows to both the rotor and the

stator. Any change in load or disturbance at either the rotor or stator will affect the current supply to the other. Thus, the torque and speed characteristics of such motors are non-linear. This motor will not be discussed further as the main concern in this thesis is with motors containing stators made of permanent magnets.

The coil windings at the rotor of brushed DC motors with a permanent magnet stator can be modelled with an equivalent circuit consisting of a resistance (R), an inductance (L) and a voltage source (E_{emf}) connected in series (as shown in Figure 3-4). Based on the Kirchhoff's Law, the voltage (E) of the equivalent circuit is derived as follows:

$$E = iR + L\frac{di}{dt} + E_{emf} \tag{3-3}$$

With this voltage, current flows through the rotor winding and induces an electromagnetic force to produce torque (T_m) at the motor shaft. The purpose of the torque (T_m) is to overcome the motor inertia ($J_{motor}\frac{d\Omega_m}{dt}$), the friction ($T_f$), and the motor's load (T_L). The equation is derived as follows:

$$T_m = J_{motor}\frac{d\Omega_m}{dt} + T_f + T_L \tag{3-4}$$

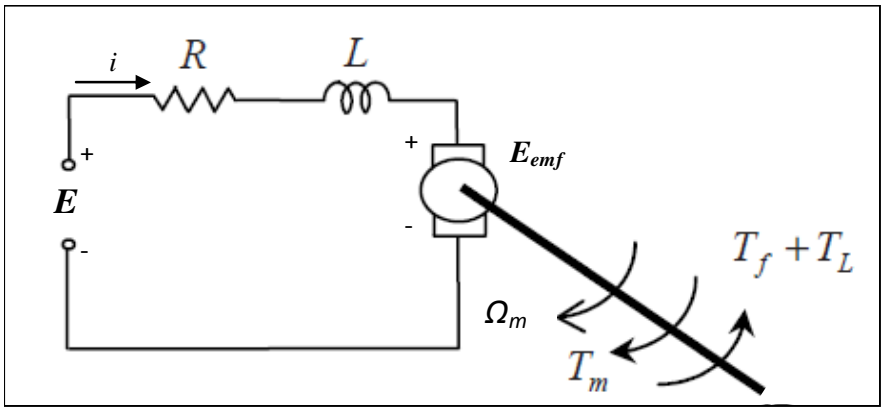

Figure 3-4 Equivalent circuit of coil winding at brushed DC motor

Normally, the motor loading (T_L) and the friction (T_f) are functions of its speed ($T_L(\Omega_m)$ *and* $T_f(\Omega_m)$). Thus, Equation (3-4) can be simplified as follows:

$$T_m = J_{motor}\frac{d\Omega_m}{dt} + T_f\left(\Omega_m\right) + T_L\left(\Omega_m\right) \tag{3-5}$$

Under steady state condition, the motor will rotate at a constant speed ($\frac{d\Omega_m}{dt} = 0$) and no current change will occur ($\frac{di}{dt} = 0$). Thus, Equation (3-3) and Equation (3-5) can be simplified as follows:

$$E = iR + E_{emf} \tag{3-6}$$

and

$$T_m = T_f\left(\Omega_m\right) + T_L\left(\Omega_m\right) = T_e\left(\Omega_m\right) \tag{3-7}$$

Equation (3-6) is the electrical equation of the motor and shows that there is a linear relationship between the voltage, current and back-emf. Equation (3-7) is the mechanical equation at the motor and simplifies the torque equation of the motor as a function of rotational speed (Ω_m). The electrical (Equation (3-6)) and mechanical equation (Equation (3-7)) can be combined together with the motor constants in Equations (3-1) and (3-2) to form the torque equation as follows:

$$T_e\left(\Omega_m\right) = \frac{k_T}{R}\left(E - k_E\Omega_m\right) \tag{3-8}$$

It can be seen from Equation (3-8) that the linear relationship between torque and rotation speed is governed by the voltage supply to the motor (E) since the other parameters (k_E, k_T, and R) are constants. Figure 3-5 shows the torque–speed curves of the motor under different applied voltages. It can be seen that the gradient of the lines between torque and speed are the same. By applying different voltages, the line is shifted up or down based on the applied voltage (V_a). For a

DC motor to achieve a higher torque and rotational output, the applied voltage needs to be increased. On the other hand, the gradient is governed by the motor constant which is based on the magnetic field on the motor. Figure 3-6 shows the torque-speed curves of the motor as the motor constant is varied from high to low (k_{TA} to k_{TC}). It can be seen that a higher motor constant causes torque to increase and rotation speed to decrease (the line is shifted to the right).

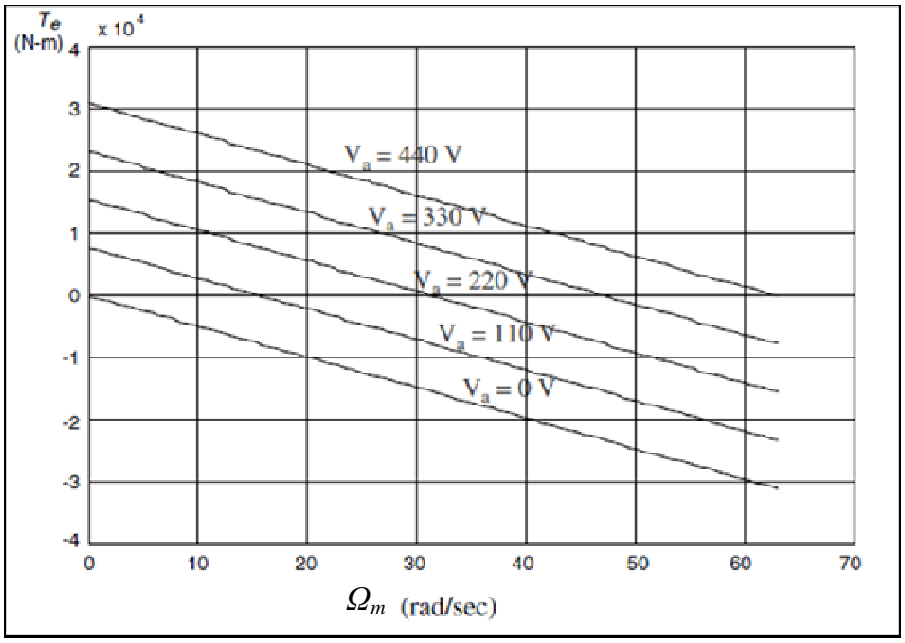

Figure 3-5 Torque-speed curves of a permanent magnet DC motor (rated armatue voltage 440V, rated power 110 kW, rated speed 560 rpm)

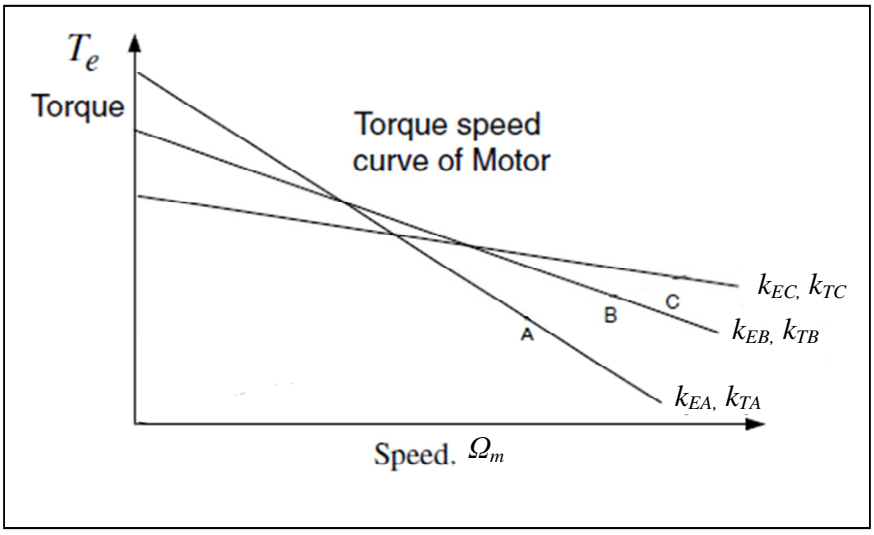

Figure 3-6 Torque-speed curve of a permanent DC motor under different motor constant

It can be seen from Equation (3-8) that under a steady state condition, the voltage of the motor is linearly related its torque and rotation speed. It can be seen from Equation (3-2) that the motor's current is linearly related with its torque. It can be seen from both equations that the electrical input of the motor (voltage and current) is linearly related its mechanical output (torque and rotation speed). Thus, we can conclude that such a motor is as a linear system. The next section explains how the motor can be modelled by using a transduction matrix.

3.1.3. Transduction matrix of brushed DC motors

In dynamic system modelling, the characteristic of the single input-single output linear time invariant system can be represented by a weighting function ($h(\tau)$) and frequency response function $H(f)$ (FRF). When the system is subjected to a well-defined single input ($x(t)$), the output of the system ($y(t)$) can be obtained from the convolution integral between the weighting function ($h(\tau)$) and the input ($x(t)$). The equation is expressed as follows:

$$y(t) = \int_0^\infty h(\tau)\, x(t-\tau)\, d\tau \tag{3-9}$$

Applying the Fourier Transform to Equation (3-9), the linear relation between the input and output of the system can be formed as follows:

$$Y(\omega) = H(\omega)\, X(\omega) \tag{3-10}$$

where

$$H(\omega) = \int_0^\infty h(\tau)\, e^{-j\omega\tau} d\tau \tag{3-11}$$

$$Y(\omega) = \int_0^\infty y(\tau)\, e^{-j\omega\tau} d\tau \tag{3-12}$$

$$X(\omega) = \int_0^\infty x(\tau)\, e^{-j\omega\tau} d\tau \tag{3-13}$$

$H(\omega)$, $Y(\omega)$, and $X(\omega)$ are the Fourier Transform of $x(t)$, $y(t)$ and $h(t)$ respectively. By rearranging Equation (3-10), $H(\omega)$ can be obtained from a known output over a known input of the system in the frequency domain and formulated as follows:

$$FRF = H(\omega) = \frac{Y(\omega)}{X(\omega)} \tag{3-14}$$

Thus, the output of the system can be directly predicted with this $H(\omega)$ from any input given to the system. The output ($Y(\omega)$) of a system with a known $H(\omega)$ can be obtained by substituting $H(\omega)$ and the input ($X(\omega)$) into Equation (3-10).

In linear systems with multiple inputs and outputs, the dynamic behaviour of the system can be described as a combination of the subsystems' FRF which can be formed into a matrix. Each subsystem is treated as a "black box" that has a single

input ($X_n(\omega)$) and a single output ($Y_m(\omega)$). The element of the matrix is FRF of each subsystem. Mathematically, the equation can be written as follows:

$$\begin{bmatrix} Y_1(\omega) \\ Y_2(\omega) \\ \vdots \\ Y_m(\omega) \end{bmatrix} = \begin{bmatrix} H_{11}(\omega) & H_{12}(\omega) & \cdots & H_{1n}(\omega) \\ H_{21}(\omega) & H_{22}(\omega) & \cdots & H_{2n}(\omega) \\ \vdots & \vdots & & \vdots \\ H_{m1}(\omega) & H_{m2}(\omega) & \cdots & H_{mn}(\omega) \end{bmatrix} \begin{bmatrix} X_1(\omega) \\ X_2(\omega) \\ \vdots \\ X_n(\omega) \end{bmatrix} \tag{3-15}$$

where $X_n(\omega)$ is the Fourier Transform of the input-n ($x_n(t)$), $Y_m(\omega)$ is the Fourier Transform of the output-m ($y_m(t)$) and $H_{mn}(\omega)$ is the FRF of subsystems between Fourier Transform of $X_n(\omega)$ and $Y_m(\omega)$.

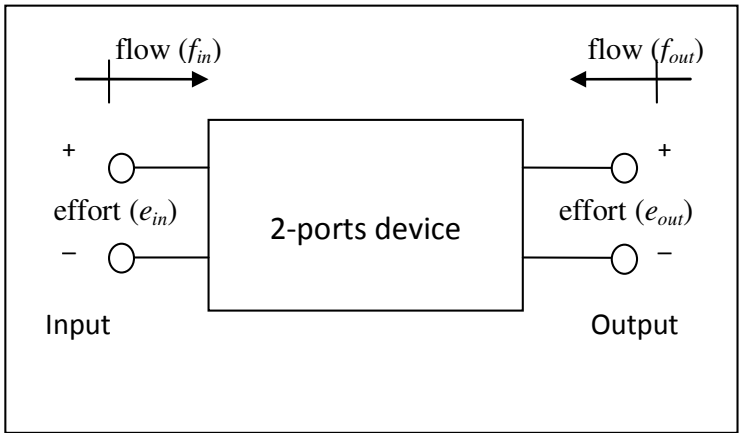

Figure 3-7 Schematic diagram of 2-ports, 4-poles system

An example of a multiple input-multiple output linear system is a 2-ports, 4-poles system (Figure 3-7). The two ports consist of an input port and an output port. Each port in the system has two poles. One pole represents the effort variable (e) and the other pole represents the flow variable (f). The system can be separated into 4 subsystems with 4 FRFs (Figure 3-8). Each FRF relates an input port's pole with an output port's pole. In theory, this relationship can be described by a 2x2 matrix as follows:

$$\begin{bmatrix} e_{in}(\omega) \\ f_{in}(\omega) \end{bmatrix} = [t] \begin{bmatrix} e_{out}(\omega) \\ f_{out}(\omega) \end{bmatrix} \tag{3-16}$$

$$\begin{bmatrix} e_{in}(\omega) \\ f_{in}(\omega) \end{bmatrix} = \begin{bmatrix} a_{11}(\omega) & a_{12}(\omega) \\ a_{21}(\omega) & a_{22}(\omega) \end{bmatrix} \begin{bmatrix} e_{out}(\omega) \\ f_{out}(\omega) \end{bmatrix} \tag{3-17}$$

The four elements of matrix are as follows:

$$a_{11}(\omega) = \left. \frac{e_{in}(\omega)}{e_{out}(\omega)} \right|_{f_{out}(\omega)=0} \tag{3-18}$$

$$a_{12}(\omega) = \left. \frac{e_{in}(\omega)}{f_{out}(\omega)} \right|_{e_{out}(\omega)=0} \tag{3-19}$$

$$a_{21}(\omega) = \left. \frac{f_{in}(\omega)}{e_{out}(\omega)} \right|_{f_{out}(\omega)=0} \tag{3-20}$$

$$a_{22}(\omega) = \left. \frac{f_{in}(\omega)}{f_{out}(\omega)} \right|_{e_{out}(\omega)=0} \tag{3-21}$$

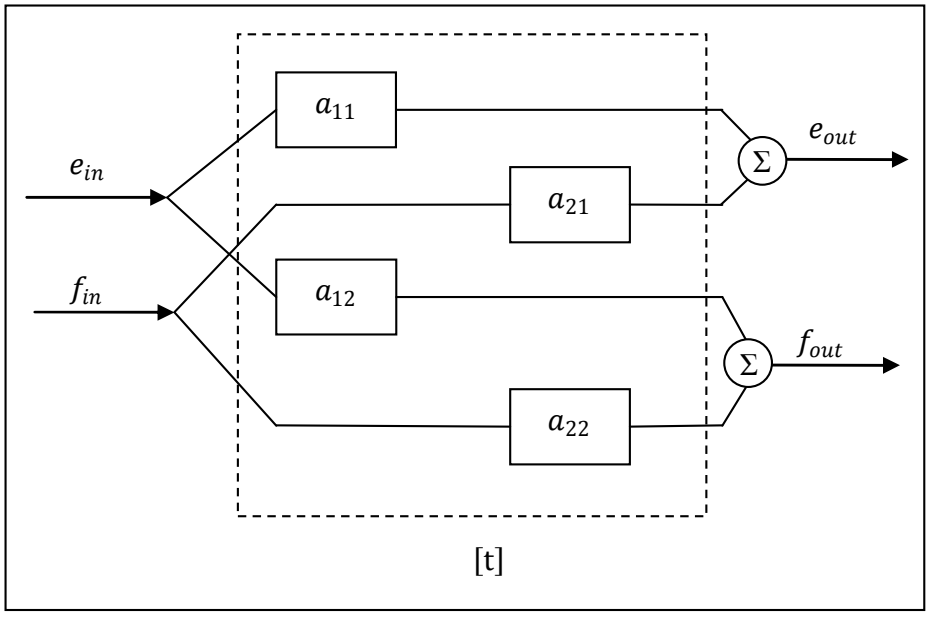

Figure 3-8 Structured FRF for 2-ports, 4-poles system

Each element of the matrix relates an input pole with an output pole and the rest of the output poles are assumed to be zero. Thus, the elements of the matrix in Equations (3-18) to (3-21) can be categorized into two conditions as follows:

a) a_{11} and a_{21} are obtained when the output flow variable is equal to zero (f_{out}=0).
b) a_{12} and a_{22} are obtained when the output effort variable is equal to zero (e_{out}=0).

In this researach, A brushed DC motor is assumed as a linear system with multiple inputs and outputs. The motor has two (2) electrical inputs, the voltage (E) and current (i). From this inputs, the motor produces two (2) mechanical output in the form of torque (T_m) and rotation speed (Ω_m). Equations (3-2) and (3-8) show that electrical input and mechanical output of the motor are linearly related. Thus, a brushed DC motor can be represented with a 2-ports and 4-pole system. The two poles of the input port are voltage (effort variable) and current (flow variable). The two poles of the output port are torque (effort variable) and rotation speed (flow variable) (Figure 3-9).

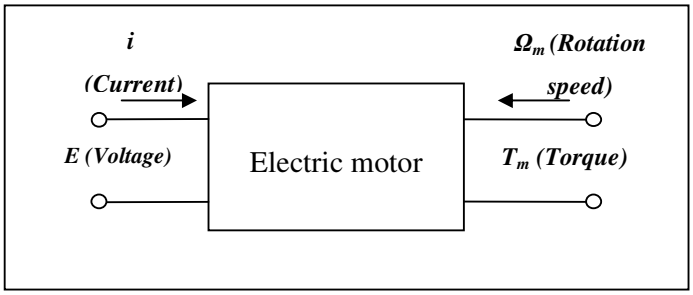

Figure 3-9 A 2-ports 4-poles model of electric motor

The relationship between the input variables and output variables of the motor can be described by the transduction matrix ([*t*]) in Equation (3-16). As the system represents a brushed DC motor which is operated under constant value (0 Hz), the elements of matrix (FRF) can be simplified into complex numbers at a frequency of 0 Hz. Therefore, the matrix is expressed as follows:

$$\begin{bmatrix} E(0) \\ i(0) \end{bmatrix} = \begin{bmatrix} t(0) \end{bmatrix} \begin{bmatrix} T_m(0) \\ \Omega_m(0) \end{bmatrix} \tag{3-22}$$

$$\begin{bmatrix} E(0) \\ i(0) \end{bmatrix} = \begin{bmatrix} t_{11}(0) & t_{12}(0) \\ t_{21}(0) & t_{22}(0) \end{bmatrix} \begin{bmatrix} T_m(0) \\ \Omega_m(0) \end{bmatrix} \tag{3-23}$$

The four elements of the matrix are as follows:

$$t_{11}(0) = \left. \frac{E(0)}{T_m(0)} \right|_{\Omega_m = 0} \tag{3-24}$$

$$t_{12}(0) = \left. \frac{E(0)}{\Omega_m(0)} \right|_{T_m = 0} \tag{3-25}$$

$$t_{21}(0) = \left. \frac{i(0)}{T_m(0)} \right|_{\Omega_m = 0} \tag{3-26}$$

$$t_{22}(0) = \left.\frac{i(0)}{\Omega_m(0)}\right|_{T_m=0} \tag{3-27}$$

where the elements of matrix are obtained under two boundary conditions. t_{11} and t_{21} are obtained by restricting the motor motion ($\Omega_m = 0$). t_{21} and t_{22} are obtained by allowing the motor to run freely ($T_m = 0$).

Each element of the matrix represents a transfer function of one electrical port and one mechanical port, where

- t_{11} represent the transfer function between the voltage and torque when the motor motion is restricted (clamp condition).
- t_{12} represent the transfer function between the voltage and rotational speed when motor motion is free running (free condition).
- t_{21} represent the transfer function between current and torque when motor motion is restricted (clamp condition).
- t_{22} represent the transfer function between current and rotational speed when motor motion is free running (free condition).

Since the matrix characterizes the transduction behaviour between the electrical input and mechanical output of electrical motor, it is termed as the "transduction matrix". [10, 56]

3.2. Identification of Transduction Matrix

In the previous section, the linearity of the brushed DC motor and how the linear relationship can be modelled by the transduction matrix were explained. The transduction matrix can be obtained theoretically or experimentally. Theoretically, the transduction matrix is obtained from the equivalent circuit of the brushed DC motor and its motor constants. The elements of the matrix are computed based on two aforementioned boundary conditions. Experimentally, the transduction matrix

is obtained based on the least square approximation of the measurement results. Both methods will be explained and compared.

3.2.1. Theoretical derivation of transduction matrix

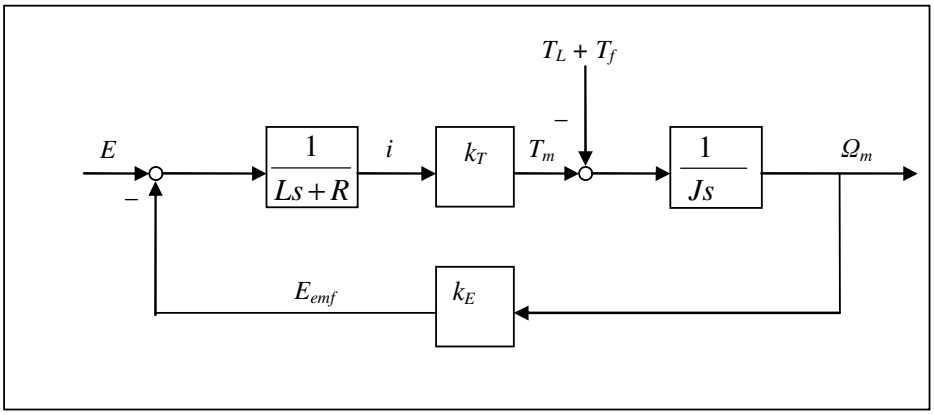

Figure 3-10 Block diagram of brushed DC motor

As mentioned in section 3.1.2, a brushed DC motor can be modelled as an equivalent circuit with a relationship as stated in Equation (3-3). To relate Equation (3-3) with the mechanical equation of the electric motor in Equation (3-5), Laplace Transform are applied to both equation and the motor constants in Equation (3-1) and (3-2) are used. The equations are arranged in a block diagram in Figure 3-10. With the block diagram, the transduction matrix can be evaluated under the two aforementioned boundary conditions stated previously:

1. The rotational speed is equal to zero ($\Omega_m = 0$)
    a. No back-EMF voltage is induced induced ($E_{emf} = 0$) as the relationship between rotational speed and back-EMF voltage is direct as seen in Equation (3-1).
    b. There is no torque to overcome the motor's inertia ($J_{motor}\frac{d\Omega_m}{dt} = 0$). Note that T_m is not equal to zero as the friction *(T_f)* and motor loading *(T_L)* have to be overcome as well.

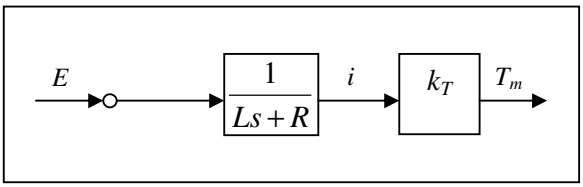

Figure 3-11 Simplified block diagram based on zero rotational speed

Based on these two conditions stated above, the block diagram can be simplified as shown in Figure 3-11. The relationships between mechanical and electrical ports of the motor in Figure 3-11 are as follows:

$$T_m = \frac{k_T}{Ls+R}E \qquad \text{and} \qquad T_m = k_T i \tag{3-28}$$

The elements for first column of transduction matrix are as follow

$$t_{11} = \frac{E}{T_m} = \frac{Ls+R}{k_T} \tag{3-29}$$

$$t_{21} = \frac{i}{T_m} = \frac{1}{k_T} \tag{3-30}$$

2. The torque produced by the motor is assumed to be zero ($T_m = 0$)
   a. The motor is assumed to be running at a no-load speed ($\Omega_m = \Omega_{no-load}$) and no extra torque is needed to accelerate the motor ($J_{motor}\frac{d\Omega_m}{dt} = 0$).
   b. The current is equal to zero ($i = 0$) due to relationship between motor torque and current as shown in Equation (3-2).

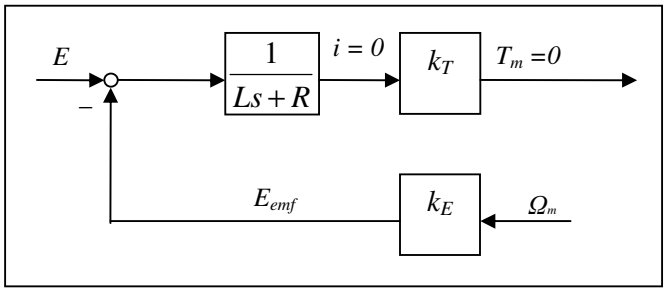

Figure 3-12 Simplified block diagram of DC motor based on zero torque

Based on the two conditions, the block diagram can be simplified as shown in Figure 3-12. The relationships between mechanical and electrical port of the motor based on the figure are as follows

$$E - E_{emf} = 0 \qquad \text{and} \qquad E = E_{emf} = k_E \Omega_m \tag{3-31}$$

Based on these relationships, the elements for second column of transduction matrix are as follows:

$$t_{12} = \frac{E}{\Omega_m} = k_E \tag{3-32}$$

$$t_{22} = \frac{i}{\Omega_m} = 0 \tag{3-33}$$

By rearranging the elements of the matrix (Equations (3-29), (3-30), (3-32), and (3-33)) and replacing *s* with *jω*, the transduction matrix is formed as follows:

$$[t] = \begin{bmatrix} t_{11} & t_{12} \\ t_{21} & t_{22} \end{bmatrix} = \begin{bmatrix} \dfrac{j\omega L + R}{k_T} & k_E \\ \dfrac{1}{k_T} & 0 \end{bmatrix} \tag{3-34}$$

Equation (3-34) shows that the matrix is a combination of the motor's inductance (*L*), resistance (*R*), and motor constants (k_E and k_T). These properties are usually provided by the motor's manufacturer.

3.2.2. Experimental identification of transduction matrix

Experimentally, the condition of null rotational motion of motor ($\Omega_m = 0$) can be restricted by placing a very high load on the motor ($T_m = \infty$). However, this is not advisable as the motor will draw a high current and may become damaged from overheating. To overcome this difficulty, another approach is used to identify the transduction matrix experimentally. As can be seen from the transduction matrix

in Equation (3-22), electrical input (E and i) and mechanical output (T_m and Ω_m) of the brushed DC motor are linearly related. When there is n-number of E, i, T_m, and Ω_m, the transduction matrix ([t]) will still be a single solution 2x2 matrix which can relate them. This relationship is written as follows:

$$\begin{bmatrix} E_1(0) & E_2(0) & \cdots & E_n(0) \\ i_1(0) & i_2(0) & \cdots & i_n(0) \end{bmatrix} = [t] \begin{bmatrix} T_{m1}(0) & T_{m2}(0) & \cdots & T_{mn}(0) \\ \Omega_{m1}(0) & \Omega_{m2}(0) & \cdots & \Omega_{mn}(0) \end{bmatrix} \tag{3-35}$$

Or

$$[Input_{elec}] = [t][Output_{mech}] \tag{3-36}$$

where $Input_{elec}$ represents the set of electrical data of the motor ($E_1(0)$ to $E_n(0)$ and $i_1(0)$ to $i_n(0)$)

$$[Input_{elec}] = \begin{bmatrix} E_1(0) & E_2(0) & \cdots & E_n(0) \\ i_1(0) & i_2(0) & \cdots & i_n(0) \end{bmatrix} \tag{3-37}$$

and where $Output_{mech}$ represents the set of mechanical data of the motor ($T_{m1}(0)$ to $T_{mn}(0)$ and $\Omega_{m1}(0)$ to $\Omega_{mn}(0)$).

$$[Output_{mech}] = \begin{bmatrix} T_{m1}(0) & T_{m2}(0) & \cdots & T_{mn}(0) \\ \Omega_{m1}(0) & \Omega_{m2}(0) & \cdots & \Omega_{mn}(0) \end{bmatrix} \tag{3-38}$$

It is not possible to obtain by experiments a single value of [t], satisfying Equation (3-36), due to the presence of experimental errors. Thus, the least squares method is employed to calculate an approximate solution to [t] as follows:

$$[t] = \left([Output_{mech}]^t [Output_{mech}] \right)^{-1} [Output_{mech}]^t [Input_{elec}] \tag{3-39}$$

where [t] in Equation (3-39) is an approximate solution. By increasing the number of data (n), the accuracy of the obtained transduction matrix can be improved.

3.2.3. Verification of the transduction matrix with the Matlab Simulink

A Simulink model is constructed to prove that the transduction matrix is able to relate the electrical input and mechanical output of a brushed DC motor. The model is constructed according to the block diagram shown in Figure 3-13. The voltage value (E) of model is set to 24 V and the other values of the electric motor component (L, R, k_T and k_E) are applied based on Appendix A. Mathematically, the transduction matrix of motor is obtained by substituting the L, R, k_T, k_E and $\omega = 0$ (DC power) into Equation (3-34) as follows:

$$[t] = \begin{bmatrix} 0.0446 & 10.634 \\ 0.138 & 0 \end{bmatrix} \tag{3-41}$$

The friction torque is assumed to be zero ($T_f = 0$) and T_L increases proportionally with the rotational angle of the motor ($T_L = K_{load}\theta_m = 50\theta_m$). The torque, rotational speed, current and voltage of the motor are recorded for 400 data point and stored in the Matlab workspace. Figures 3-14 to 3-17 show the recorded torque, rotational speed, voltage and current.

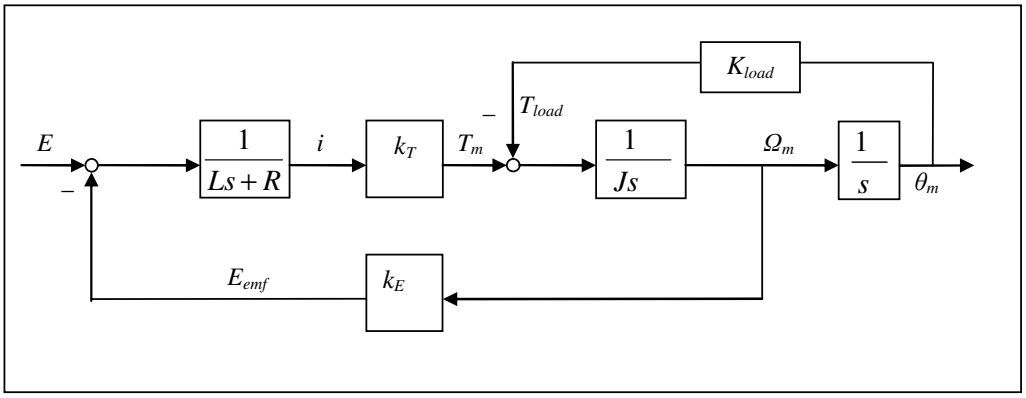

Figure 3-13 Block diagram model for simulink

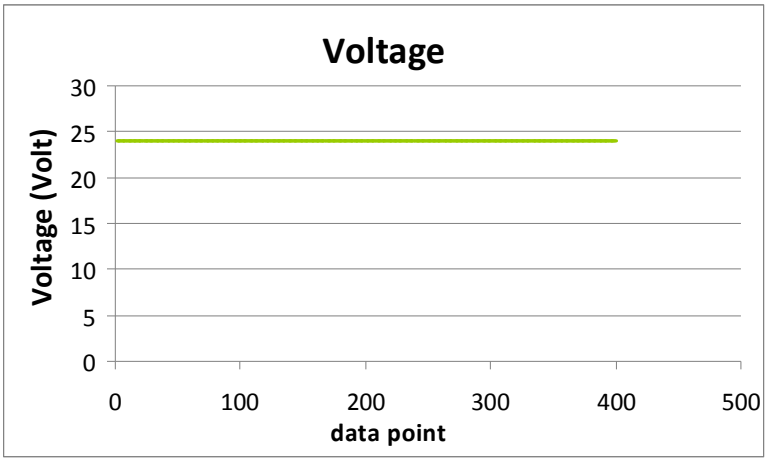

Figure 3-14 Voltage obtained from Simulink model of electric motor

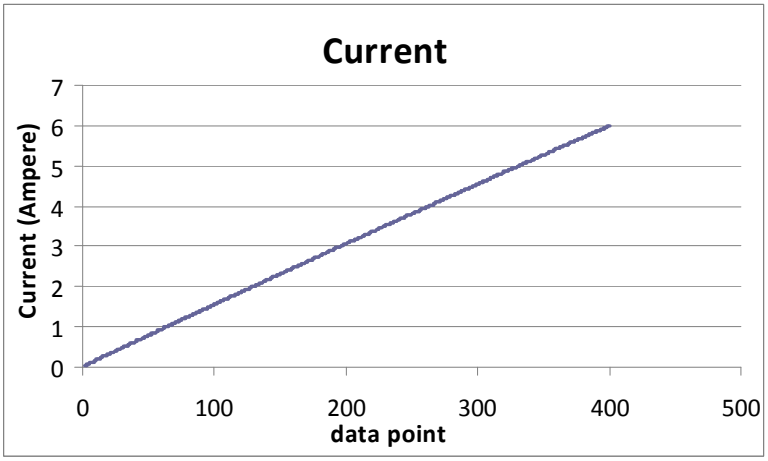

Figure 3-15 Current obtained from Simulink model of electric motor

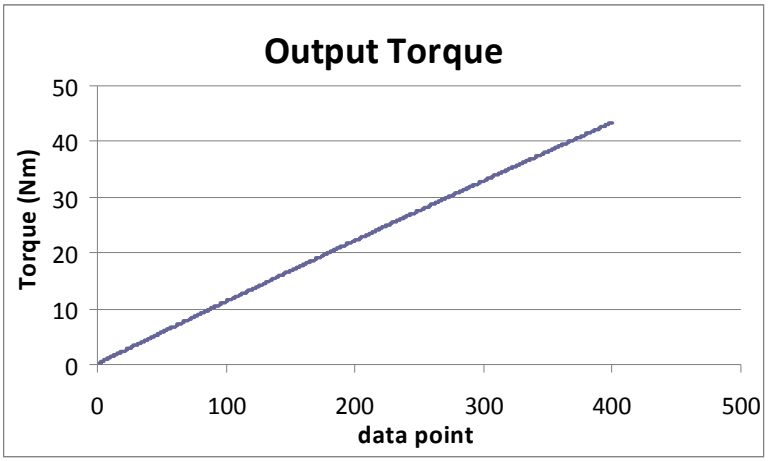

Figure 3-16 Output torque obtained from Simulink model of electric motor

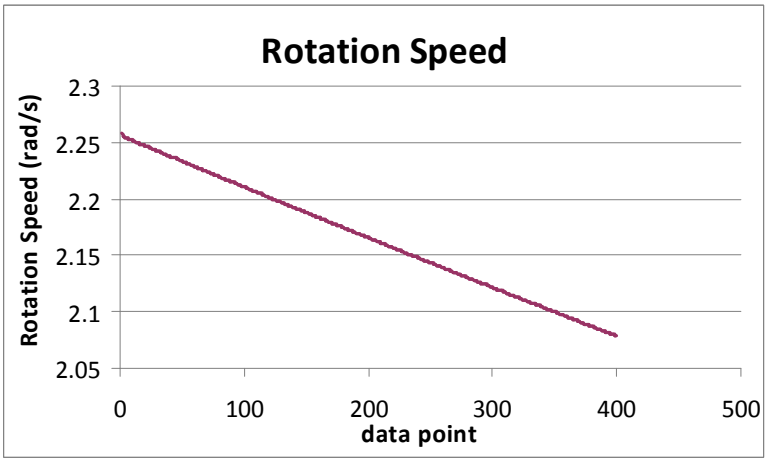

Figure 3-17 Rotation speed obtained from simulink model of electric motor

By substituting the recorded torque, rotational speed, voltage and current into Equation (3-39), the transduction matrix is calculated as follows:

$$[t] = \begin{bmatrix} 0.0446 & 10.634 \\ 0.138 & 0 \end{bmatrix} \tag{3-41}$$

It can be seen that the transduction matrix obtained from the Simulink model (Equation (3-41)) matches the transduction matrix obtained from the equivalent circuit of the motor (Equation 3-40). Thus, the transduction matrix's ability to

relate the electrical input and mechanical output of the motor is proved. By substituting the electrical input of the motor model into the transduction matrix in Equation (3-40), the mechanical output can be predicted. In the next section, transduction matrix of a brushed DC motor will be identified experimentally. The motor parameters are shown in Appendix A and Equation (3-39) is used to calculate the transduction matrix.

3.3. Experimental Calibration of Transduction Matrix

3.3.1. Experimental setup

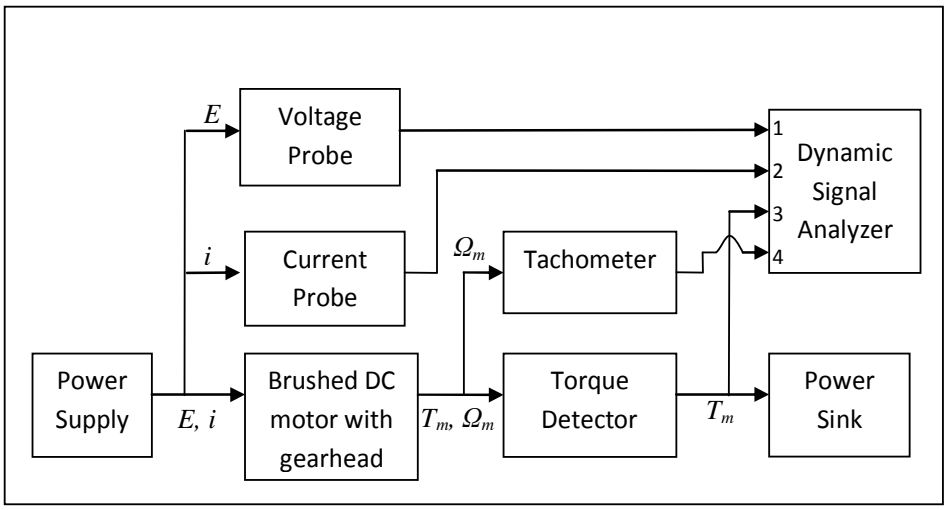

Figure 3-18 Schematic diagram for experimental setup

The experimental setup used to obtain the transduction matrix of a chosen brushed DC motor is shown in Figure 3-18. The setup consists of a power supply, a DC motor with a gearhead, a voltage probe, a current probe, a torque detector, a tachometer, a power sink and a dynamic signal analyzer. The specifications of the equipment used for the experiment can be found in Appendix A. The motor is powered by a 24 V power supply (E =24 V) and its current is limited at 12 A (i_{max} =12 A) for overcurrent protection. At the applied voltage, the motor runs at a constant speed (Ω_m = constant) and generates a torque (T_m). The power sink is

installed at the motor's output to generate resistance torque on the motor. The voltage and current probes are used to measure the E and i. The torque detector and tachometer are used to measure the T_m and Ω_m. All the four parameters (T_m, Ω_m, E and i) are sampled and recorded with the dynamic signal analyzer.

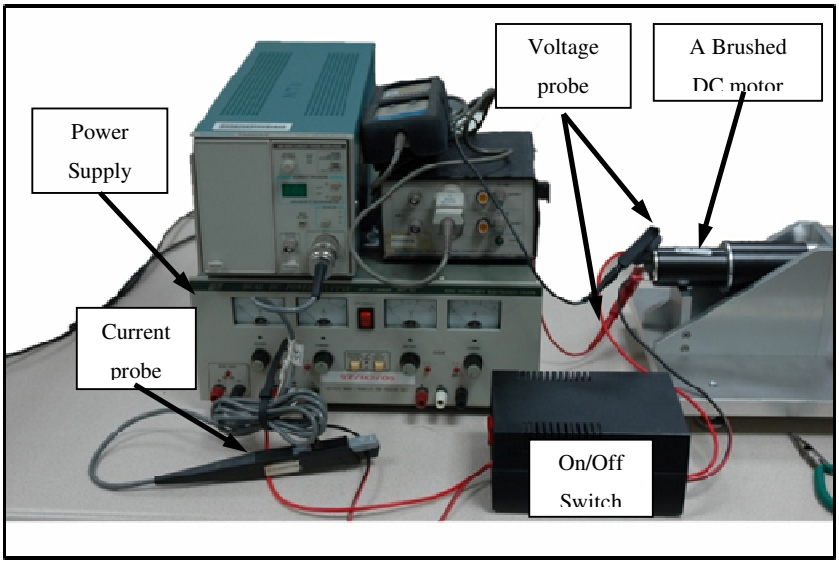

Figure 3-19 Current and voltage probe

The setup of the voltage and current probes is shown in Figure 3-19. The motor is connected with a power supply and on/off switch thru two power cable (red cable and red/black cable). The red cable is connected to positive terminal of the motor and the black cable is connected to negative terminal. The voltage probe is clipped to the terminal of the motor. The voltage probe consists of a pair of clips (red and black colour clips). The red clip is connected to the positive terminal of the motor and the black clip is connected to the negative terminal. The current probe is clamped around in either one the power cable. There is an arrow direction located at the current probe. The arrow direction must be positioned in the direction of current flow to obtain the correct sign for the current signal. The outputs of voltage and current probes are connected to dynamic signal analyzer.

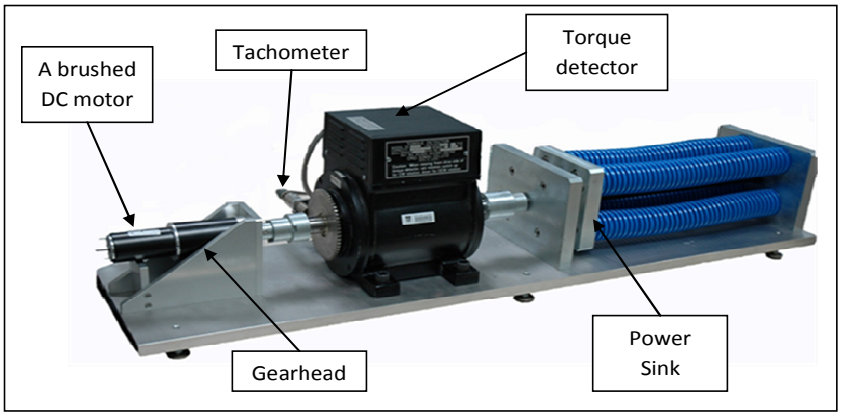

Figure 3-20 Equipment setup for torque detector and tachometer

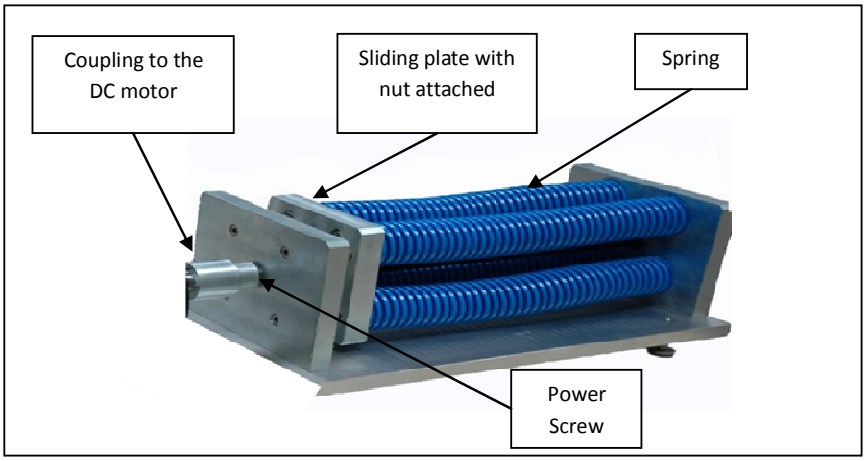

Figure 3-21 Load Torque

The setup for the torque detector and tachometer are shown in Figure 3-20. The selected brushed DC motor with a gearhead is coupled with the torque detector with uses of a coupling. The tachometer is attached at the side of torque detector. The torque detector is coupled with a custom-made power sink to provide load to the motor. The power sink uses a power screw to transform the rotary motion into linear motion (Figure 3-21). As the motor turns the power screw, the nut is moved in a linear direction. Since the sliding plate is attached to the nut, it will move together with the nut to compress the springs. Due to the compression, the springs provide a resistance load on the shaft of the motor. This resistance load is an

incremental torque that can be calculated using the power screw formula as shown:

$$T = \frac{FD_p}{2}\left(\frac{L_{screw} + \pi f_{screw} D_p}{\pi D_p - f_{screw} L_{screw}}\right) \tag{3-42}$$

where D_p is the pitch diameter of power screw, L_{screw} is lead length of the screw and f_{screw} is friction coefficient.

As the force (F) is exerted by compressed springs with stiffness k_{spring},

$$F = k_{spring} x \tag{3-43}$$

Hence, the load torque can be calculated as follows:

$$T = \frac{k_{spring} D_p}{2}\left(\frac{L_{screw} + \pi f_{screw} D_p}{\pi D_p - f_{screw} L_{screw}}\right) x \tag{3-44}$$

All the quantities in Equation (3-44) (D_p, L, f, and k) are known value (constant) except for the displacement of the springs, (x). Hence, this power sink supplies the load torque to the motor that is proportional to the displacement of springs. The equation shows that as the power screw turns, the plate travels further to compress the springs and the motor generates a higher torque.

3.3.2. Experimental procedure

The experiment is started by supplying a 24 V DC current to the motor. With this voltage, the motor runs at 19.631 RPM (Ω_m = 2.0547 rad/s) to move the sliding plate. The sliding plate compresses the spring and torque is supplied by the motor shaft. The measurement stops when the springs are fully compressed. The voltage is cut off from the motor immediately to avoid overloading. The four parameters are sampled and recorded with a sampling frequency of 2000 Hz. The chosen sampling frequency has to be high enough to avoid aliasing. The data points of

each recorded signal are 16,000 points/sample which is sufficient to capture the entire process. A low pass digital filter with cut-off frequency at 10 Hz is employed to remove any high frequency noise from the recorded signal.

3.3.3. Experimental results

Voltage (V)	**Current (A)**	**Torque (Nm)**	**Rotational speed (rad/s)**
22.93	1.5872	9.5329	2.1338
23.456	1.7755	10.508	2.2084
23.267	1.9758	11.751	2.1943
23.432	2.0602	12.666	2.2043
22.906	2.2745	14.587	2.0685
23.398	2.3133	14.453	2.2075
23.303	2.4838	15.676	2.1293
22.907	2.5745	16.847	2.0763
22.886	2.7907	18.365	2.0726
23.226	2.9567	18.789	2.1288
23.339	3.1554	20.577	2.1362
23.49	3.3855	22.656	2.157
23.354	3.5379	23.048	2.1386
22.796	3.6786	24.213	2.0356
23.123	3.8606	24.998	2.0672
22.794	3.884	25.579	2.0115
23.502	4.1023	27.343	2.0932
22.791	4.2125	28.074	2.0059
23.298	4.4539	29.73	2.0743
23.489	4.5985	30.691	2.101
23.492	5.4391	35.768	2.0367

Table 3-1 Measurement results in experimental calibration of transduction matrix

Table 3-1 shows 20 samples from the measurement results. The measurement results are plotted in Figures 3-22 to 3-25. It can be seen that the torque increases from 10 Nm when the motor starts to 40 Nm when the spring is fully compressed. During this process, an increase in current from 1.7 to 6 A can be observed. The values of the voltage and rotational speed remain almost constant. The torque, rotational speed, voltage and current are measured with 16,000 data points. These data points are substituted into Equation (3-39) to obtain the transduction matrix as follows:

$$[t] = \begin{bmatrix} 0.0566 & 10.4075 \\ 0.1419 & 0.1109 \end{bmatrix} \tag{3-45}$$

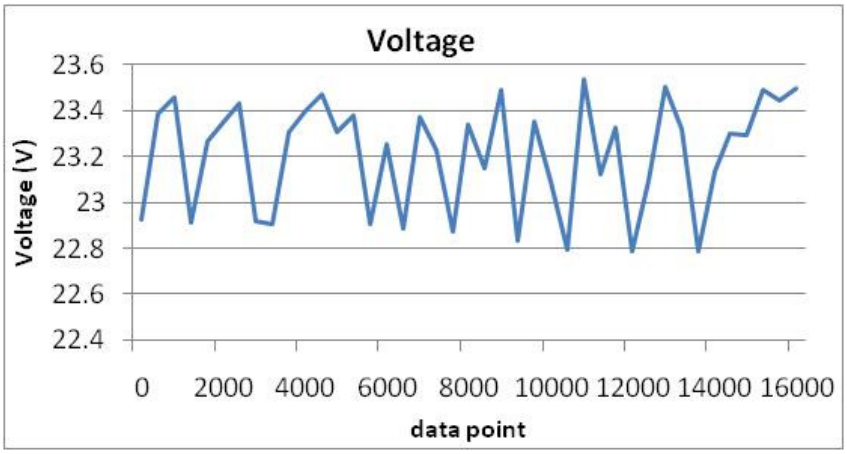

Figure 3-22 Voltage based on measurement

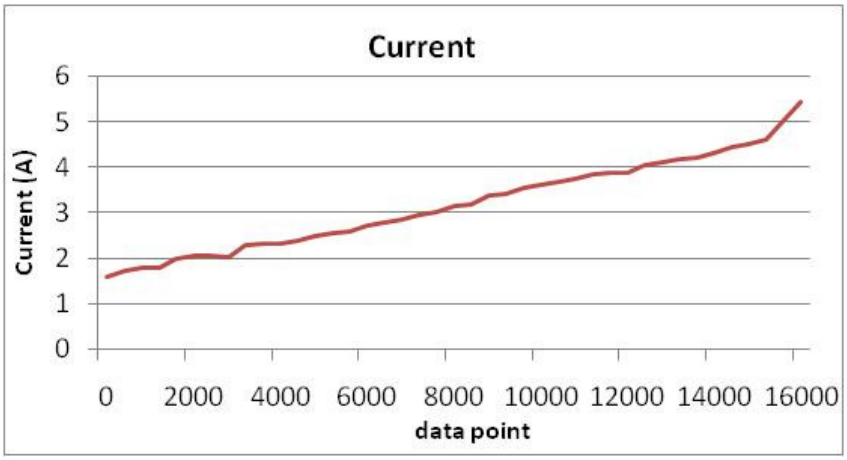

Figure 3-23 Current based on measurement

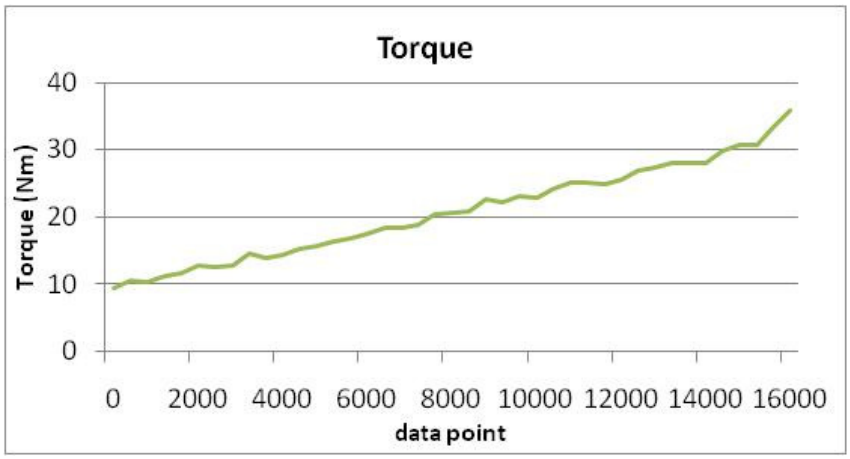

Figure 3-24 Torque based on measurement

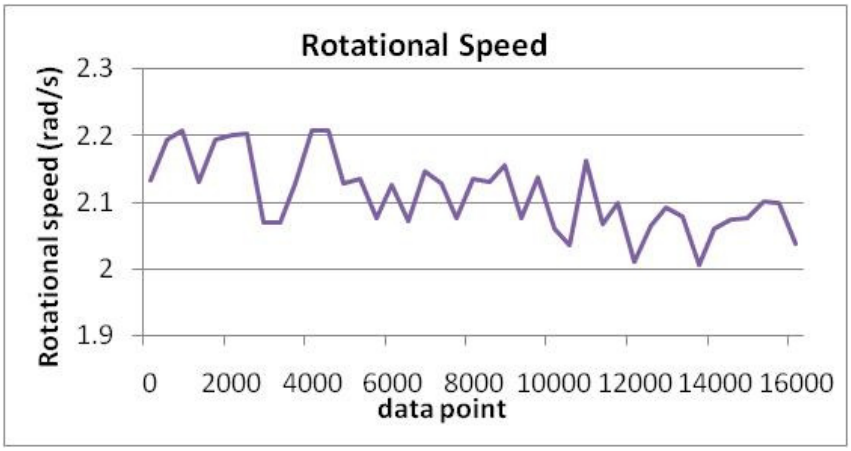

Figure 3-25 Rotational speed based on measurement

This transduction matrix in Equation (3-45) differs from the one in Equation (3-41), especially for the value of t_{22}. The t_{22} from the Equation (3-45) is 0.1109 instead of zero in Equation (3-41). This difference may be explained by the assumption made in the derivation of the transduction matrix in Equation (3-41) that there is zero friction in the motor (T_f=0). In reality, friction arises, for instance, from the viscosity of the air gap and electromagnetic field. Hence, the value of t_{22} is actually not zero.

The second row of the transduction matrix in Equation (3-34) shows that the current of the motor is equal to the motor's torque (T_m) multiplied by the motor constant (k_T) and zero rotational speed. Mathematically, this is written as follows:

$$[i] = \begin{bmatrix} \frac{1}{k_T} & 0 \end{bmatrix} \begin{bmatrix} T_m \\ \Omega_m \end{bmatrix} \tag{3-46}$$

It can be seen from Equation (3-7) that T_m consists of both T_f and T_L. Equation (3-7) is substituted into Equation (3-46) as follows:

$$i = \frac{\left(T_f + T_L\right)}{k_T} + 0\left(\Omega_m\right) \tag{3-47}$$

If T_f is not zero and a function of rotational speed, it can be formulated as follows:

$$T_f\left(\Omega_m\right) = B\Omega_m \tag{3-48}$$

where B is the friction coefficient.

By substituting Equation (3-48) into Equation (3-47), the transduction matrix in Equation (3-34) is as follows:

$$[t] = \begin{bmatrix} t_{11} & t_{12} \\ t_{21} & t_{22} \end{bmatrix} = \begin{bmatrix} \dfrac{j\omega L + R}{k_T} & k_E \\ \dfrac{1}{k_T} & \dfrac{B}{k_T} \end{bmatrix} \tag{3-49}$$

It can thus be seen that t_{22} is not zero.

A comparison of the results is done to prove that the transduction matrix in Equation (3-45) is more accurate than Equation (3-41). The voltage and current from Table 3-1 are substituted into Equations (3-45) and (3-41) to obtain the torque and rotational speed for each equation. The torque and rotational speed so obtained are compared with the torque and rotational speed in Table 3-1, as shown in Figures 3-26 and 3-27. It can be seen from Figures 3-26 and 3-27 that the torque calculated from Equation (3-41) has a higher value compare to the others. The torque calculated from Equation (3-45) shows a similar result with the measured torque. The results of the comparison for rotational speed are similar.

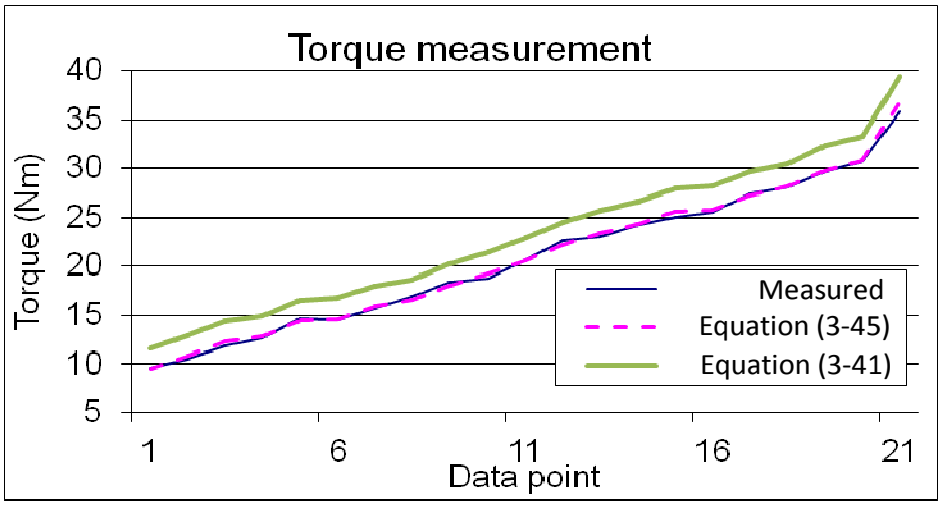

Figure 3-26 Comparison of torque

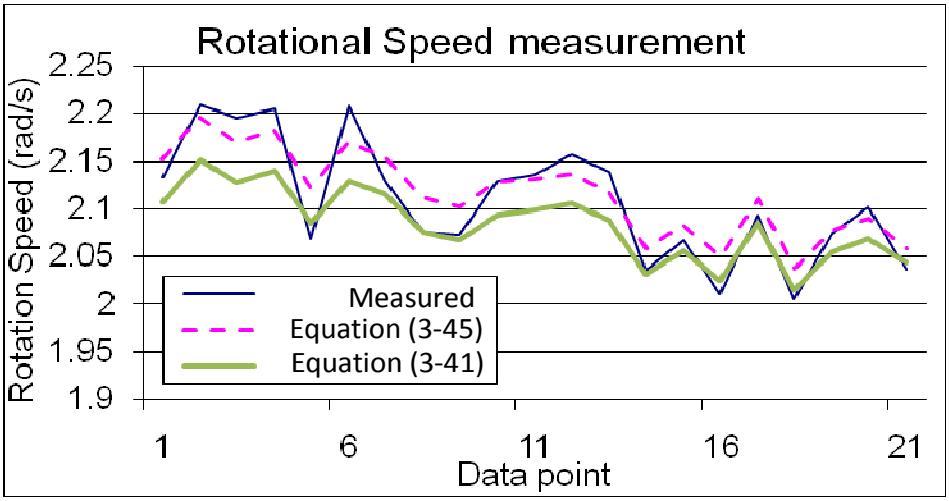

Figure 3-27 Comparison of rotation speed

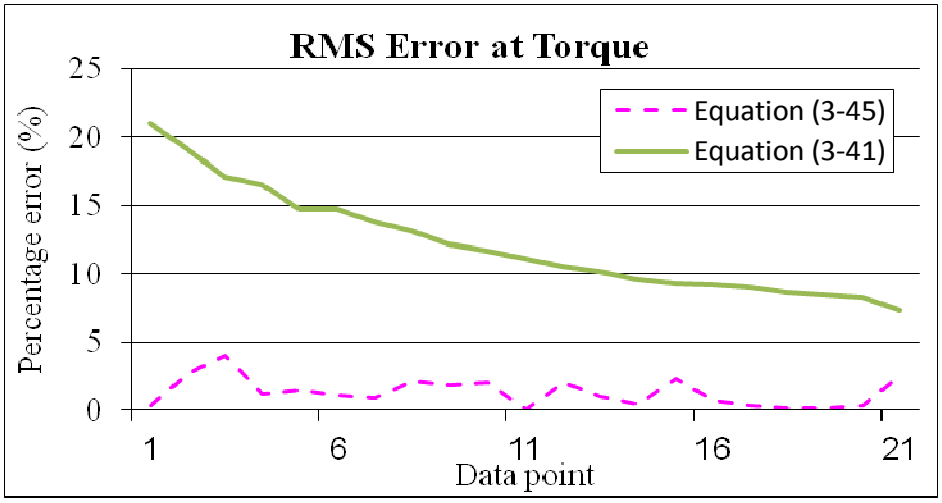

Figure 3-28 Normalized RMS error at torque

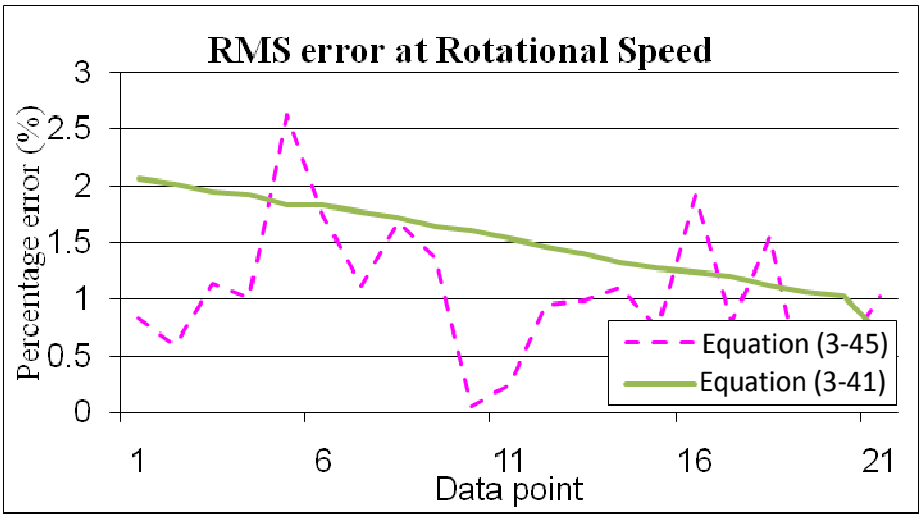

Figure 3-29 Normalized RMS error at rotational speed

To calculate the error of the transduction matrix for Equations (3-45) and (3-41), the normalized root mean square (RMS) error for both are calculated and the plotted in Figures 3-28 and 3-29. Taking the average of the normalised error, it can be seen that the RMS error of the torque calculated from Equation (3-45) is 1.32% and Equation (3-41) is 12.18%. The RMS error of the rotational speed calculated from Equation (3-45) is 1.06% and Equation (3-41) is 1.51%.

Therefore, it is concluded that the transduction matrix obtained in Equation (3-45) can be used in this thesis to calculate the torque and rotational speed of motor.

The errors of the torque calculated from Equation (3-41) arise mostly from the torque's offset value, which is the friction torque (T_f). It can be seen from Equation (3-7) that T_m consists of both T_f and T_L. In the experimental condition, the torque measured by the torque meter is T_L, while T_f is immeasurable. Thus, the torque calculated from Equation (3-41) is bigger than the experimental torque because the torque calculated from Equation (3-41) is T_m whereas the experimental torque is T_f.

3.4. Summary

A brushed DC motor transduces the supplied electrical power into mechanical power. Voltage and current supplied to the motor are transformed into the form of torque and shaft rotation. As the motor uses a permanent magnet in the stator and the electrical power is directly supplied to the rotor, the relationship between electrical power and mechanical power is linear which can be shown by Equation (3-1) and Equation (3-2). Thus, transduction behaviour of brushed DC motor can be described with a transduction matrix.

The transduction matrix is a 2x2 transfer matrix with each of its four elements is a FRF that linearly relate an input pole with an output pole in frequency domain. The matrix can be obtained by the theoretical or experimental method. For a brushed DC motor, its transduction matrix is obtained theoretically from an equivalent electric circuit of the motors and motor constant by applying two boundary conditions to the motor. The matrix is obtained experimentally by calculations from the experimental measurements of the electrical input and mechanical output of the motor based on Equation (3-39). A brushed DC motor with known transduction matrix can be used as a self-sensing actuator. Mechanical output of the motor (torque and rotational speed) can be calculated from its electrical input (voltage and current) with help of Transduction matrix in

real time. Thus, the matrix helps in reduction the usage of mechanical sensor that is bulky and space constraint and enabling real time measurement of torque and rotational speed.

In this project, a brushed DC motor (motor specifications is listed in Appendix A) has been calibrated to obtain its transduction matrix. The transduction matrix is obtained theoretically and experimentally. A comparison both matrixes show that there is less error in the calculation of the mechanical output of the DC motor in the matrix in Equation (3-45) (mean error of 1.32%) than the matrix in Equation (3-40). Thus, transduction matrix in Equation (3-45) is employed for an in-process measurement of the tightness of bolted joints with the motor. The motor's torque and rotational speed applied to the bolted joints can be calculated from the motor's input electrical during the tightening process with the help of the transduction matrix from Equation (3-45).

CHAPTER 4
TIGHTNESS ASSESSMENT OF BOLTED JOINTS

The tightness of a bolted joint is an important parameter in its design. The tightness, which depends on the clamping force, quantifies the resistance of the bolted joint under loading. The clamping force should be higher than the load to withstand it but should not be too high such as to cause the breakage at the joint. Thus, it is necessary to measure the clamping force needed to tighten the bolted joint accurately.

In the previous chapter, the transduction matrix, which relates the electrical input with the mechanical output of a brushed DC motor, was introduced. The transduction matrix plays a major role in the development of a novel method to measure the torque and rotational speed outputted by a motor-driven mechanical system indirectly without the use of conventional force and motion sensors. This chapter reports on the use of such a method to measure the tightness of bolted joints tightened with a DC motor. The transduction matrix facilitates the measurement of the torque and rotation speed during tightening.

Section 4.1 explains the tightening method used in industries and their advantages and disadvantages. Section 4.2 presents the setup and procedure used to develop the brushed DC motor into a real time tightness measurement tool for in-process tightening of the bolted joints. Section 4.3 discusses the measurement results acquired based on this novel method. Section 4.4 introduces and discusses a new tightening indicator observed from the measurement results. Section 4.5 summarizes this chapter.

4.1. Tightening method

Bolted joints are fastener elements that can withstand high working loads and are re-usable. They are tightened by turning the nut relative to the bolt to clamp the

jointed members. This process places the bolt under tension and generates a clamping force at the jointed members. The clamping force is normally equal in value to the preload (tension force) on the structures to be fastened, indicating that the jointed members are intact. Thus, the objective in the tightening process is to generate sufficient preload at the bolt to clamp the jointed members through several tightening methods. This section discusses the different tightening methods based on their indicator.

4.1.1. Tightening method based on torque

Torque is the least expensive and easiest way to control tightness at the bolted joints because it is considered an input to the bolted joints. When the bolted joints are tightened, torque is applied to turn the bolt and generate preload. The tightening process stops when torque reaches a certain value, because it is assumed that the bolt has attained the desired tightness (preload). The torque's value is derived from the linear relationship between the torque (T) and the preload (P), which is expressed as follows:

$$T = P \times C \tag{4-1}$$

Experimental and theoretical analyses have defined the constant (C) in two known equations, which are:

$$T_{in} = K \times D \times P \tag{2-5}$$

and

$$T_{in} = P\left(\frac{p}{2\pi} + \frac{\mu_t r_t}{\cos\alpha} + \mu_n r_n\right) \tag{2-6}$$

In both equations, C is derived into several parameters based on the bolt geometry and coefficient of friction.

Equation (2-5), known as the short-form equation, shows that the relationship between torque and preload is governed by the bolt diameter (D) and nut factor (K). This equation is used for practical application as the nut factor, a single constant, represents all the factors that affect the torque and preload relationship. The nut factor is determined experimentally and its value varies for each application. In fact, many investigators have found that the nut factor obtained from a sample or prototype joint differs significantly from that obtained from the actual joint. This discrepancy may be caused by the conditions of the threads, the lubricant used, operator skill, bolting procedure and the coefficient of friction.

Equation (2-6), known as the long-form equation, shows that the torque given to the bolted joint is resisted by three reaction torques. They are the bolt stretching torque, the frictional torque between the nut threads and bolt threads, and the frictional torque between the nut surfaces with joint surfaces. The combination of Equations (2-5) and (2-6) shows the relationship between the nut factor (K), the bolt geometry (r_t, r_n, p, and D) and the coefficient of friction (μ_n and μ_t). The combined equation is written as follows:

$$K = \frac{p}{2\pi D} + \frac{\mu_t r_t}{cos\alpha D} + \frac{\mu_n r_n}{D} \tag{4-2}$$

Where the bolt is of the same size, D, r_n, r_t and p are constant, the coefficient of friction is the only factor which affects the value of the nut factor. Thus, for bolts of the same size, the relationship between the torque and the preload is also affected by the coefficients of friction.

Several laboratory tests have shown that coefficient of friction of a single material varies significantly. The coefficient of friction between heavily loaded metal surfaces coated with molydisulfide lubricants ranges from 0.026 to 0.273 based on measurements by the Brookhaven National Laboratories [57]. This variation in the coefficient of friction affects the accuracy of the predicted preload when torque is used as an indicator.

Besides the coefficient of friction, there are other factors such as bolt geometry, strain energy loss, hole interference, frequency of tightening and retightening which affect the relationship between torque and preload. These factors also affect the accuracy of the preload produced by torque. This means, even though the input torque to the bolted joint can be measured accurately, the preload at the joint may still vary due to the aforementioned factors. Several strategies, in the tightening of the bolted joints with torque, are used to compensate for those factors:

a) The value of the tightening torque is considered based on minimum-maximum range of the nut factor and desired preload. Normally, the supplier of the fastener material and coating will provide the minimum, mean, and maximum values of the nut factor of the material. The torque value is calculated from the mean value of the nut factor and the desired preload. The minimum and maximum values of the nut factor are used to calculate the minimum and maximum preload achieved under the calculated torque. The sufficiency of the maximum and minimum preload values to avoid joint failure is then considered.
b) Lubricant is applied to reduce the preload scatter. Before tightening, it is suggested that lubricant should be applied to the surface at the bolt and nut to reduce their friction. A lubricated surface reduces uncertainties at bolted joint and scatter in the preload generated.

4.1.2. Tightening method based on turning angle

The turning angle is the other input to bolted joints beside torque. When torque is applied to the nut, the nut is simultaneously turned relative to the bolt. This turning causes the nut to advance linearly with a linear displacement equal to exactly one pitch of the threads in one rotation. When the bolt is stretched, we can assume that the linear stretch of bolt behaves similarly. Thus, the stretch amount of the bolt can be predicted from the turning angle. The angle can be used as the control parameter for bolted joints to indicate when the tightening process should

be stopped. Equation (2-3) can be used to calculate the preload generated at the bolted joint from the turning angle. However, it is noted that the initial turns of the nut will not stretch the bolts. Thus, the relationship of the preload and turning angle is not linear at the beginning of the stretch (Figure 2-6). To overcome this problem, the nut is first tightened to a certain degree of torque before it is further tightened by the desired turning angle.

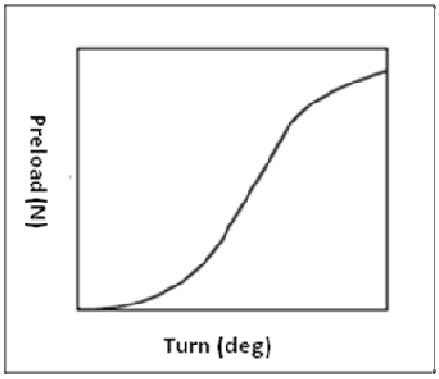

Figure 2-6 The preload vs Angle of turn graph [2]

Usually, the relationship between the turn and preload is one that is depicted by a S-shaped curve as shown in Figure 2-6. However, the shape of curve may be different due to several factors:

a) Sheet metal joint

   When the joint members are very thin, they become very stiff. This causes a sudden vertical rise in the turning angle-preload relationship, shown in Figure 4-1. The sudden rise causes a problem when tightening the joint at high speed. The preload value can increase suddenly and cause the joint to break.

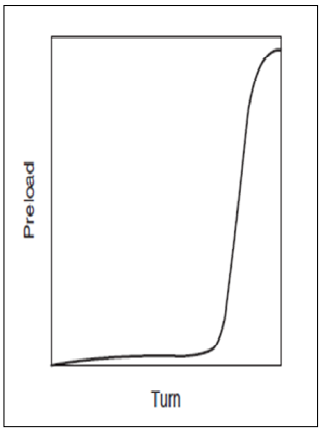

Figure 4-1 Turn-preload curve for tightened a sheet metal [2]

b) Gasketed joint

The tightening process of a gasketed joint normally is divided into several stages to permit the gasket to relax and prevent damage. Due to the relaxation of the gasket, the preload drops after some time. Thus, the curve showing the relationship of turn and preload resembles the teeth of a saw (Figure 4-2), and is thus an additional weakness of using turning angle to predict preload.

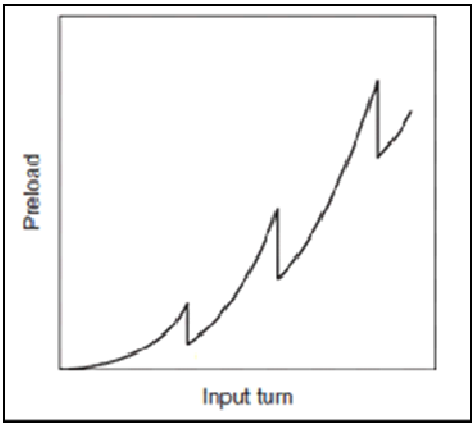

Figure 4-2 Turn-preload curve for gasketed joint [2]

c) Reference of measurement

The reference of measurement of the turning angle affects the turning angle-preload curve. Equation (2-3) assumes that the measured angle is the

relative angle between the nut and bolt. In practice, however, the measured angle is usually the relative turn between the nut and the machine or some other fixed reference. Due to the slippage between the bolt and the fixed frame (machine), the turning angle-preload curves may vary for each tightening process (Figure 4-3).

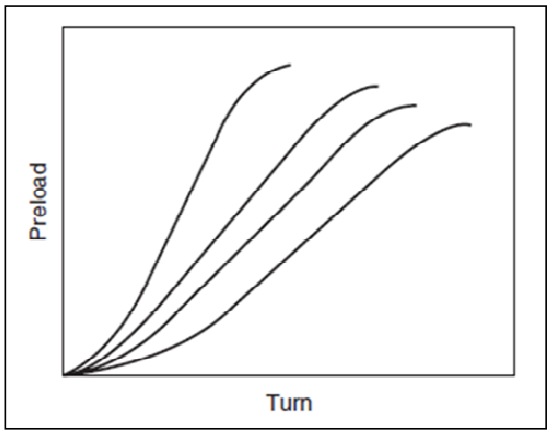

Figure 4-3 Turn-preload curve due to fixed reference [2]

4.1.3. Tightening method based on preload

The main purpose of tightening is to generate clamping force to secure the joint. The clamping force is generated as a reaction of the joint members from the bolt stretching (preload). To predict the preload, the input torque and turn are measured during stretching. However, there is a big variation between the preload generated from the torque and the aforementioned turn measurement most of the time. Thus, several techniques have been developed to control the preload directly. They are as follows:

a) Measurement of the bolt stretch

   This technique is based on the assumption that the bolt is a heavy spring. When a tension force is applied to a bolt, it will stretch for a certain distance. The relationship between the stretch and the force applied was shown in Equation (2-1). Equation (2-1) shows that the tension force generated at the bolt (preload) is equal to its stretch distance multiplied by its stiffness. The stretch is calculated from the difference in the length of

bolt before and after tightening. This technique is more suitable for inspection rather than for controlling the amount of preload during tightening since the preload value is calculated after, not during, the process.

b) Strain measurement technique

This measurement method uses a washer with an attached strain gauge to measure preload. The washer is installed in series with the bolt and joint members to measure the preload directly. When the bolt is tightened and stretched, it generates a tension force on the washer and joint members. Thus, preload can be monitored during the tightening process. However, this method introduces additional weight and material to the bolted joints.

c) Bolt tensioner

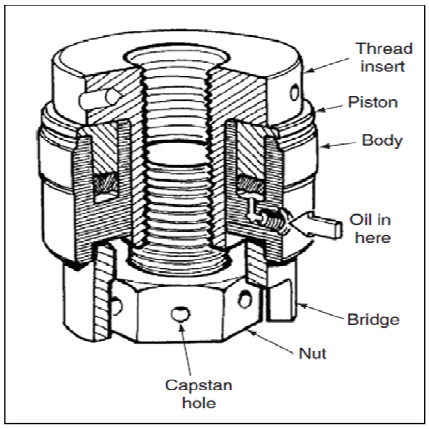

Figure 4-4 Bolt Tensioner [2]

A bolt tensioner is a tool that directly applies preload to a bolt by pulling instead of turning it. Normally, hydraulic power is utilized for this tightening process. Figure 4-4 shows a cutaway view of the hydraulic tensioner. Figure 4-5 shows the sequence of operation of the bolt tensioner. Firstly, the thread insert of tensioner is run down a bolt stud (Figure 4-5a). Secondly, the hydraulic fluid is pumped into the tensioner to stretch the bolt (Figure 4-5b). Thirdly, after the desired value of preload is achieved, a

nut is run down the bolt threads to secure the joint (Figure 4-5c). Finally, the tensioner is removed from the bolted joint to allow the tension force of bolt to apply directly to the joint members (Figure 4-5d). With this technique, an accurate measurement of the value of the preload at the bolt can be achieved. However, this technique can only work for big bolts and nuts due to the use of the hydraulic power and mechanism.

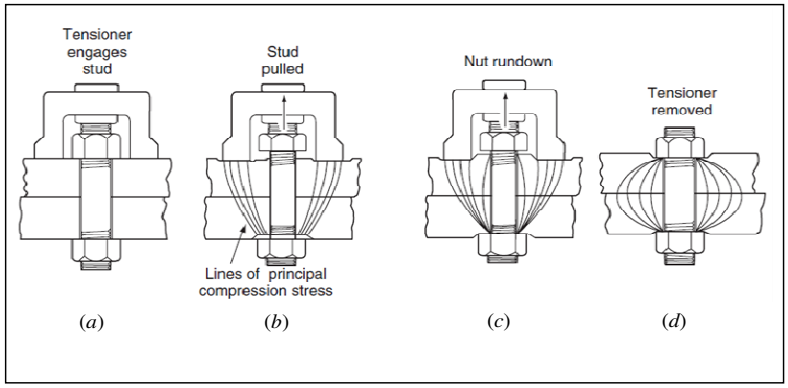

Figure 4-5 Sequences of operation of bolt tensioner [2]

4.1.4. Tightening method based on torque and turning angle

In the discussion thus far, the torque or turning angle is controlled in the tightening process to achieve the desired preload. The accuracy of the preload is affected by parameters such as the coefficient of friction, fastener geometry and the joint elasticity. In practice, there are other problems that affect the accuracy, such as blind holes, holes that are not tapped deeply enough, wrongly size holes, dirt in the holes, crossed threads, partially stripped threads, soft parts, gross misalignment of parts, chips under the head or in the hole, tool malfunctions, warped mating parts and burrs. These may cause a sudden change in the torque or turning angle leading the operator to conclude mistakenly that the desired preload has been achieved. These problems have led to the development of simultaneously using torque and turning angle to control the tightening process. Higher accuracy can be achieved by using torque and turn together as opposed to using torque or turn separately. Some of the measurement strategies that use torque and turn as control parameters are as follows:

1. Turn–of-nut method

   This is the oldest tightening technique using both torque and turn in controlling the tightness of the bolted joints. A nut is first tightened with torque to stretch a bolt a little. After that, the nut is turned to its desired turning angle. The torque is used at the start of the tightening process to compensate for the non-linear relationship between turning angle and preload. Turning angle is then used to control tightness of bolted joints. Note that the turning angle is linearly related with the preload after a certain region of tightness.

2. Torque-angle window to monitor tightness of bolted joint

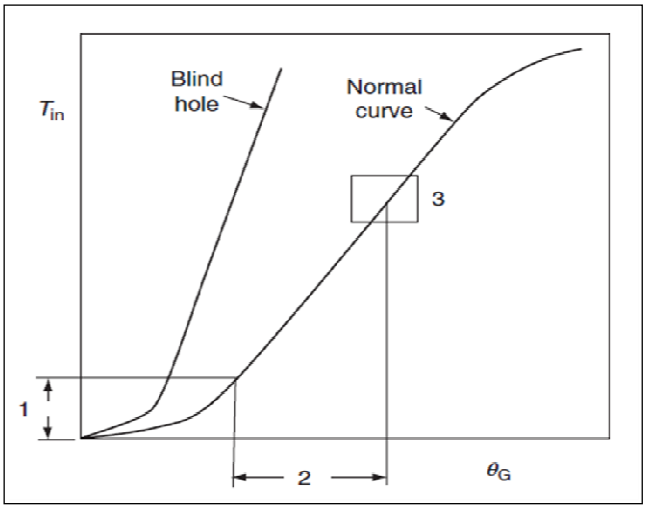

Figure 4-6 Torque-angle window to monitor blind hole [2]

The torque and turning angle can be measured with a torque sensor and encoder. Based on both measurements, the torque-angle window can be constructed as shown in Figure 4-6. This window can be used to evaluate the torque and turning angle when the tightening process is stopped. If the measured torque and turning angle falls within an acceptable "window" of suggested values, the tightened bolted joint is fine. In the case of a blind hole or that of the threads galled in a bolted joint, more torque is needed to turn the bolt. Based on an observation of torque alone, one may conclude that the

desired tightness has been achieved. However, an observation of both torque and turning angle shows that the final value of torque and turn does not fall within the acceptable "window". This indicates to the operator that there is something wrong with the bolted joint.

3. Torque-time window

   Another approach besides using a torque-turn window is to monitor the amount of time required to build up the torque to a desired level. This method is easier and cheaper than torque-time window as only torque and time are measured. However, unlike torque-turn window, the torque-time window does provide an improved control over the preload because turning angle is not considered.

4. Yield control

   Yield control is a technique to tighten a fastener to its yield point. This technique can be achieved by monitoring the torque along the time and is similar to the turn-of-nut method. At the start, the nut is in free run-down (Figure 4-7 point 1). When the nut is engaged with the joint members, the initial torque starts to build up. After this point, the torque increases linearly over time (Figure 4-7 point 2). The tightening process is paused when the bolt starts to yield. The bolt yield can be observed from radiant change in the torque-time window (Figure 4-7 point 3). After that, torque pulsations are applied to the bolt to permit short relaxation of the bolt. The bolted joint is tightened to its yield point because the preload scatter less at this point. At the yield point, the torque-preload curve is flat and any additional torque does not produce much preload. However, this method is not recommended because stretching the bolt up to the yield point imposes additional load on the joint and may cause additional plastic deformation.

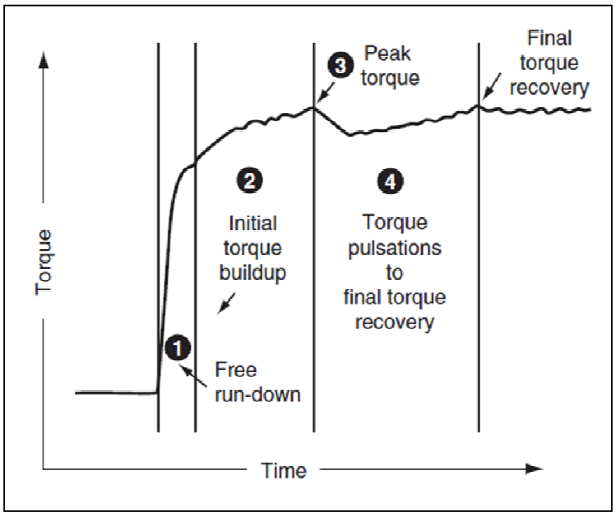

Figure 4-7 Tighten to the yield point [2]

4.2. DC motor as tightness measurement tool of bolted joints

The previous section has shown that for current bolted joint tightening techniques, the torque and turn, as inputs to a bolted joint, are controlled to achieve the desired preload. However, there is always a scatter of preload due to uncertainties in their relationship (friction, uneven bolt geometry). Controlling preload is the best choice to achieve greater accuracy in the measurement of preload but the equipment needed to control preload are bulky and expensive. A load cell needs to be installed into each joint whereas bolt tensioners cannot access certain joint connection and only works on big bolts (with diameter bigger than 18 mm).

The advantages of tightening based on the torque and turning angle are the ability to monitor the tightening process, and observe problems that may arise and the behaviour of the bolt and nut. In this section, a method to monitor tightness with a brushed DC motor is introduced. The torque and turn produced by the motor can be calculated from the electrical input with the help of a transduction matrix. The calculated data can be monitored and analyzed in real-time with a Dynamic Signal Analyzer. This method thus provides a solution for real-time monitoring of the tightening process.

4.2.1. Transduction matrix to enable simultaneous torque and turn measurement

In the previous chapter, it was shown that the transduction matrix relates the voltage and current of a brushed DC motor with the torque and rotation speed. This characteristic of the transduction matrix aids us in the development of a tightening and monitoring tool for bolted joints. As the bolted joint is tightened by the motor, the torque and rotation speed that is applied to the joint can be calculated from the measured voltage and current. By inversing the matrix from Equation (3-23), the relationship between the torque and rotational speed of the motor with its voltage and current can be written as follows:

$$\begin{bmatrix} T_m(0) \\ \Omega_m(0) \end{bmatrix} = \frac{1}{t_{11}(0)t_{22}(0) - t_{12}(0)t_{21}(0)} \begin{bmatrix} t_{22}(0) & -t_{12}(0) \\ -t_{21}(0) & t_{11}(0) \end{bmatrix} \begin{bmatrix} E(0) \\ i(0) \end{bmatrix} \tag{4-3}$$

In chapter 3, the transduction matrix for a specific brushed DC motor was obtained. This specific motor will be used in this chapter as a tightening tool. The transduction matrix of the motor based on Equation 3-45 is as follows:

$$[t] = \begin{bmatrix} 0.0566 & 10.4075 \\ 0.1419 & 0.1109 \end{bmatrix}$$

By substituting the matrix element into Equation (4-3), the torque and rotational speed during the tightening process can be calculated as follows:

$$\begin{bmatrix} T_m \\ \Omega_m \end{bmatrix} = \begin{bmatrix} -0.0754 & 7.0773 \\ 0.0965 & -0.0385 \end{bmatrix} \begin{bmatrix} E \\ i \end{bmatrix} \tag{4-4}$$

Thus, the turning angle of bolt can be calculated by integrating the rotation speed over time:

$$\theta_{bolt} = \int \Omega_m dt \tag{4-5}$$

The equation can be digitized by applying the Trapezoidal rule, which is represented by the following equation:

$$\theta_{bolt} = \sum_{i=0}^{n} \frac{\left((\Omega_m)_{i+1} + (\Omega_m)_i\right)}{2} \Delta t \tag{4-6}$$

where n is the number of sample and Δt is the sampling time.

Based on Equations (4-4) and (4-6), the torque, rotation speed and turning angle of the bolt can be calculated from voltage and current of the motor. By connecting the voltage and current probe to the dynamic signal analyzer, the measured voltage and current can be calculated in real time and stored for further reference. The in-process measurement of bolted joint tightening in this thesis is developed from this concept.

4.2.2. Experimental setup for tightness measurement of bolted joints

The experiment setup for measuring the tightness of the bolted joints is shown in Figure 4-8. The experiment consists of a brushed DC motor with a known transduction matrix, a bolted joint, a load cell, a voltage probe, a current probe and a dynamic signal analyzer. The specifications of equipments are mentioned in Appendix A and the transduction matrix of the motor can be found in Equation (3-45). The motor is used to tighten a bolted joint and the load cell is used to measure preload. The voltage and current probes are used to measure the voltage and current of the motor. The installation of the voltage and current probe is similar to that in the experiment to calibrate of transduction matrix explained earlier in Chapter 3.

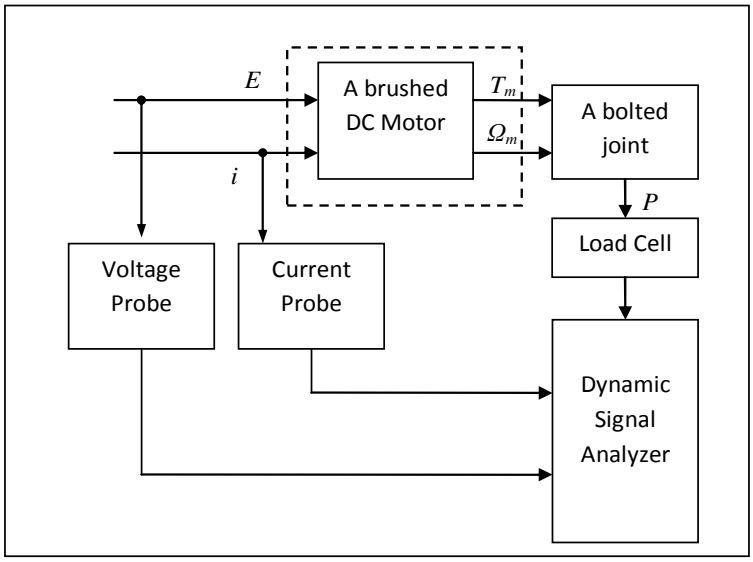

Figure 4-8 Experimental setup

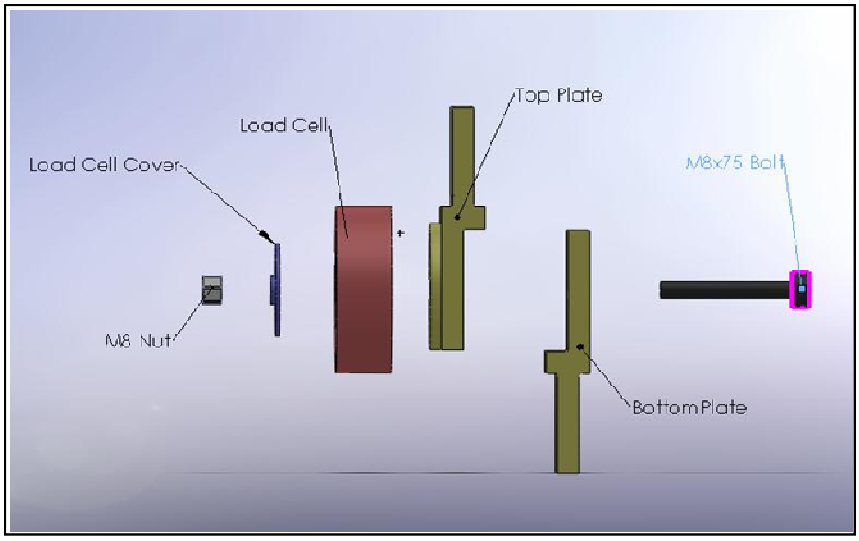

Figure 4-9 A bolted joint with a load cell

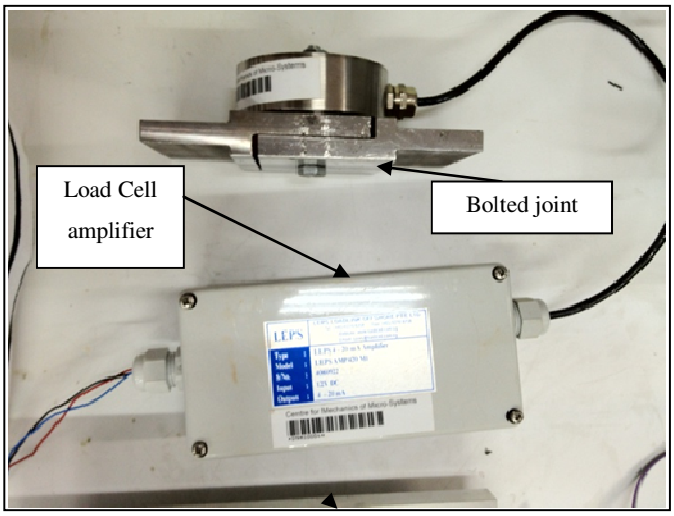

Figure 4-10 A bolted joint with load cell and amplifier

Figures 4-9 and 4-10 show a bolted joint designed for this experiment. The bolted joint consists of a M8 bolt, a M8 nut, two steel plates, a load cell and a load cell cover. The plates serve as the parts to be fastened. The bottom plate is fixed to a table to prevent movement during tightening process. The top plate has a circular shape to allow for load cell placement. The load cell is located behind the plate to prevent damage to the load. The load cell cover is designed in a ring shape to distribute the force evenly from the M8 nut to the load cell. A circular coupling (Figure 4-11) is designed to connect the motor and a bolted joint. Figure 4-12 shows how the motor and the bolted joint are connected with the coupling.

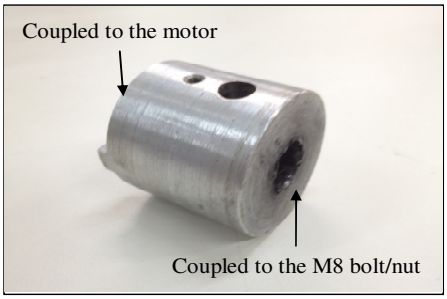

Figure 4-11 A coupling

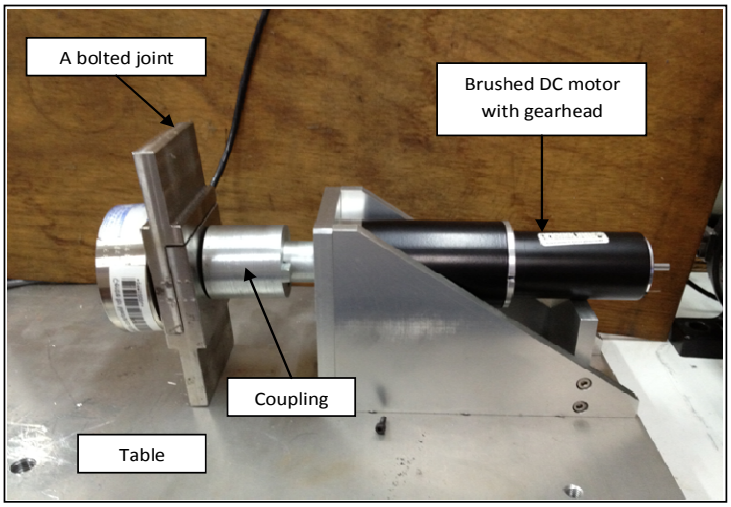

Figure 4-12 A bolted joint couple with a brushed DC motor

4.2.3. Experimental procedure

As the coefficient of friction is the main factor affecting tightness of the bolted joint, the experiment was conducted by tightening normal and lubricated bolts. The lubricant used is WD-40, which is a common lubricant find in hardware store. The lubricant was applied at the surface of bolt thread and nut thread. Three set of experiments were performed for each type of bolt. The voltage was set to 24 V based on the motor's operating condition and the current was limited to 2 A to prevent over-tightening of bolt. When the current was at 2 A, the power supply maintained this current value due to its configuration. The voltage and current of the motor, and the bolt preload were measured during the tightening process. The torque, rotational speed, and turning angle were then calculated from the measured voltage and current with the transduction matrix in Equation (4-4). The measurement was started when voltage was supplied to the motor and was stopped after 5 seconds. The data was then sampled and recorded with a sampling frequency of 2,000Hz. A low pass digital filter with cut-off frequency at 10 HZ was applied to the data to smooth the graph. For signal processing purposes, data was extracted from the time when the current starts to increase to the time when the motor stops. The bolt preload, voltage and current were measured during the

tightening process. The torque and rotational speed applied on the bolted joint were then calculated by substituting the voltage and current into Equation (4-4).

4.3. Experimental results

The results obtained are presented and discussed as follows:

4.3.1. Observation of tightening process

Samples of the measurement results for lubricated bolts and non-lubricated bolts ("normal bolts") are shown in Figures 4-13 to 4-18. It can be observed from Figures 4-13 to 4-18 that the tightening process of lubricated and normal bolts follow the same pattern but differs in their execution time. Thus, an explanation of the tightening process of a normal bolted joint applies to both lubricated and normal bolted joints. The explanation is broken into different sequences as follows:

a) Point A

   This is the point where the nut starts to touch the plate surface. Further turning of the nut will stretch the bolt. An increase in the motor torque and bolt preload are observed after this point.

b) Point A-B

   The bolt is stretched at an almost constant speed in this region. Due to the stretching, the motor torque increases and additional current is drawn. The stretching creates an incremental preload in the bolt. A small decrease in rotational speed is observed during the stretching.

c) Point B-C

   The current reaches the limit value of 2 A and therefore the voltage and rotational speed decreases significantly. At this point, it is observed that the torque increases at a slower rate while the preload increases at normal rate.

d) Point C

The motor stops as maximum torque is reached.

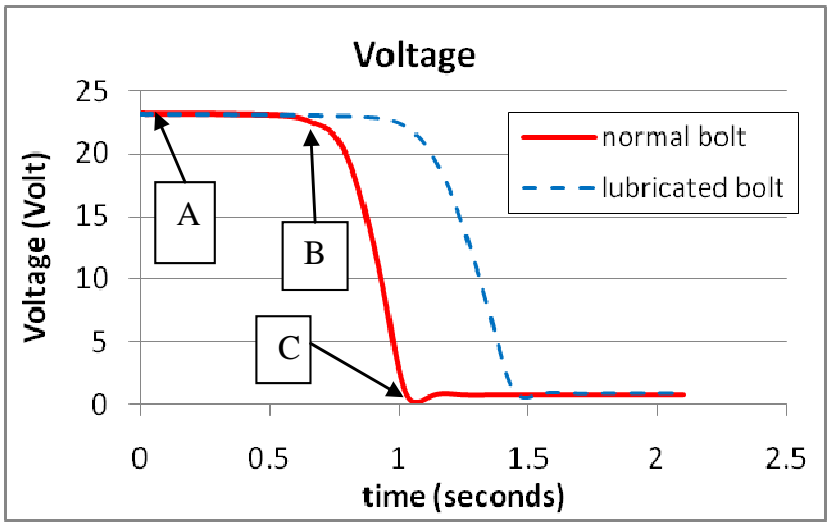

Figure 4-13 Voltage of the motor during tightening

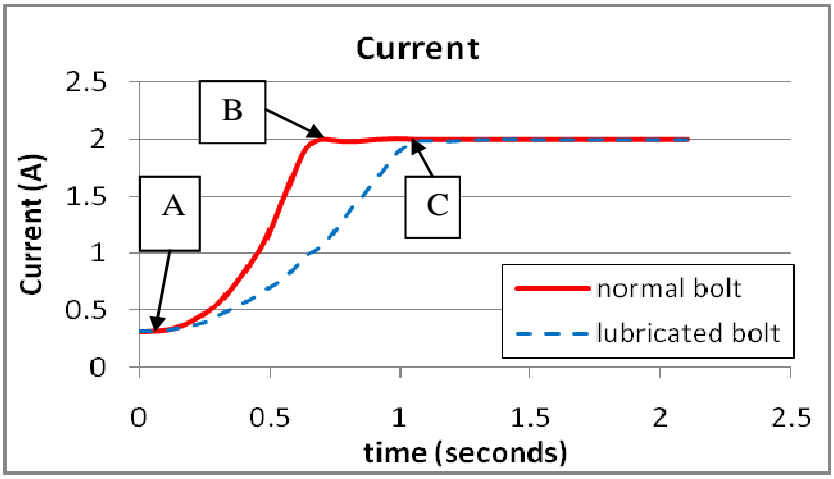

Figure 4-14 Current of the motor during tightening

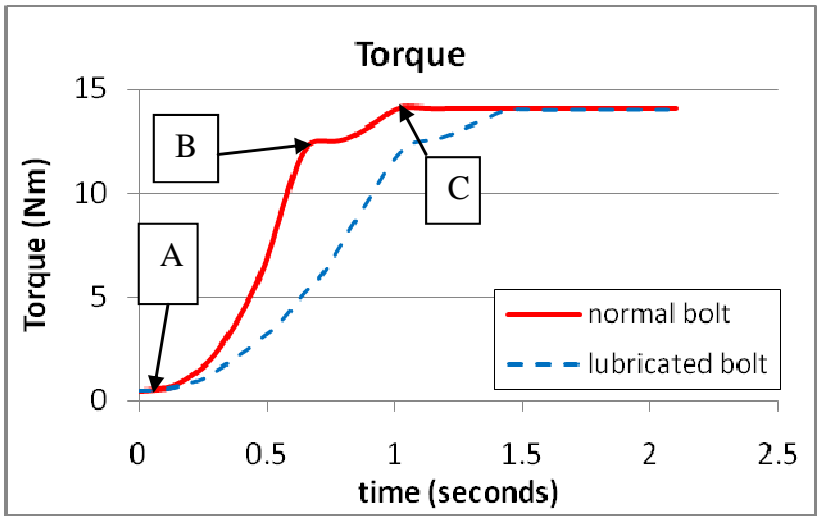

Figure 4-15 Torque of the motor during tightening

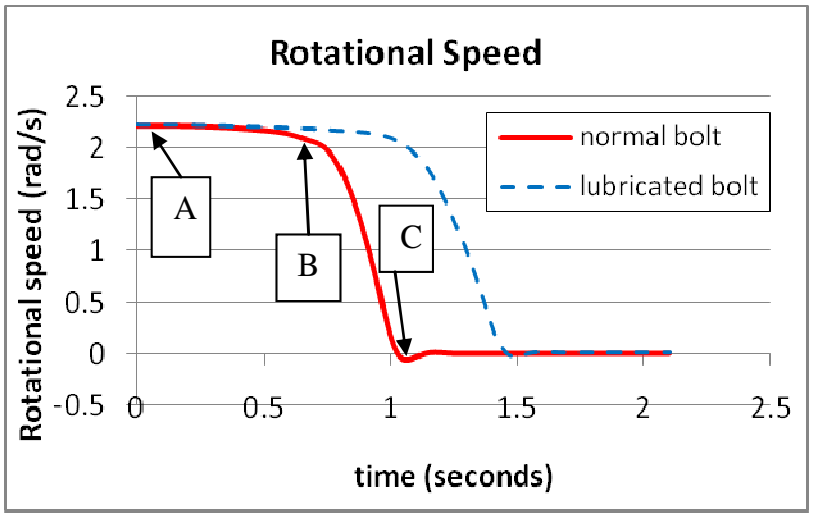

Figure 4-16 Rotational speed of the motor during tightening

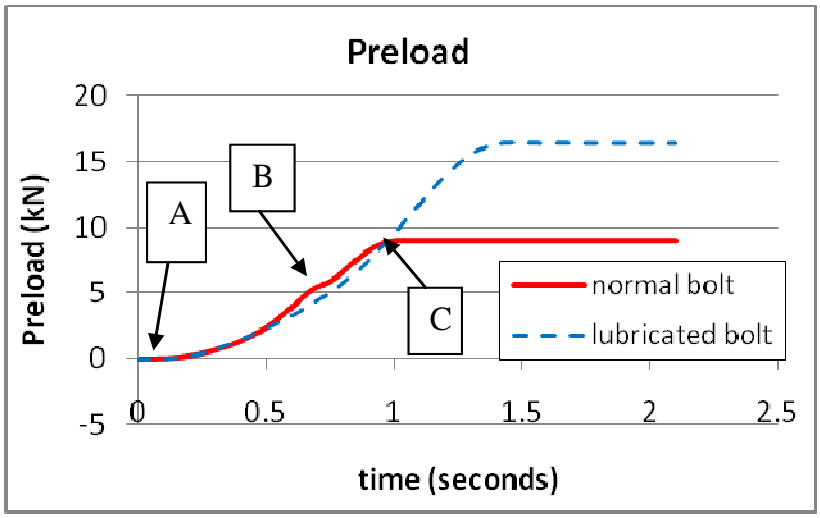

Figure 4-17 Preload of the bolt during tightening

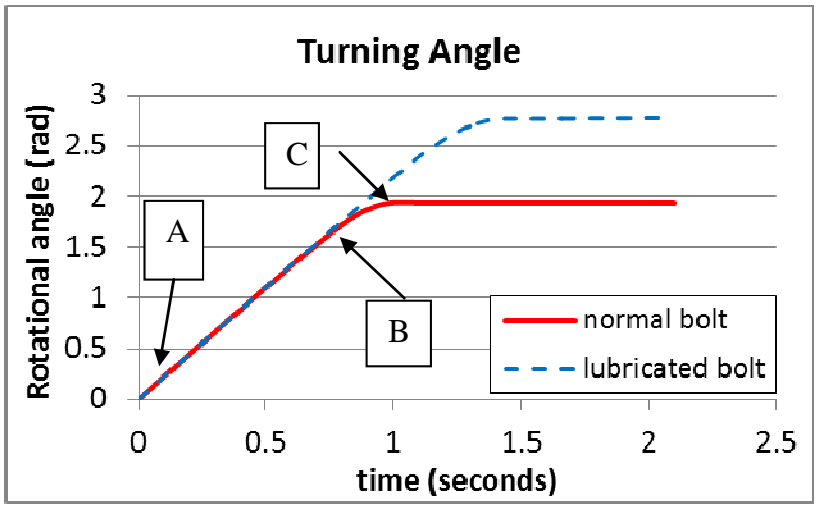

Figure 4-18 Turning angle of the bolt

4.3.2. Tightening torque

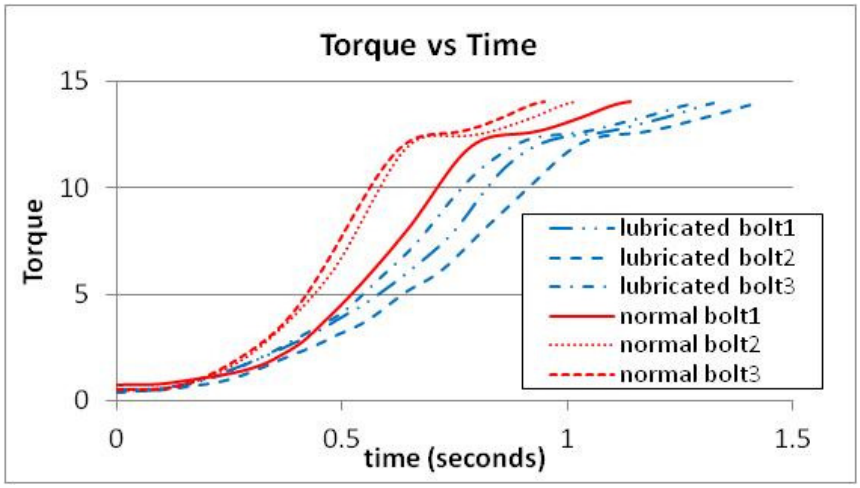

Figure 4-19 Tightening torque of the bolted joint over time

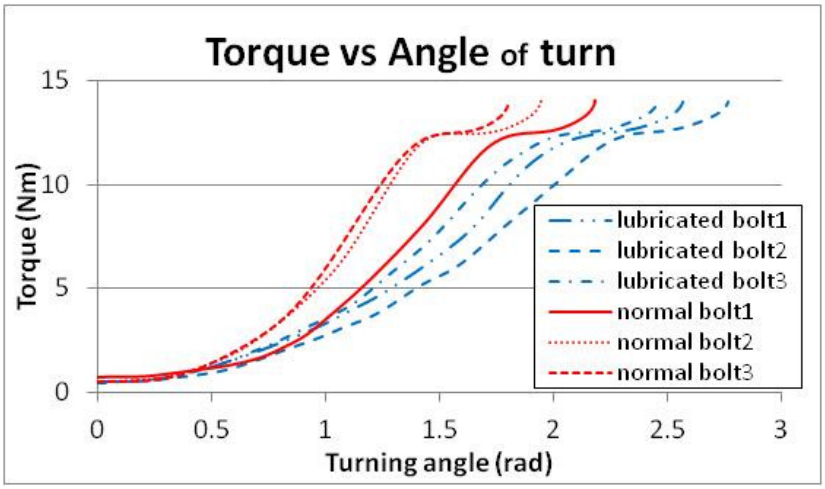

Figure 4-20 Tightening torque vs Turning angle

Torque values between both types of bolts are compared because it is the common indicator of tightness of bolted joints. Based on the comparisons, the maximum torque applied to both lubricated and normal bolts is 14 Nm. Figure 4-19 shows that torque increases at a higher rate for normal bolts as compared to lubricated bolts, which produces greater friction. Additionally, the normal bolts reach maximum torque faster than the lubricated ones and turn less due greater friction

(Figure 4-20). Hence, the preload generated at normal bolt is smaller as shown in Figure 4-21. This observation can be consistent with the short form equation mentioned earlier in Chapter 2 ($T_{in} = K \times D \times P$). The torque applied to a bolted joint is equal to the preload (P) generated at the bolt multiplied by the diameter of the bolt (D) and the nut factor (K). K is a constant that includes the friction coefficient and the dimensional information of bolt (pitch, lead angle, etc.). In the present case, the equation can be simplified to $K \times P =$ constant, because the input torque and the bolt diameter are the same for the lubricated and normal bolts (T_{in} and D are constant). This simplified equation shows that K is inversely proportional with preload (P). Hence, a higher K (higher friction) will produce a smaller preload (P). Therefore, it can be concluded that the same magnitude of tightening torque may produce different preload at the bolted joints due to variation in friction. Therefore, torque is not a good indicator of tightness since friction varies easily from variations in different conditions of the tightening process such as the lubrication applied, the tightening speed, and the material used.

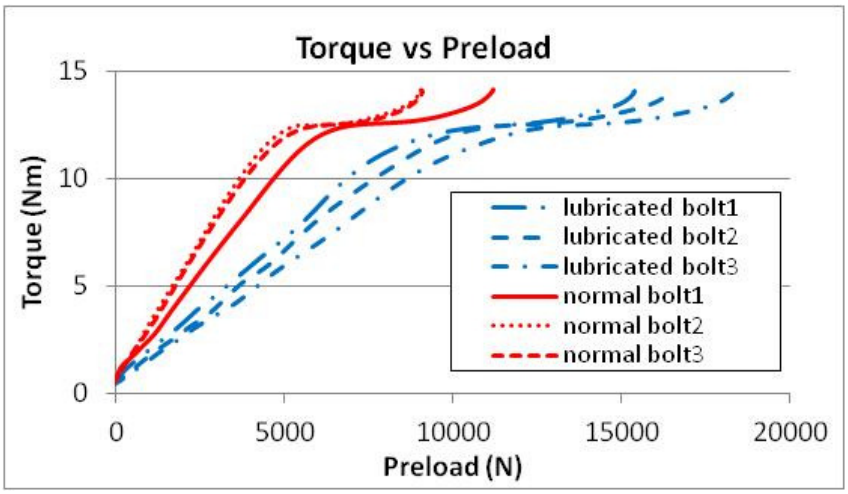

Figure 4-21 Tightening torque of bolt versus preload

Figure 4-21 shows that two regions of distinct patterns in the relationship between torque and preload during tightening process. In the first region, the relationship is represented by a straight line, which is governed by the short form equation

($T_{in} = K \times D \times P$). In the second region, the relationship is non-linear. This is because the motor's current has reached its pre-set limit. At this region, the torque increases at a slower rate and the preload increases at a normal rate.

4.4. Total Energy input as a tightness indicator

The bolted joint can be viewed as an energy storage device. When a bolted joint is tightened, energy is applied to the bolt in the form of torque and turn. The bolt stores the energy in the form of bolt stretches (potential energy). This energy is used to help the bolt resist external disturbance. This section will introduce tightening energy as tightness indicator. Comparisons between the tightening energy with two other tightness indicators are done to show the accuracy of the energy as tightness indicator.

4.4.1. Total energy input to a bolted joint versus time

Since torque and rotational speed can be obtained simultaneously by the proposed method, the total energy input to a bolted joint during the tightening process can be calculated as follows:

$$E_{bolt} = \int T_m \Omega_m dt \tag{4-7}$$

The equation can be digitized by applying trapezoidal rule, which is written as follows:

$$E_{bolt} = \sum_{i=1}^{n} \left((T_m)_{i-1} + (T_m)_i \right) \frac{(\Omega_m)_i}{2} \Delta t \tag{4-8}$$

Based on this formula, we try to observe total energy input given to the bolted joint and propose it as the tightness indicator

Figure 4-22 shows measurements of the total energy input to the bolts. Both normal and lubricated bolts have the same value at the starting point. As the bolt

is tightened, the normal bolts need more energy due to its rougher surface (higher friction). However, at the end of tightening process, the total energy of the lubricated bolt is greater than that of the normal bolt. This shows that the lubricant aids in the tightening process. It reduces surface friction and permits more energy to be transferred to the bolt. As a result, a higher tightness is achieved. However, it will be suggested in the next chapter that the lubricant should be removed after tightening, as greater friction is needed to prevent the bolted joint from self-loosening.

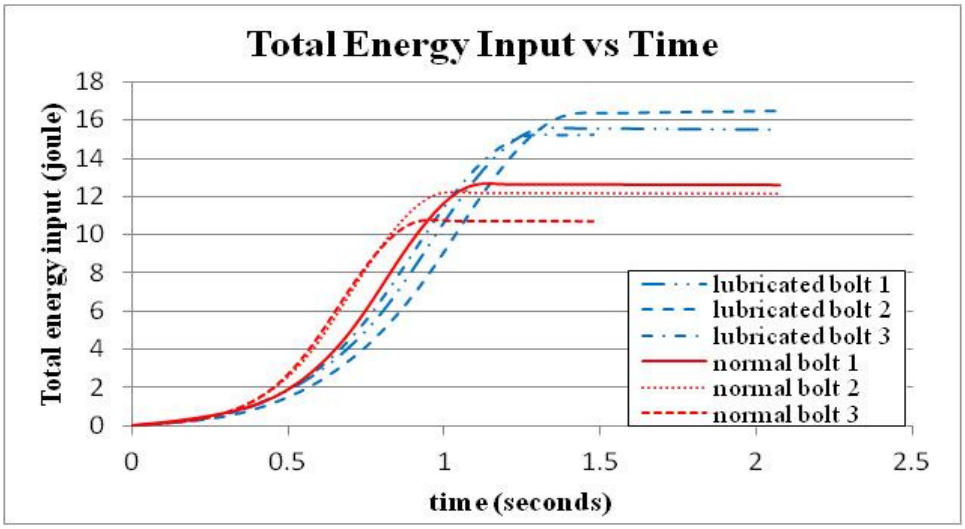

Figure 4-22 Total energy input vs time

4.4.2. Comparison between total energy input and preload

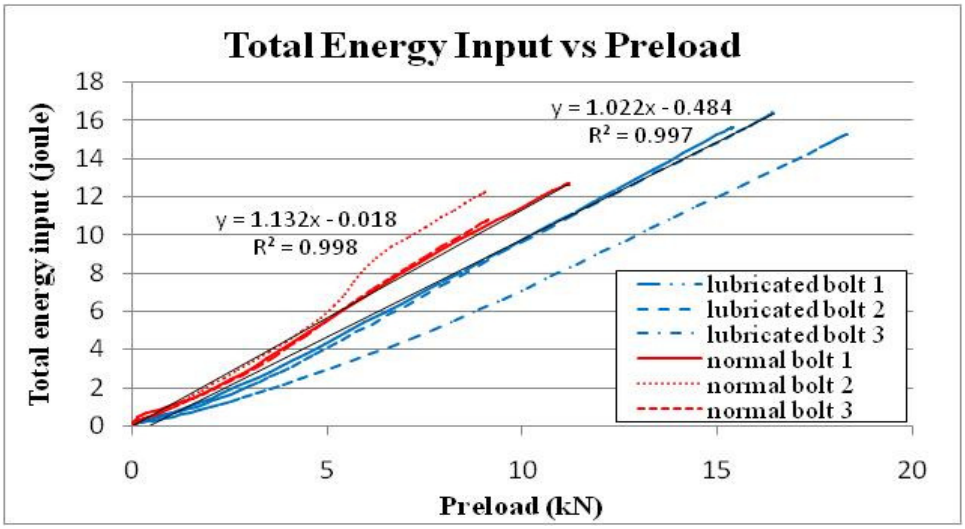

Figure 4-23 Total energy input vs preload

The total energy input and preload have a linear relationship as shown in Figure 4-23. The relationship is represented by a straight line with different gradients for normal and lubricated bolts. Normal bolt 1 and lubricated bolt 2 are used to represent their respective group. Using the curve fitting functionality provided in Microsoft Excel, equations to determine the relationship are obtained as follows:

a) Lubricated bolt:

$$E_l = 1.022P - 0.484 \tag{4-9}$$

b) Normal bolt:

$$E_n = 1.132P - 0.018 \tag{4-10}$$

The values of the correlation coefficients (R^2) for both equations are close to 0.99, which shows a good correlation. Thus, it can be concluded that preload can be also indirectly measured from the total energy input by obtaining the gradient of the graph. However, the gradient needs to be obtained experimentally. In addition, it is observed that the normal bolt has a higher gradient than lubricated bolt. This

shows that friction also affects the relationship between total energy and preload. However, the effect of friction is smaller compared to the relationship between the torque and preload.

4.4.3. Comparison between tightening torque and total energy input

Table 4-1 Comparison value of the tightness indicator

	Torque (Nm)	***Preload (kg)***	***Total Energy (joule)***
Lubricated bolt 1	14.082	1569.036	15.647
Lubricated bolt 2	14.065	1676.163	16.466
Lubricated bolt 3	14.076	1870.967	15.270
Normal bolt 1	14.107	1140.936	12.687
Normal bolt 2	14.144	922.762	12.248
Normal bolt 3	14.082	929.767	10.795

The relationship between the total energy input and preload is linear throughout the entire tightening process. On the other hand, the relationship between torque and preload can be divided into two regions. This shows that total energy input can be used to calculate the preload accurately during the tightening process compare to torque. Table 4-1 compares values of the torque, preload and total energy input at the end of tightening process. It can be seen that the preload generated to tighten the lubricated bolt is higher, but the same result does not show in the torque value. On the other hand, a higher preload is clearly indicated by using the total energy input. This is because most of the total energy input to the bolt is caused by the stretching of the bolt, which is influenced by preload but not friction. Hence, it is concluded that the total energy input is a better indicator of the tightness of a bolted joint compare to torque because it can predict preload accurately.

4.5. Summary

The tightness of bolted joints can be measured using a brushed DC motor with a known transduction matrix. The torque and rotational speed are calculated from the motor's input electrical with the help of the transduction matrix. Two types of bolt specimens — bolts with lubricant applied (lubricated bolt) and bolts without lubricant (normal bolt) — were prepared to study effect of friction in bolted joints. As shown in Figure 4-12, the tightening torque is affected by the bolted joint's friction conditions. The greater the friction is, the greater the increment rate of torque will be and the smaller that of the preload will be. This is consistent with the torque equation of the bolt, which shows that torque applied to the bolt depends on a combination of preload, friction and bolt diameter. Towards the end of tightening process, a non-linear relationship between torque and preload is observed. Hence, it is concluded that the tightening torque is not a good tightness indicator for use during the tightening process.

The energy input to the bolted joint can be calculated from the torque and rotational speed using Equation (4-6). Based on the measurement results, it can be concluded that the energy input is a better tightness indicator than the tightening torque. Figure 4-15 shows that the energy input has a linear relationship with the bolt preload throughout the entire tightening process. The preload can be predicted from the energy input by experimentally obtaining gradient of the linear relationship. Besides that, an indicator based on the energy input can also distinguish different preloads for the two different cases of lubricated and normal bolted joint, which have the same value of tightening torque. Due to the lower surface friction, the lubricated bolt has a higher preload compare to the normal bolt. This is indicated by the higher total energy input to the lubricated bolt.

Based on the aforementioned results and findings, it is recommended that the total energy input should be used as the tightness indicator of bolted joints. As shown in Table 4-1, different preloads are generated from the same torque under different surface conditions. This is because the relationship between torque and

preload is affected by friction as reflected in the torque equation as well. On the other hand, the influence of friction on the total energy input is little and it is more influenced by the preload. Hence, the total energy input is a better tightness indicator than the tightening torque.

Lastly, we observe that lubricant aids the tightening process in allowing a bolt to be tightened more. Figure 4-17 and Figure 4-18 show that lubricated bolts are tighter than normal bolts. Turning angle and preload generated under the same value of tightening torque at lubricated bolts are higher than normal ones. This is because lubricant reduces surface friction of material and input torque can be utilized to stretch the bolts more rather than overcome surface friction. However, higher surface friction is needed to keep the bolted joint intact because it aids in preventing loosening of bolted joints. Thus, a quick drying lubricant is helpful in aiding the tightening process. During the tightening process, the lubricant reduces surface friction to permits more tightening. After tightening process, the lubricant will dry out and increase the surface friction back to normal for loosening prevention.

CHAPTER 5
LOOSENING OF BOLTED JOINTS

Bolted joints tend to lose their tightness under vibration. The vibration excites the joints and causes it to loosen, thereby reducing the bolted joint's capability to support loads. Furthermore, the looseness allows the bolt to rotate freely and separate from the joint. As reviewed in Chapter 2, the behaviour and response of bolted joints under vibration has historically been described and studied using dynamic models. In particular, the model's system properties are helpful in studying the mechanism by which the joints are loosened.

This chapter presents a method to identify the dynamic model of bolted joints. A brushed DC motor and a calibrated transduction matrix are used to identify the model. The motor is used to excite bolted joints of a fixed tightness at a single excitation frequency. Both the excitation and response of the bolted joints are calculated from the motor's electrical input with the help of a transduction matrix. A dynamic model of the bolted joints is then constructed from the measurements. Based on the identified model, loosening bolted joints under vibration is simulated in order to validate the identified model and investigate the mechanism of loosening

Section 5.1 reviews the concept of system identification for time invariant and time variant systems. Section 5.2 presents an experimental method to identify the system properties of bolted joints and construct dynamic model of bolted joints with the motor. Section 5.3 simulates the response of the bolted joint based on identified model to simulate loosening. Section 5.4 summarizes the results and findings.

5.1. Introduction of System Identification

A linear system under a certain excitation will give out a certain response. The relationship between the excitation and the response can be described by

Frequency Response Function (FRF). FRF is formed by dividing the excitation signal by the response signal in the frequency domain. After obtaining FRF of the system, the system properties can be derived from its FRF. In this section, the mathematical methods to obtain FRF of time invariant and variant system are described. Following which, a mathematical derivation to link between system properties and FRF will be presented.

5.1.1. Impedance of time invariant system

FRF is a transfer function that explains the system's dynamic behaviour over a frequency range. It is formed by dividing the excitation signal by the response signal or vice versa in the frequency domain. Normally, the excitation and response signals are transformed from the time domain to the frequency domain by the Fourier Transform. There are 6 forms of FRF based on response parameters and function arrangements. These are shown in Table 5-1 [58]. Each form of FRF serves as a system signature based on its function arrangement.

Response Parameter (R)	**Response/Force excitation**	**Force excitation /Response**
Displacement	Receptance	Dynamic Stiffness
Velocity	Mobility	Mechanical Impedance
Acceleration	Inertance	Apparent Mass

Table 5-1 Definitions of Frequency Response Functions

This thesis focuses on mechanical impedance. Mechanical impedance is a function of force divided by velocity in the frequency domain. It measures the dynamic system's resistance of motion when subjected to a given force. Mathematically, mechanical impedance is expressed by the following formula:

$$Z_m(\omega) = \frac{F(\omega)}{v(\omega)} \tag{5-1}$$

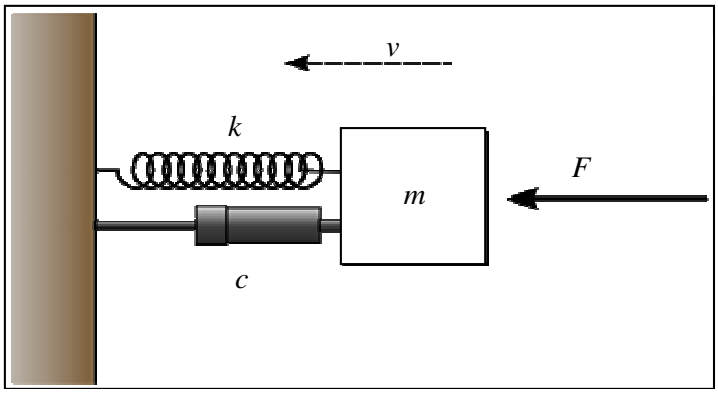

Figure 5-1 Simple mechanical system

For a simple time invariant mechanical system consisting of constant mass (m), constant damping (c) and constant spring (k) (Figure 5-1), the excitation ($F(t)$) and response ($v(t)$) of the system can be described with the equation as follows:

$$F(t) = m\frac{dv(t)}{dt} + cv(t) + k\int v(t)dt \tag{5-2}$$

By transforming the $F(t)$and $v(t)$ into the frequency domain with Fourier Transform, $F(t)$and $v(t)$ become $F(\omega)$and $v(\omega)$ *respectively*. The linear relationship between $F(\omega)$and $v(\omega)$ can be described by the equation as follows:

$$F(\omega) = \left(jm\omega + c + \frac{k}{j\omega} \right) v(\omega) \tag{5-3}$$

The mechanical impedance of the system can be expressed as follows:

$$Z_m(\omega) = \frac{F(\omega)}{v(\omega)} = c + j\left(\frac{m\omega^2 - k}{\omega} \right) \tag{5-4}$$

As shown in Equation (5-4), the mechanical impedance is only presented in the frequency domain, and the system properties (m, c, and k) are assumed to be constants. If the system properties vary with time, a different approach is used. This is explained in the next section.

5.1.2. Impedance of the linear time variant system

A time variant system is a system with its properties that vary with time. The mechanical impedance of the time variant system is a function of frequency and time ($Z_m(t,\omega)$). For a simple time variant system consisting of $m(t)$, $c(t)$ and $k(t)$, the mechanical impedance can be represented as follows:

$$Z_m(t,\omega) = \frac{F(t,\omega)}{v(t,\omega)} = c(t,\omega) + j\left(\frac{m(t)\omega^2 - k(t)}{\omega}\right) \tag{5-5}$$

where $m(t)$, $c(t)$ and $k(t)$, are function in time domain.

Hilbert Transform is used in this project to help in the calculation of the mechanical impedance of the time variant system. Hilbert Transform is a signal-processing tool that behaves like Fourier Transform except that it transforms the time-domain function into the same domain. Because the result of transformation is in time domain, the change of mechanical impedance over time can be observed. This is the reason why Hilbert Transform is used to help in obtaining impedance for linear time variant system.

Hilbert Transform is a convolution integral between real-valued function ($x(t)$) and $1/\pi t$ over the range $-\infty < t < \infty$. [59]. Mathematically, it is written as:

$$\tilde{x}(t) = \mathrm{H}\left(x(t)\right) = \int_{-\infty}^{\infty} \frac{x(u)}{\pi(t-u)} du \tag{5-6}$$

By applying Hilbert Transform to real-valued function ($x(t)$), it will phase shift the function for $\pi/2$ and generate imaginary part of the function. Together with the real part, it create analytic signal of the system. Mechanical impedance of the signal is obtained from the division of analytic signal of the force and velocity signal of the system.

In a case of a linear system is excited with a single frequency (ω_f) continuous force ($F(t)=Fe^{\omega ft}$), the system will produce a velocity response with the same

frequency ($v(t)=ve^{\omega ft}$). Hilbert Transform is applied to the force (F*(t)*) and velocity (*v(t)*) signal to generate the imaginary representative. Mathematically, this is written as follows:

$$\tilde{F}(t) = \mathrm{H}\left(\tilde{F}(t)\right) \tag{5-7}$$

$$\tilde{v}(t) = \mathrm{H}\left(v(t)\right) \tag{5-8}$$

where $\tilde{F}(t)$ and $\tilde{v}(t)$ are the imaginary parts of force (F*(t)*) and velocity (*v(t)*). By adding the real part and imaginary part of each signal, analytic signals of force ($F_{analytic}$) and velocity ($v_{analytic}$) are formed. The mechanical impedance of the system for that particular frequency (ω_f) can be obtained by dividing the analytic signal of force and velocity signal. Mathematically, it is expressed as follows:

$$Z_m(t) = \frac{F_{analytic}}{v_{analytic}} = \frac{F(t) + j\tilde{F}(t)}{v(t) + j\tilde{v}(t)} \tag{5-9}$$

The mechanical impedance in Equation (5-9) is obtained in the time domain and solved only at the particular frequency ($\omega=\omega_f$). If there is more than one frequency, the obtained mechanical impedance is less accurate. Thus, it is advisable to limit the frequency excitation to one single excitation frequency to obtain the accurate value of mechanical impedance. To show that the mechanical impedance obtained with Equation (5-9) is equal to the mechanical impedance obtained with Equation (5-5) at a particular frequency ($\omega=\omega_f$), sample calculations are carried out in Appendix B. The calculation also shows that more than one frequency will affect the accuracy of obtained mechanical impedance and averaging is needed to obtain a near value of impedance.

5.1.3. Identification of system properties from mechanical impedance

Previous section has shown mechanical impedance of time variant and time invariant system. Both the mechanical impedance are characteristic functions of the system properties. For a case of simple linear system, mechanical impedance

is described as combination of mass, damping coefficient and stiffness coefficient, which is shown in Equation (5-4) and Equation (5-5) for time invariant and time variant system.

According to the equations, mechanical impedance is a complex number consisting of real and imaginary numbers. The real number is called resistance and it represents the damping coefficient. The imaginary number is called reactance and it represents mass and stiffness coefficient. Mathematically, the relationship can be simplified as:

$$Z_{real}(t) = c(t) \tag{5-10}$$

$$Z_{imag}(t,\omega) = \frac{m(t)\omega^2 - k(t)}{\omega} \tag{5-11}$$

Based on Equation (5-10) and Equation (5-11), the system properties can be obtained from the measured mechanical impedance. Equation (5-10) shows that the damping coefficient (*c(t)*) is obtained from the real part of impedance (resistance). Equation (5-11) shows that the imaginary number of impedance consists of three variables which are mass (*m(t)*), stiffness (*k(t)*) and excitation frequency (*f*). Ideally, mass (*m(t)*) and stiffness (*k(t)*) of the linear system are independent of excitation frequency (*f*). Thus, any variant of excitation frequency (f_1,f_2,..,f_n) given to the system will not affect mass (*m(t)*) and stiffness (*k(t)*) of the system but generate variant value of imaginary part of impedance (Z_{imag-1}, Z_{imag-2}, ..., Z_{imag-n}). This relationship can be written in matrix form as follow:

$$\begin{bmatrix} Z_{imag-1}(t) \\ Z_{imag-2}(t) \\ \vdots \\ Z_{imag-n}(t) \end{bmatrix} = \begin{bmatrix} \omega_{f1} & -\frac{1}{\omega_{f1}} \\ \omega_{f2} & -\frac{1}{\omega_{f2}} \\ \vdots & \vdots \\ \omega_{fn} & -\frac{1}{\omega_{fn}} \end{bmatrix} \begin{bmatrix} m(t) \\ k(t) \end{bmatrix} \tag{5-12}$$

Based on Equation (5-12), *m(t)* and (*k(t)*) can be solved with two excitation frequency and taking inverse matrix. In experiment, it is advisable to use more than two (n>2) excitation frequency to reduce the experimental error. However, this will create an overdetermined equation and the least square method is needed to solve *m(t)*and *k(t)*. Mathematically, the solution is expressed as follows:

$$\begin{bmatrix} m(t) \\ k(t) \end{bmatrix} = \left(\begin{bmatrix} \omega_{f1} - \frac{1}{\omega_{f1}} \\ \omega_{f2} - \frac{1}{\omega_{f2}} \\ \vdots \\ \omega_{fn} - \frac{1}{\omega_{fn}} \end{bmatrix}^T \begin{bmatrix} \omega_{f1} - \frac{1}{\omega_{f1}} \\ \omega_{f2} - \frac{1}{\omega_{f2}} \\ \vdots \\ \omega_{fn} - \frac{1}{\omega_{fn}} \end{bmatrix} \right)^{-1} \begin{bmatrix} \omega_{f1} - \frac{1}{\omega_{f1}} \\ \omega_{f2} - \frac{1}{\omega_{f2}} \\ \vdots \\ \omega_{fn} - \frac{1}{\omega_{fn}} \end{bmatrix}^T \begin{bmatrix} Z_{imag-1}(t) \\ Z_{imag-2}(t) \\ \vdots \\ Z_{imag-n}(t) \end{bmatrix} \quad (5\text{-}13)$$

With Equation (5-13), *m(t)* and (*k(t)*) can be obtained experimentally. Both Equations (5-10) and (5-13) can be used to obtain the system properties of linear system from the mechanical impedance. By applying single excitation frequency to the system, mechanical impedance of the system is obtained. The next section will explain this system identification method applied at the bolted joints using a Brushed DC motor as the sensing and actuating device.

5.2. System identification of bolted joints

A bolted joint under excitation is considered as a dynamic system. The joint gives out response in a small displacement and dissipates excitation energy to protect the jointed structure. In order to understand this dynamic response and dissipative behaviour of bolted joint, system properties of the joint are needed. In this project, a brushed DC motor with a known transduction matrix is used to obtain the mechanical impedance of the bolted joints. The motor applies a single frequency sinusoidal excitation of small amplitude to the bolted joints and the response of joints is reflected at the rotational speed of the motor. Both the torque and rotational speed are calculated from the input electrical of the motor with the help of the transduction matrix. The mechanical impedance of bolted joints is calculated based on the Equation (5-14). Following which, the system properties

will be derived from the measured mechanical impedance using Equations (5-10) and (5-13). This section introduces the aforementioned experimental method and the derivation to obtain the system properties. The experimental setup and procedure will also be described.

5.2.1. Dynamic model of bolted joint

A bolted joint under small range of frequency excitation can be modelled as a simple mechanical system. The system consists of mass, spring and damping. Each component of the system represents the dynamic behaviour of the system. The mass component represents the inertia of the joint, the spring component represents the stiffness of the joint and the damping represents the dissipative behaviour of the joint. Stiffness describes the elasticity behaviour of the joint. It describes displacement of the joint under given excitation. Damping describes the dissipative behaviour of bolted joint. It describes how energy is dissipated from the joint.

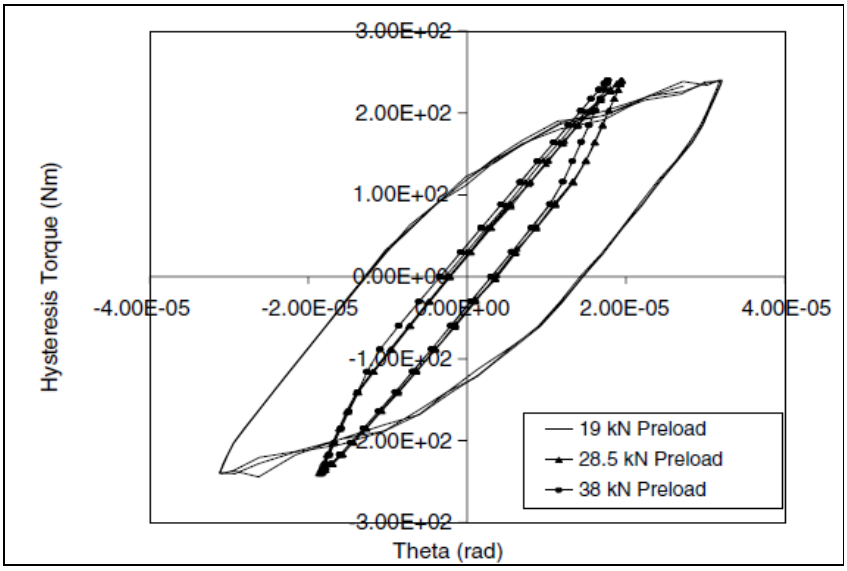

Figure 5-2 Hysteresis curve [49]

Tightness of bolted joint affects the value of those components. Figure 5-2 shows hysteresis graph of bolted joints with different preload under excitation of single value of torque. This graph is obtained from FEM model of bolted joint generated by Oldfield [49]. In the figure, the displacement of each bolted joint is observed to be varied. This implies that the components of a bolted joint is a function of its tightness (preload)

In order to obtain value of each component, mechanical impedance of bolted joint is measured. The mechanical impedance of bolted joint are formed from combination of coefficient of mass, spring, and damping. By assumed a simple mechanical model (mass, spring and damping), relationship of mechanical impedance with coefficient of mass, spring and damping can be shown from Equation (5-10) and Equation (5-11). The mechanical impedance of bolted joint can be obtained by dividing the analytic signal of the excitation torque over the rotational speed. This is mathematically expressed as follows:

$$Z_m(t) = \frac{T_{analytic}}{\Omega_{analytic}} = \frac{T(t) + j\tilde{T}(t)}{\Omega(t) + j\tilde{\Omega}(t)} \tag{5-14}$$

Based on this measured mechanical impedance of bolted joint, the coefficients of system can be measured by using Equation (5-10) and Equation (5-13). In order to obtain relationship between components of bolted joint, experimental is conducted with a calibrated electric motor to apply a sinusoidal excitation to a bolted joint with different preload. Based on this experimental measurement, the relationship between each component of bolted joint with its tightness can be described.

5.2.2. Experimental setup

To measure the mechanical impedance of bolted joints, the experiment shown in Figure 5-3 was set up. The experiment setup is similar with the experimental setup in Chapter 4 with an additional motion control card to control the motor movement. The experiment consisted of an electric motor, a motion control card,

a voltage probe, a current probe, a dynamic signal analyzer, and a tightened bolted joint with a load cell. The detail and model of the equipments can be found in Appendix A.

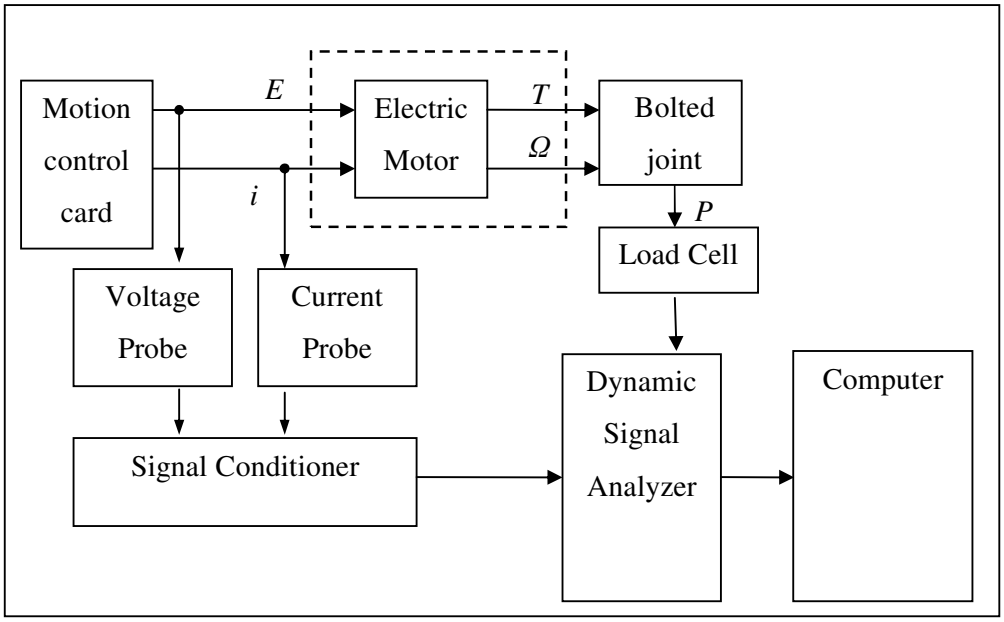

Figure 5-3 Experimental Setup to obtain Mechanical Impedance

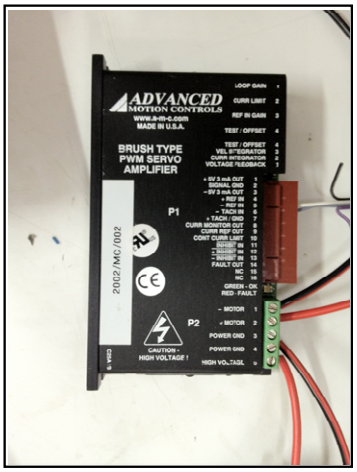

Figure 5-4 Advanced Motion Control (Motion Control Card)

The electric motor used in this experiment is a brushed DC motor. The transduction matrix for the motor has already been identified in Chapter 3. The motion control card is attached to the motor to control the motor's motion and

supply power. Figure 5-4 shows the motion control card. The motion control card amplifies any signal input to it to generate enough power to run the motor. In this experiment, the input signal is a sinusoidal signal with frequency is varied from 0.7 Hz to 1.2 Hz. The signal amplitude after amplification is 24 Volt. This signal from motion control card causes the motor to rotate in sinusoidal to excite the tightened bolted joint. The tightened bolted joint is attached at the motor with similar configuration in Chapter 4 (Figure 4-12).

Voltage and current probes are attached to the cable between the motor and motion control card. The setups for the voltage and current probe are similar to the setup mentioned in Chapter 3. The output ports of the probes are connected to the dynamic signal analyzer for sampling and storing the collected data. The bolted joint is attached to the motor shaft. The design of bolted joints and their setup are mentioned in Chapter 4. The load cell is also connected to the dynamic signal analyzer for storing purpose.

5.2.3. Experimental procedure

The experiment was conducted by applying sinusoidal excitation to the bolted joints. The samples of bolted joints were prepared in five different preloads (2,000 N, 4,000 N, 6,000 N, 8,000N and 10,000 N) and two different friction conditions (lubricated and non-lubricated) were applied for each preload. Six different excitation frequencies (0.7 Hz, 0.8 Hz, 0.9 Hz, 1.0 Hz, 1.1 Hz, and 1.2 Hz) are used to excite the bolted joint. Thus, there are 60 cases of bolted joint for each different preload, surface condition and excitation frequency. Four sets of bolted joints were prepared for each of the cases mentioned. During the excitation, the voltage and current of the motor were measured with the probes. The preload was measured from the load cell and the voltage, current and the preload were sampled and recorded with a digital signal analyzer for 3 seconds. The data were sampled at 2000 Hz frequency. A digital low pass filter with a cut off frequency of 10 Hz was applied to smooth the data. The applied torque and rotation speed were calculated from the measured voltage and current with the help of the

transduction matrix. The formula used to calculate torque and rotation speed is shown in Equation (4-2). The calculated torque and rotation speed were used to calculate mechanical impedance of bolted joints by substituting them into Equation (5-15).

5.2.4. Experimental result

A sample of measurement results is shown in Figures 5-5 to 5-8. The sample is taken from a bolted joint with preload of 10kN, rough surface condition and under 1.0 Hz excitation frequency. The figure shows that the torque and rotation speed oscillates with a frequency of 1 Hz. The preload decreases whereas the real and imaginary parts of the mechanical impedance are oscillating. Thus, the mean values of the mechanical impedance for each cycle are calculated to get the close value of mechanical impedance as suggested from Appendix C. The calculation result is plotted in Figure 5-9. Figure 5-9 shows that the real part of mechanical impedance decreases while the imaginary part of mechanical impedance increases. These results show that mechanical impedance is related to the preload.

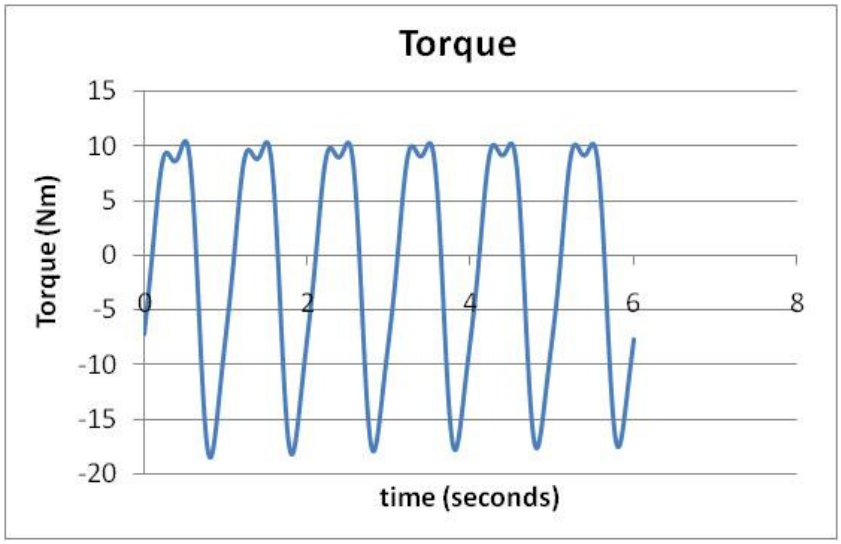

Figure 5-5 Excitation torque of the bolted joint

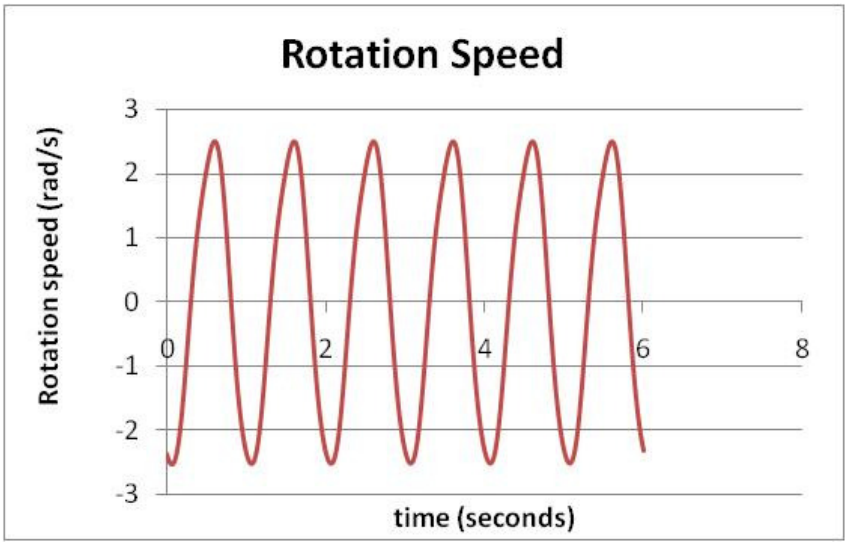

Figure 5-6 Rotation speed response of the bolted joint

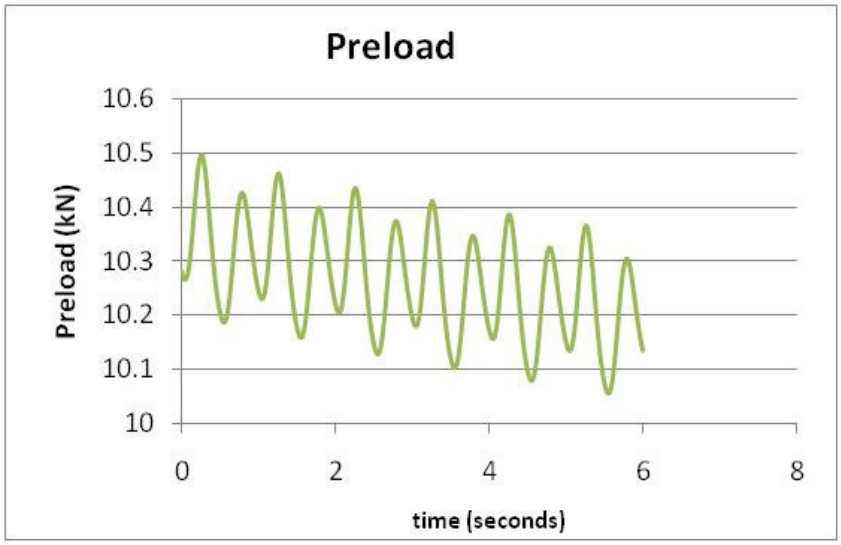

Figure 5-7 Preload of the bolted joint during the excitation

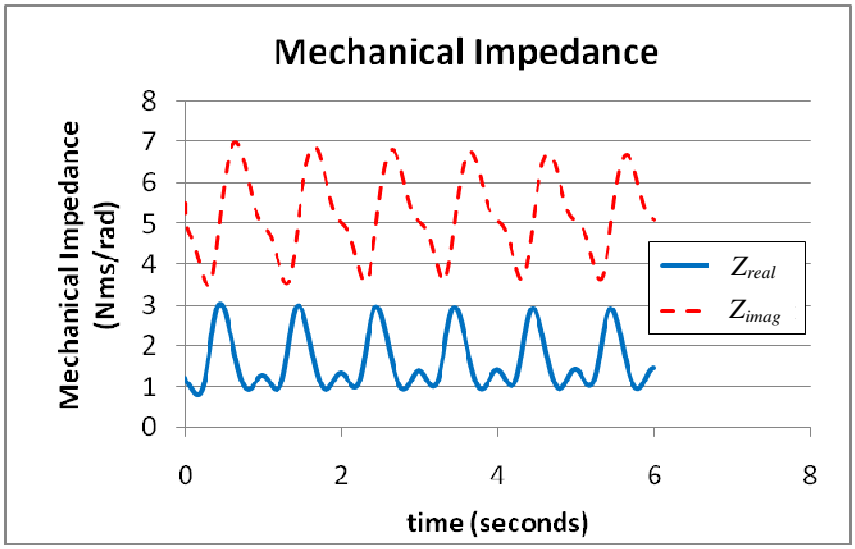

Figure 5-8 Impedance of the bolted joint

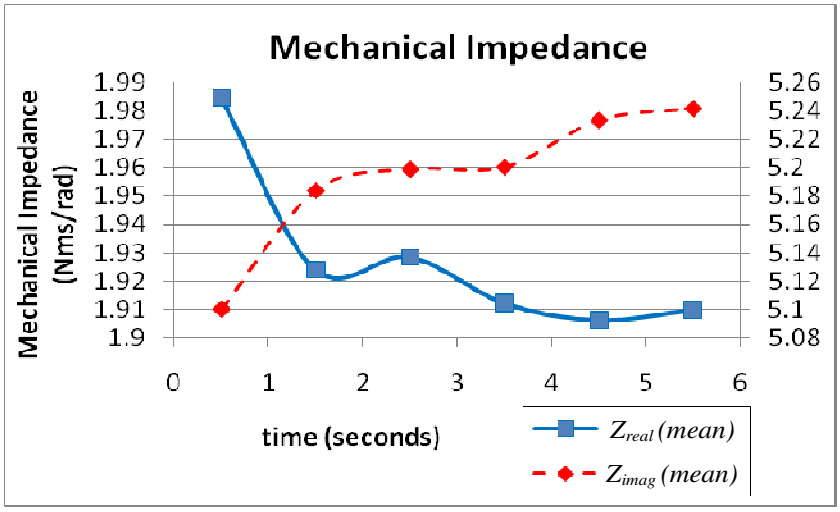

Figure 5-9 Mean value of mechanical impedance

Figures 5-10 to 5-15 show how the mechanical impedance of the bolted joints changes under different friction conditions, excitation frequencies, and preloads. The real part increases with an increase of the bolt preload whereas the imaginary part decreases. Apart from the preload, the surface friction (no lubricant) and the excitation frequency also affect the mechanical impedance. An increase in surface friction causes the real part to increase and imaginary part to decrease. On the

other hand, an increase in excitation frequency causes both the real and imaginary part to decrease.

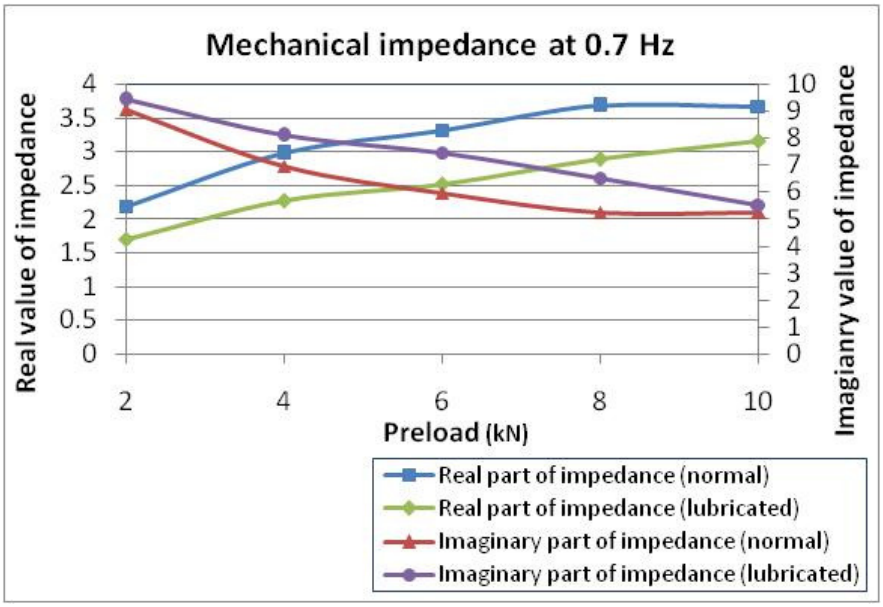

Figure 5-10 Real and Imaginary part of Impedance for frequency 0.7 Hz

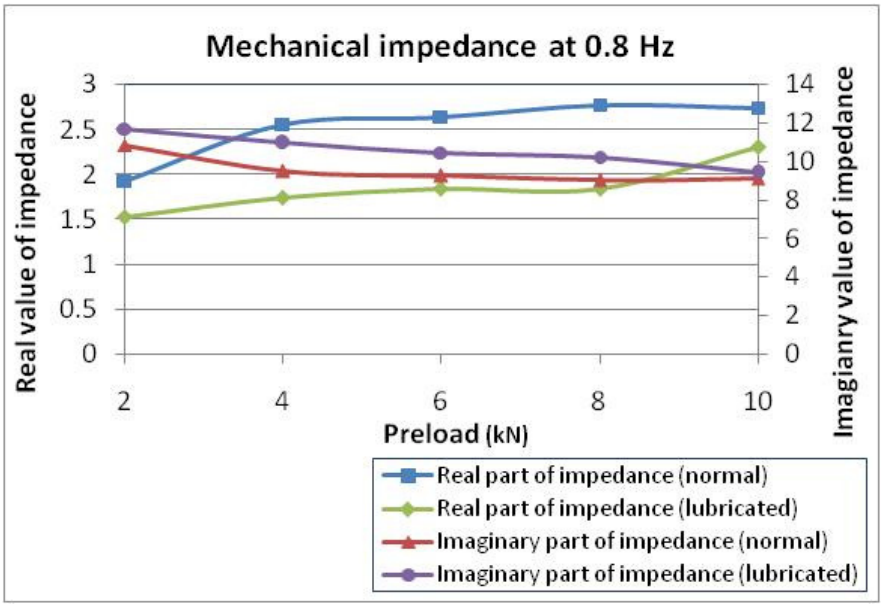

Figure 5-11 Real and Imaginary part of Impedance for frequency 0.8 Hz

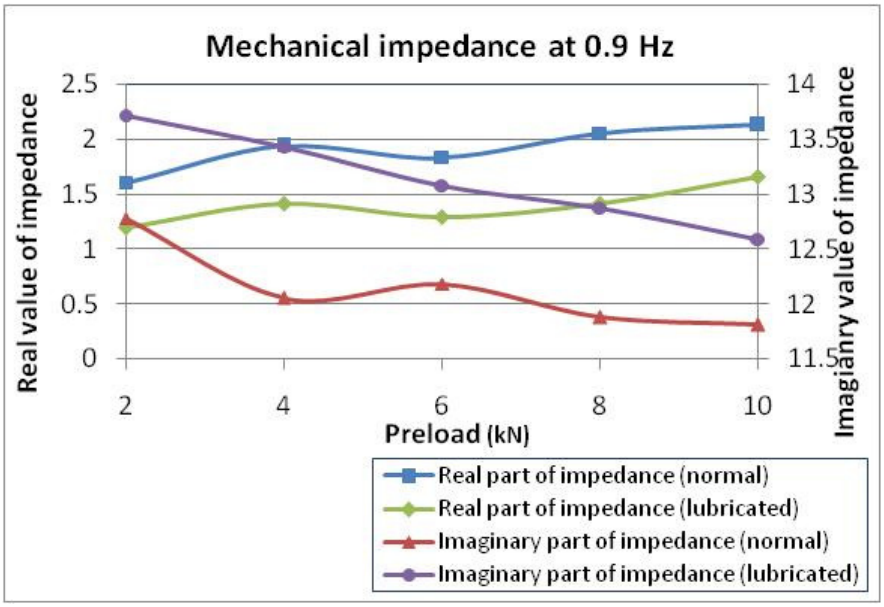

Figure 5-12 Real and Imaginary part of Impedance for frequency 0.9 Hz

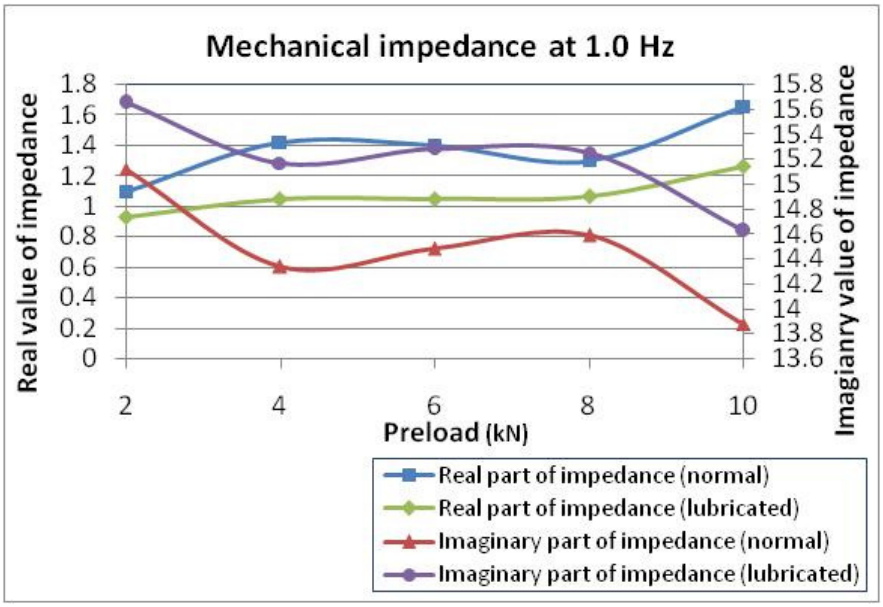

Figure 5-13 Real and Imaginary part of Impedance for frequency 1.0 Hz

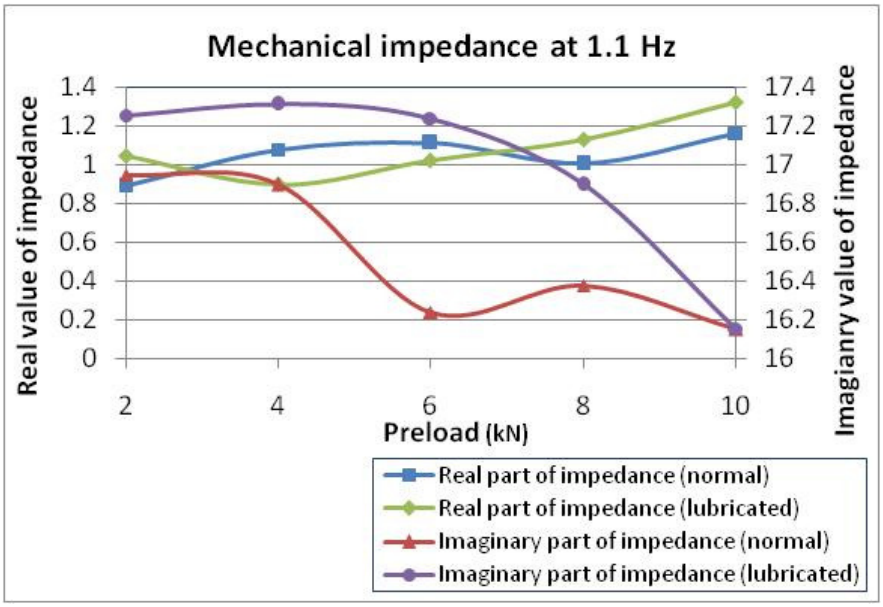

Figure 5-14 Real and Imaginary part of Impedance for frequency 1.1 Hz

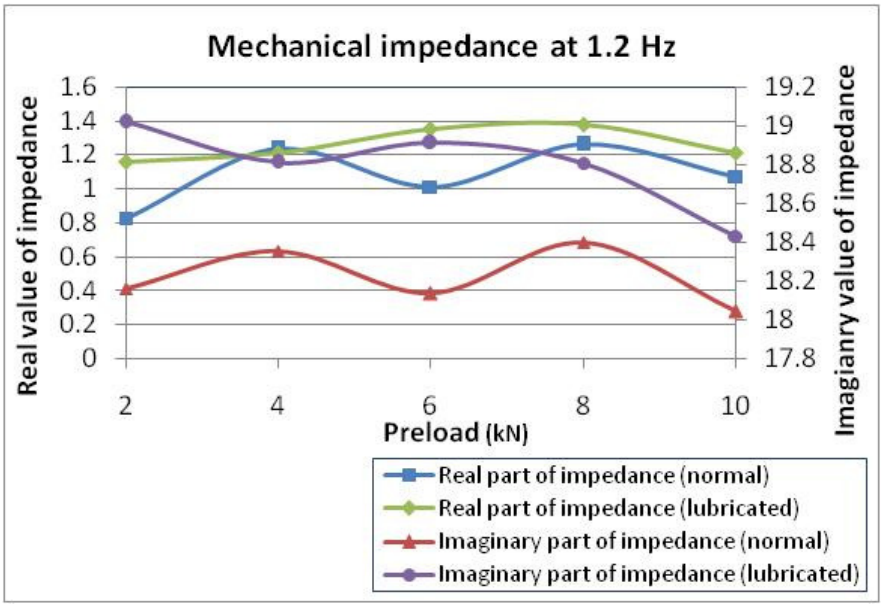

Figure 5-15 Real and Imaginary part of Impedance for frequency 1.2 Hz

Equation (5-10) is used to calculate the damping of the bolted joints. The results show that the damping is affected by the excitation frequency. This indicates that there is a hysteretic damping in the bolted joint. The hysteretic damping is the internal damping of the material and is related with excitation frequency.

However, this thesis does not explore further regarding this hysteretic damping due to its less importance in affecting loosening.

Beside excitation frequency, the preload and the surface friction also affect the damping coefficient. The relationship between the damping value and the excitation frequency, preload and friction conditions of bolted joint are divided into several parts first before it is determined. Table 5-2 shows the linear relationship between the damping value and the preload for each excitation frequency and surface friction.

The plots in Figures 5-16 and 5-17 show the relationship between the damping value and the excitation frequency, preload and friction conditions of bolted joint.

Frequency (Hz)	Relationship	
	Normal Condition	Lubricated
0.7	$C_{bolt} = \frac{0.252P}{1000} + 1.557$	$C_{bolt} = \frac{0.204P}{1000} + 1.257$
0.8	$C_{bolt} = \frac{0.139P}{1000} + 1.631$	$C_{bolt} = \frac{0.080P}{1000} + 1.374$
0.9	$C_{bolt} = \frac{0.113P}{1000} + 1.167$	$C_{bolt} = \frac{0.055P}{1000} + 1.052$
1.0	$C_{bolt} = \frac{0.067P}{1000} + 0.948$	$C_{bolt} = \frac{0.043P}{1000} + 0.802$
1.1	$C_{bolt} = \frac{0.031P}{1000} + 0.853$	$C_{bolt} = \frac{0.046P}{1000} + 0.795$
1.2	$C_{bolt} = \frac{0.016P}{1000} + 0.997$	$C_{bolt} = \frac{0.038P}{1000} + 1.005$

Table 5-2 Linear relationship between damping and preload

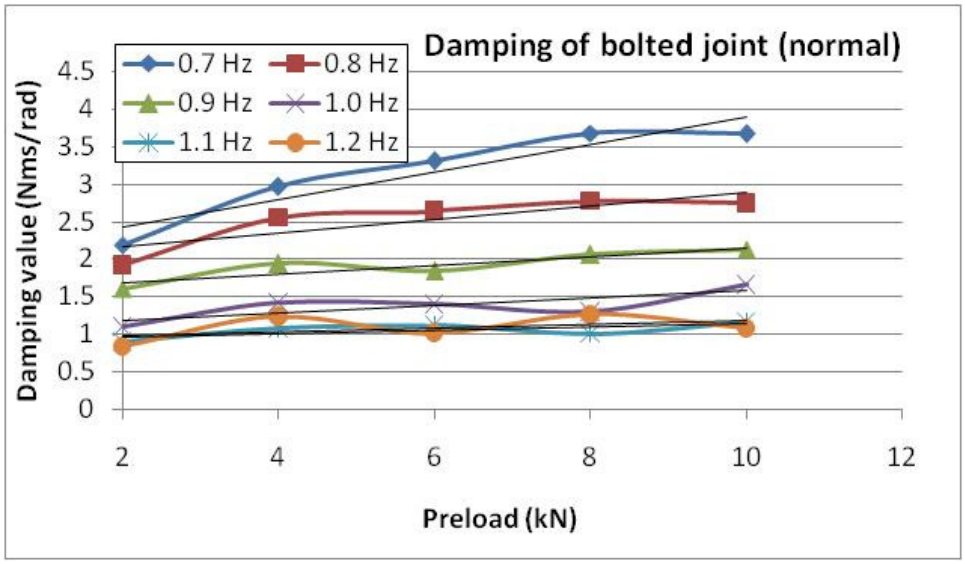

Figure 5-16 Damping of bolted joints under normal friction condition

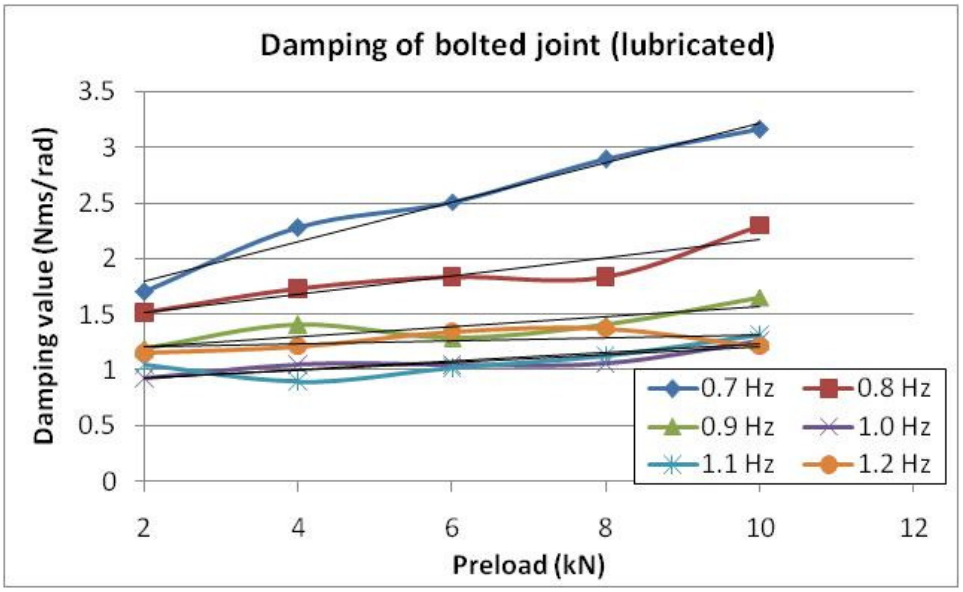

Figure 5-17 Damping of bolted joints under lubricated condition

Equation (5-13) is used to calculate the mass and stiffness of bolted joints. The imaginary parts of the mechanical impedance from different excitation frequencies are substituted into the equation. It is observed that the surface friction and preload of the bolt affect the imaginary part as well. Hence, the imaginary parts to be substituted into the equation have to be obtained under the

same bolt preload and surface condition. The calculated mass and stiffness values were obtained from different preload and surface friction conditions and the results are plotted in Figures 5-18 and 5-19. The results show that the effective mass and stiffness increase as the bolt preload increases. The mass in both normal and lubricated conditions is around 2.65 to 3 kgm^2whereas the stiffness of bolted joints varies from 2.00 to 35.00 Nm/rad. As the mass is always constant, the average value from the measurement can be calculated and the mass of bolted joint is as follows:

$$I_{bolt} = 2.87\,\text{kgm}^2/\text{rad} \tag{5-15}$$

The relationship between stiffness and preload of the bolt is assumed to be linear. Hence:

a) In a normal condition:

$$K_{bolt} = \frac{3.2137P}{1000} + 6.725 \tag{5-16}$$

b) In a lubricated condition:

$$K_{bolt} = \frac{3.0369P}{1000} + 3.1349 \tag{5-17}$$

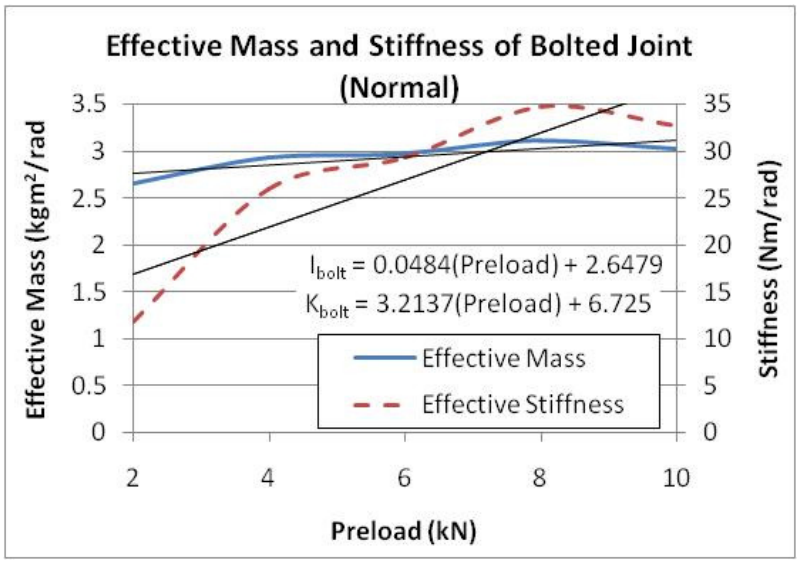

Figure 5-18 Effective mass and stiffness of bolted joints under normal friction condition

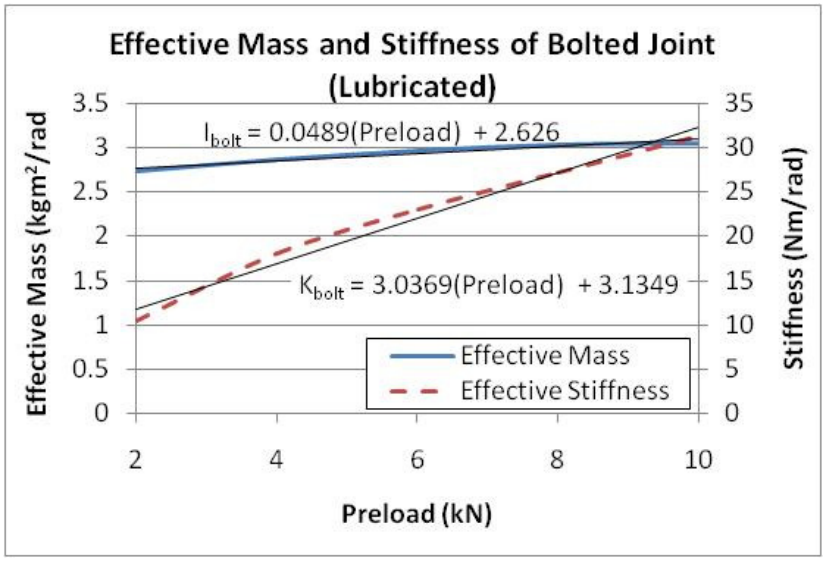

Figure 5-19 Effective mass and stiffness of bolted joints under lubricated condition

5.2.5. Hysteresis graph of the mass, spring, and damping model of bolted joints

To verify the mass, spring and damping model of bolted joints, hysteresis graphs between the torque and angle displacement of the model were formed and compared. The angle displacements are calculated by substituting the measured rotation speed into Equation (4-5). The torque of bolted joint model is then calculated from the measured rotation speed, mass, damping and rotation speed values based on the following formula:

$$T_{exc} = I_{bolt}\dot{\Omega}_{resp} + C_{bolt}\Omega_{resp} + K_{bolt}\int \Omega_{resp} dt \tag{5-18}$$

Both the hysteresis graph of measured and system models for different excitation frequencies are plotted in Figures 5-20 to 5-25

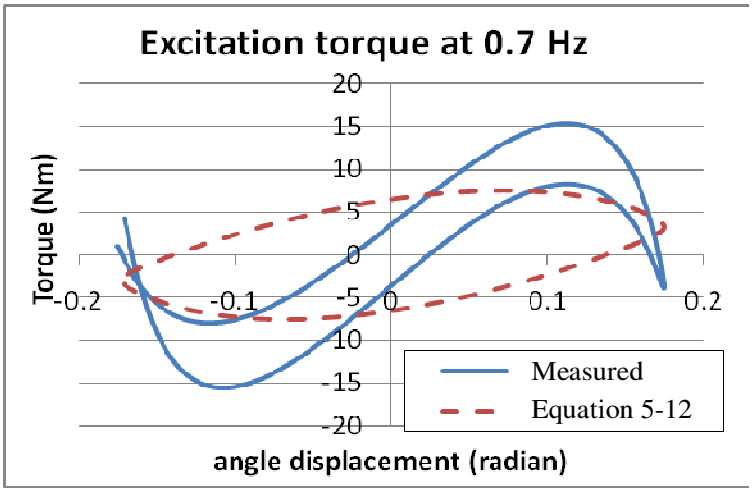

Figure 5-20 Hyteresis graph based for excitation frequency 0.7 Hz

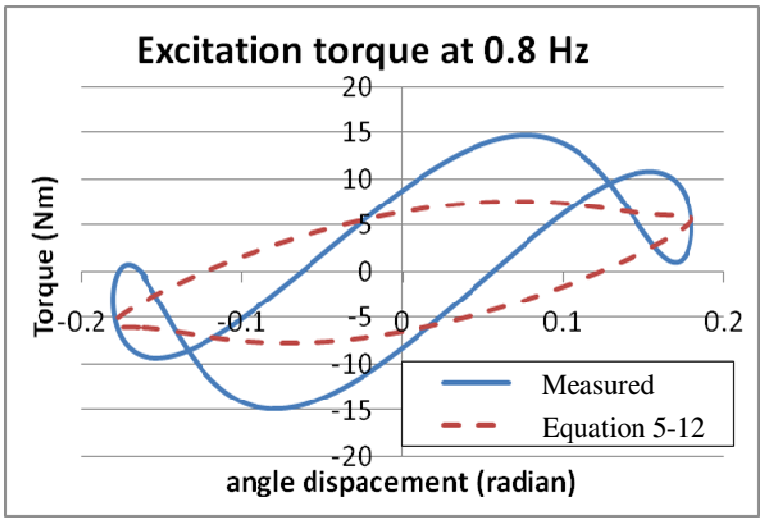

Figure 5-21 Hyteresis graph for excitation frequency 0.8 Hz

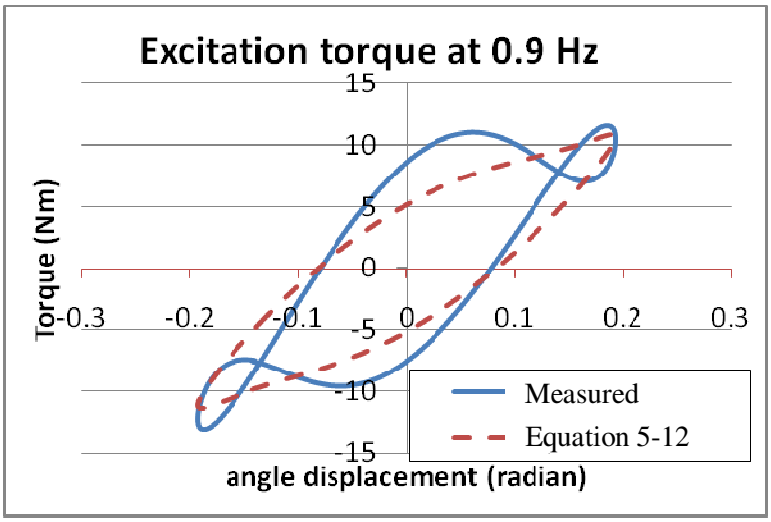

Figure 5-22 Hyteresis graph for excitation frequency 0.9 Hz

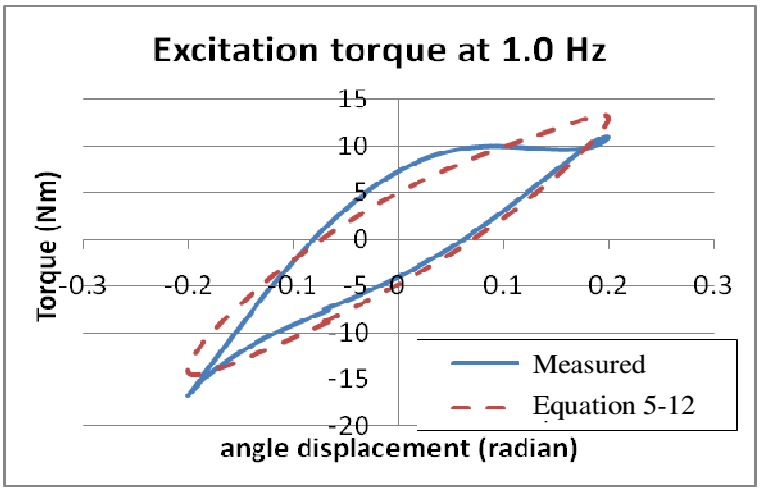

Figure 5-23 Hyteresis graph for excitation frequency 1.0 Hz

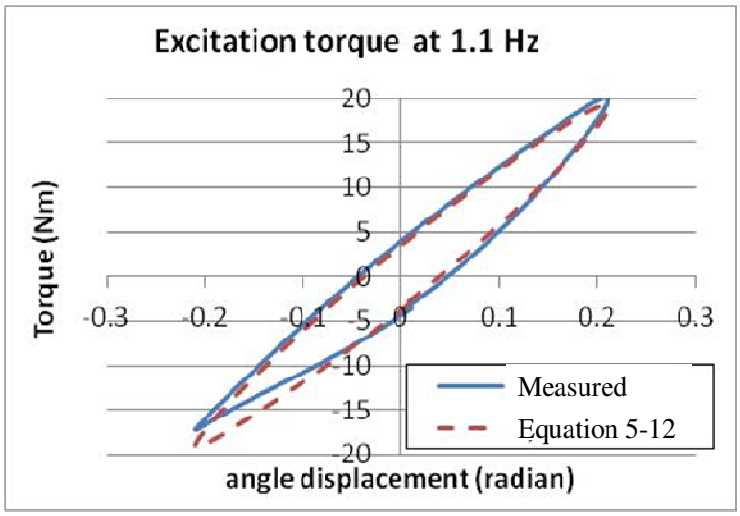

Figure 5-24 Hyteresis graph for excitation frequency 1.1 Hz

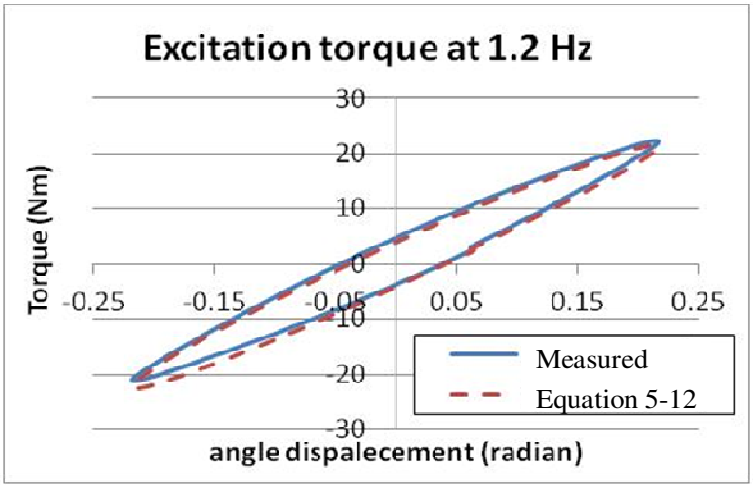

Figure 5-25 Hyteresis graph for excitation frequency 1.2 Hz

From the results, it can be seen that the hysteresis shape of the system model matches almost perfectly with the shape of experimental measured model for excitation frequencies from 1.0 to 1.2 Hz. For excitation frequencies from 0.7 to 0.9 Hz, the shape does not match perfectly. Towards the end when the angle changes direction, a drop in torque can be observed. This is caused by the change in dry friction at the bolt. Thus, a simple m, c, and k system is not suitable for modelling bolted joints excited with frequencies from 0.7 to 0.9 Hz.

5.3. Angular response of bolted joint to transverse vibration

After obtaining the dynamic model of the bolted joints, the response of the bolted joint can be simulated with a defined excitation. As mentioned in the literature, transverse vibration is a common cause of the self-loosening of bolted joints. Due to the configuration and geometry of the bolt, a torque at the bolted joint is generated by the transverse vibrations. The generated torque excites the joint and causes the loosening. The loosening torque is derived in Appendix C. The derivation shows that sinusoidal transverse force ($|F\ sin\omega_f t|$) on the bolted joint is transformed into a continuous shock spectrum ($|T\ sin\omega_f t|$). To evaluate the response of bolted joints under the loosening torque the calculations steps, shown below in this section, are taken.

5.3.1. Response of simple mass, spring and damping system in discrete time

As explained previously, the bolted joints are modelled as a simple mass (I_{bolt}), spring (K_{bolt}) and damping (C_{bolt}) system. When an impulse excitation is applied to the system, the response of the system is calculated as follows:

$$g(t) = \begin{cases} \dfrac{1}{I_{bolt}\omega_d} e^{-\varsigma\omega_n t} \sin\omega_d t & for\ t > 0 \\ 0 & for\ t < 0 \end{cases} \tag{5-19}$$

where ω_n, ω_d, and ζ are the natural frequency, damped natural frequency, and damping ratio of the system. They are each calculated as follows:

$$\omega_n = \sqrt{\frac{K_{bolt}}{I_{bolt}}} \tag{5-20}$$

$$\varsigma = \frac{C_{bolt}}{2\sqrt{K_{bolt} I_{bolt}}} \tag{5-21}$$

$$\omega_d = \omega_n \sqrt{1-\varsigma^2} \tag{5-22}$$

When the system is excited under a arbitrary torque (T_{exc}), its response can be obtained using the superposition method. The arbitrary torque is assumed to be a

superposition of impulses with varying magnitude applies at different times. The response is then calculated by summing the responses of each impulse as follows:

$$\theta_{bolt}(t) = \int_0^t T_{exc}(\tau)\, g\left(t-(\tau)\right) d\tau \tag{5-23}$$

As the torque and system properties are stored in the discrete time, the equation should accordingly be changed into discrete time to calculate the response of bolted joints. To change the equation into discrete time, a sample time, *T* seconds, is chosen to divide the normal time (*t*) into *n* number of samples. The relationship between them can be expressed as follows:

$$t = nT \tag{5-24}$$

For each sample, there is an impulse excitation (*g(n)*) given to the system for *T* second. The impulse response is formulated as follows:

$$g(n) = Tg(t) \tag{5-25}$$

By substituting Equations (5-24) and (5-25) into Equation (5-19), the impulse response in discrete mode can be expressed as follows:

$$g(n) = \frac{T}{I_{bolt}\omega_d} e^{-\varsigma\omega_n nT} \sin \omega_d nT \tag{5-26}$$

The response of the system in discrete mode can then be calculated by transforming Equation (5-23) as follows:

$$\theta_{bolt}(n) = \sum_{k=0}^{n} T_{exc}(k)\, g(n-k) \tag{5-27}$$

Using Equation (5-27), the response of bolted joint under an excitation torque can be calculated. The next part shows sample calculations of bolted joint under excitation torques.

5.3.2. Samples calculation of response of bolted joint under excitation torque due to transverse vibration

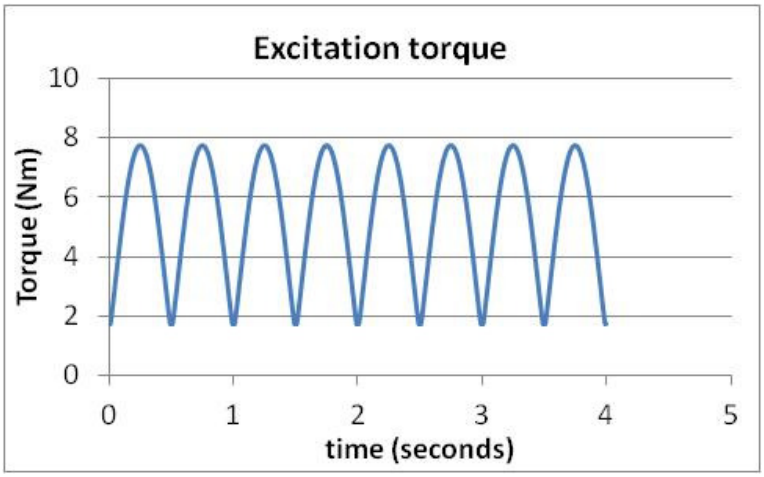

Figure 5-26 Excitation torque to bolted joint

A bolted joint without a lubricant is tightened with a preload value of 8,000 N. A transverse vibration is then applied to the joint with an excitation frequency of 1 Hz. The vibration generates a continuous loosening torque, shown in Figure 5-26, at the bolted joint. The derivation and values of the loosening torque are shown in Appendix C. Based on the preload and excitation frequencies, the system properties of the bolted joint are as follows:

- $I_{bolt} = 2.87$ kgm^2/radian (5-28)

- $C_{bolt} = \frac{0.067P}{1000} + 0.948$ Nms/radian = 1.484 Nms/radian (5-29)

- $K_{bolt} = \frac{3.2137P}{1000} + 6.725$ Nm/radian = 32.4354 Nm/radian (5-30)

The impulse response of the joint is plotted in Figure 5-27.

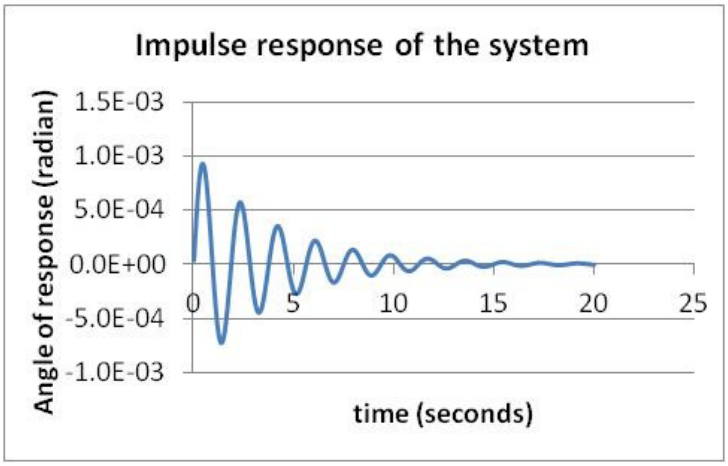

Figure 5-27 Impulse response of the system

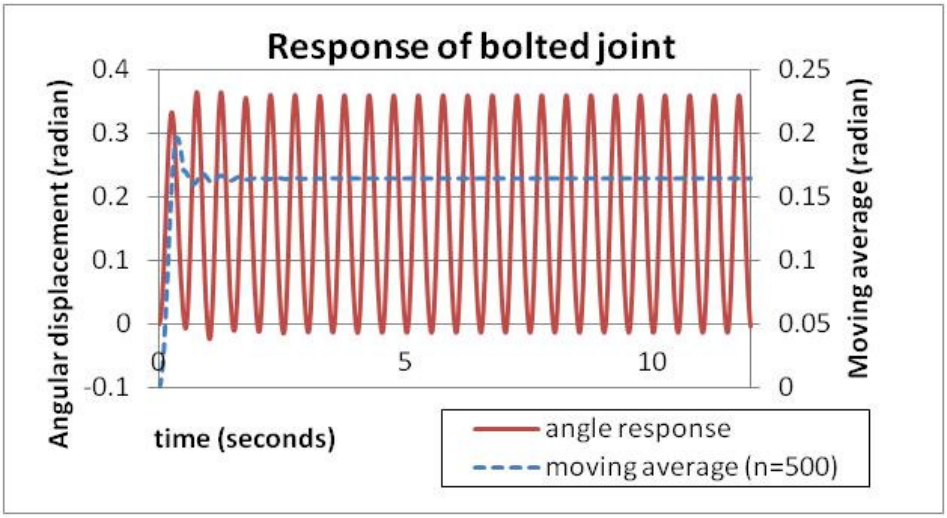

Figure 5-28 Response of bolted joint under given excitation for a constant stiffness

The loosening torque and impulse response are digitized with a sampling time of 0.002 s (T) and 8,000 data points. The sampling time, system properties, response of the bolted joint, and excitation torque are substituted into Equation (5-27) and the moving average for every 500 points is applied to the result. Figure 5-28 shows the result and the moving average of the result. Based on the moving average, it is observed that the response of the bolted joint have the same sign as the torque. This implies that the bolt is rotating in the same direction as the torque (loosening direction). After a certain point, there is no further increment in the

response angle and bolt oscillates around this point. The oscillation is caused by the stiffness of the bolted joint and existence of the torque.

As mentioned in the literature, the preload and response angle have a linear relationship. When a bolt is turned to a certain degree, a certain value of preload is acquired or lost depending on the turning direction. This preload also affects the stiffness and damping of the bolted joint as mentioned earlier. Thus, the bolted joints' damping and stiffness changes when the bolt turns.

The relationship between the preload and response angle of the bolted joint is normally obtained experimentally. Figure 5-29 shows an example of the relationship for the normal bolt used in the experiment. Based on the figure, the relationship is written as follows:

$$\Delta P = 6413.3 \ \Delta\theta_{bolt} \tag{5-31}$$

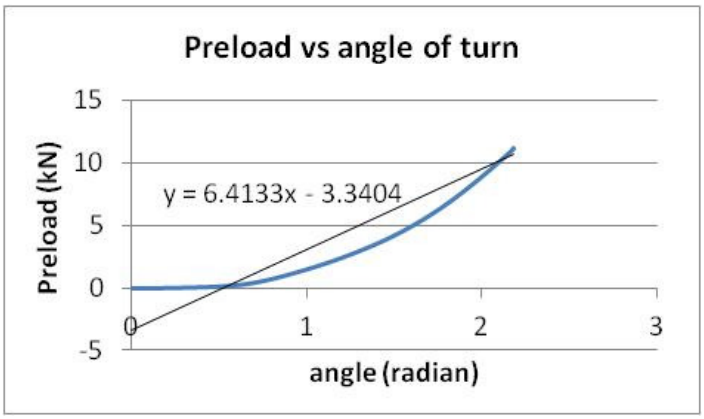

Figure 5-29 Relationship between Preload and angle of turn

Thus, the damping and stiffness of bolted joint for a 8,000 N preload in terms of response angle can be written by substituting Equation (5-31) into Equations (5-29) and (5-30), where

$$C_{bolt} = 1.484 - 0.4297\theta_{bolt} \tag{5-32}$$

$$K_{bolt} = 32.4354 - 20.61047\theta_{bolt} \tag{5-33}$$

Using Equations (5-32) and (5-33), response of bolted joint is solved by changing the value C_{bolt} and K_{bolt} for each response angle. Thus, to find the new value of C_{bolt} and K_{bolt}, the response angle needs to be solved for every data point. Based on their values, the next response angle can be calculated. For this purpose, the Matlab code shown in Appendix D is used. The code is used to obtain the response of bolted joint under an arbitrary torque. By substituting the torque response in Figure 5-26, the response of bolted joints is obtained and plotted in Figure 5-30. The result shows that the amplitude response of the system is higher than previous result in Figure 5-28. To smooth the line, the moving average for 500 data points is applied to the response. The trend shows that the response of bolted joint gradually increases in the loosening direction. Thus, it is concluded that a change of system properties affects loosening.

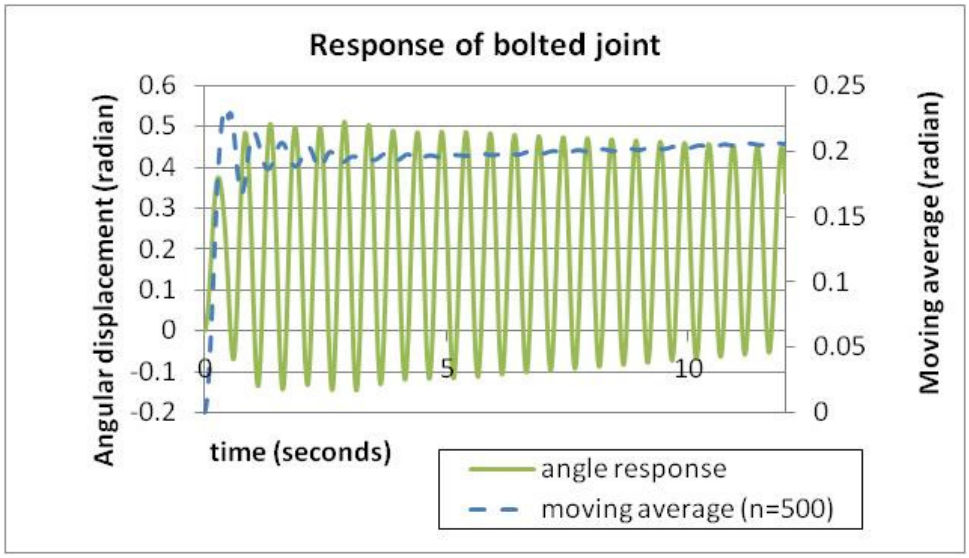

Figure 5-30 Response of bolted joint due to stiffnes reduction

5.3.3. Factors affecting the response of the bolted joint

Based on the sample calculation shown earlier, it can be seen that the response of the bolted joint to excitation is affected by the system properties and amplitude of the excitation. The effects of these factors are as follows:

a) Amplitude excitation of torque

Equation (5-23) shows that the response of the bolted joint is linearly related with the excitation torque of bolted joint. A higher excitation value leads to a higher response value. In this case, the higher the excitation torque given to bolted joint is, the faster the bolted joint is loosened. Figure 5-31 shows the response of bolted joint under different excitation torques (0.1, 0.5, and 1 time). By taking the moving average value of the response, the trend of each response are obtained and plotted in Figure 5-32. Figure 5-32 shows that a higher amplitude of excitation leads to a high increment of response (i.e. faster rate of loosening).

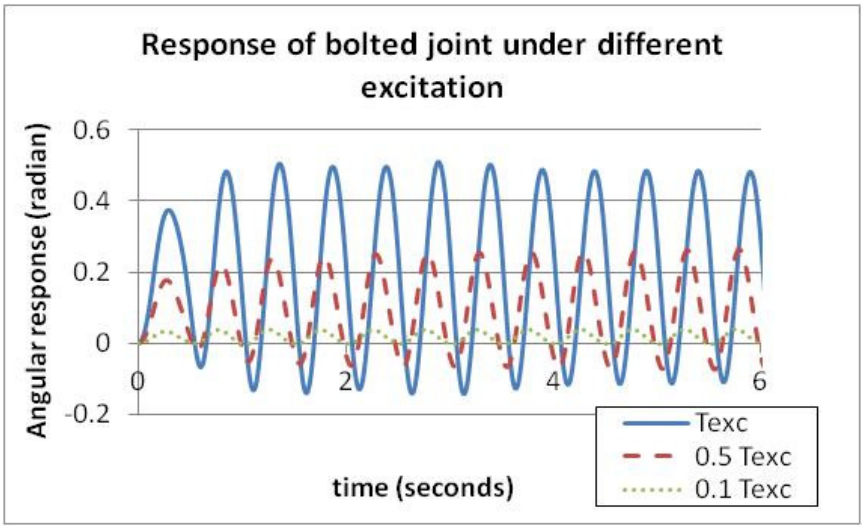

Figure 5-31 Response of bolted joint under different excitation

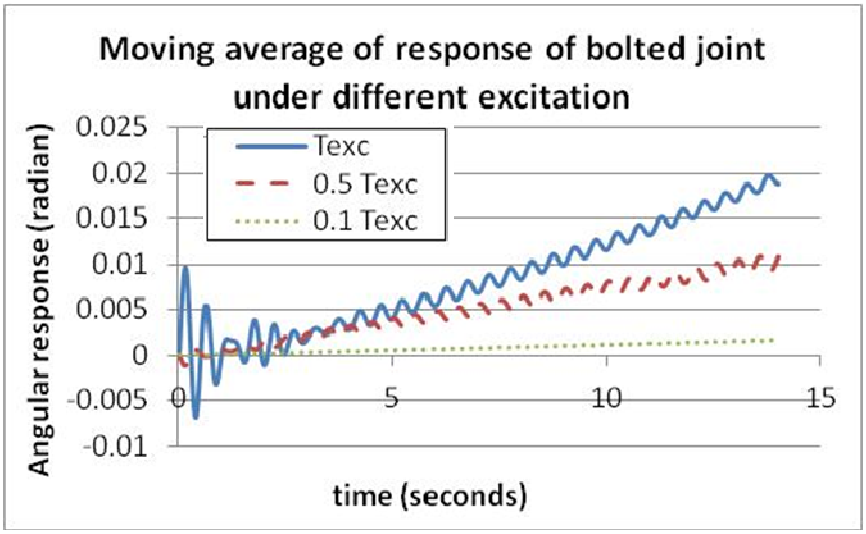

Figure 5-32 Moving average of the response of bolted joint under different excitation

b) Damping of bolted joint

Damping is a system property that dissipates energy. In the previous section, it was mentioned that the damping of bolted joint varies with the excitation frequency. A higher excitation frequency leads to a lower value of damping. Figure 5-33 shows response of bolted joint under different damping conditions. It also shows that a higher damping value will lead to a reduction of amplitude of response. However, the damping does not affect the rate of loosening. Figure 5-34 is plotted by taking the moving average of the results, and shows that the loosening rates of response are similar.

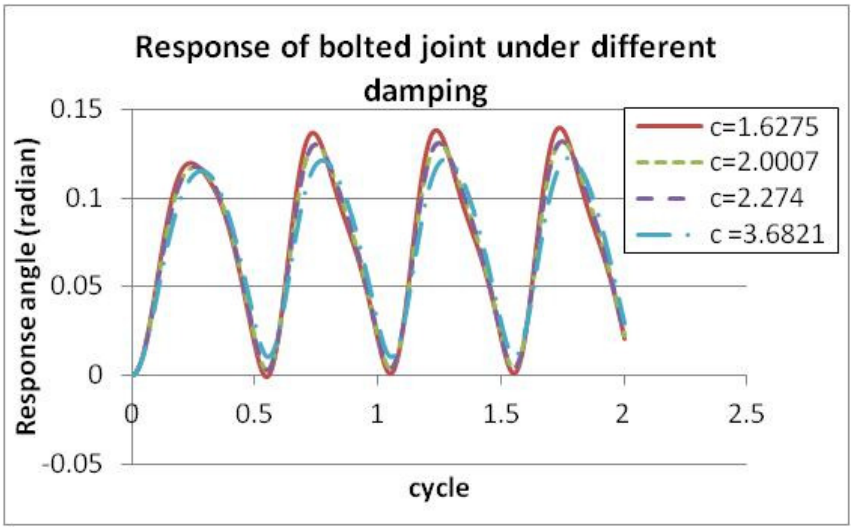

Figure 5-33 Response of bolted joint under different damping

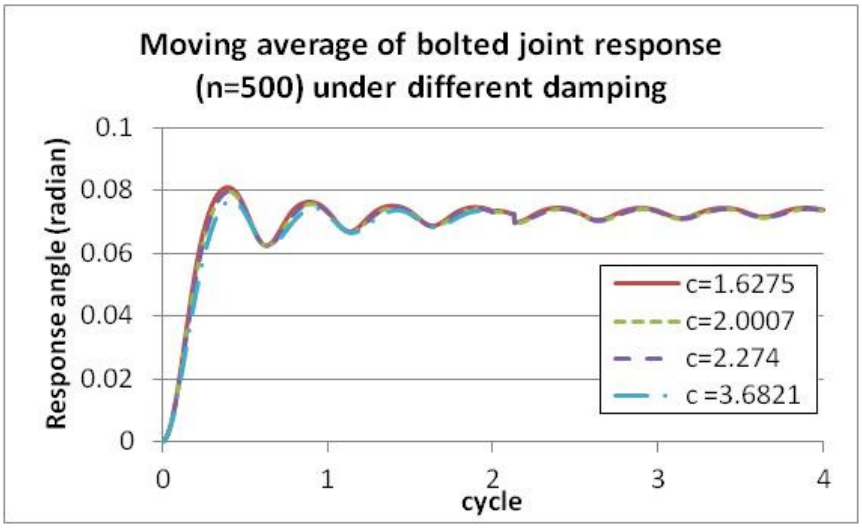

Figure 5-34 Average value of response of bolted joint under different damping

c) Stiffness of bolted joint

Stiffness is a system property that measure flexibility of the system. A higher stiffness value leads to less flexibility in the system. As discussed earlier, the stiffness of bolted joint is linearly related with preload of bolted joint. A higher preload value implies a higher stiffness. The effect of a higher value of stiffness on the response of the bolted joint is shown in Figure 5-35 below. A higher stiffness value leads to lower amplitude of response of the bolted joint.

Figure 5-36 shows that a bolted joint which is less stiff loosens faster. Hence, it is advisable to have a bolted joint with higher stiffness to reduce loosening due to vibration.

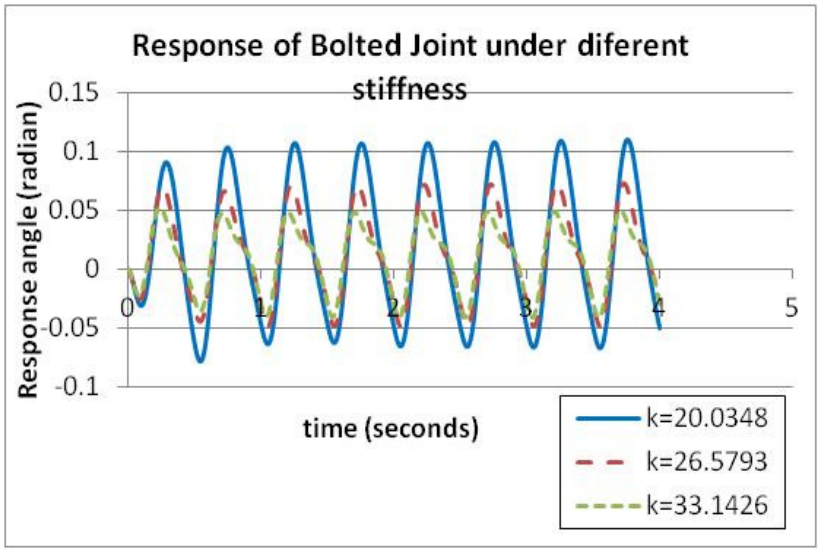

Figure 5-35 Response of bolted join under different stiffness

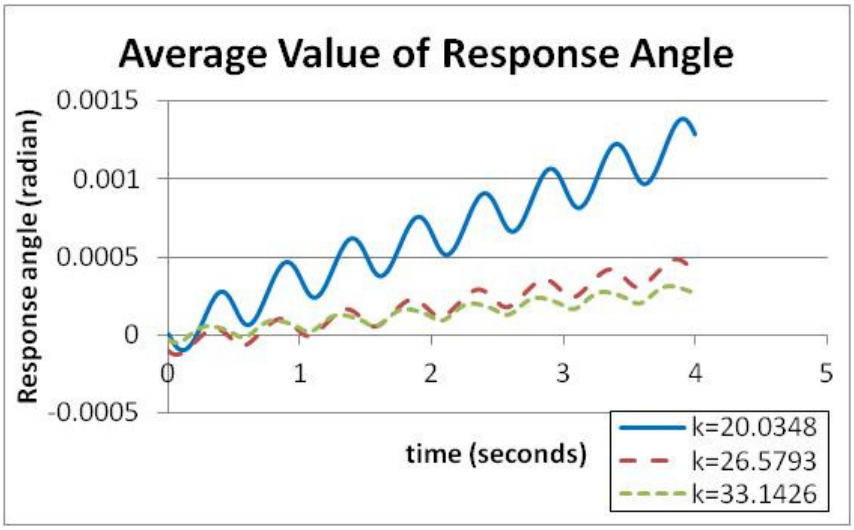

Figure 5-36 Average value of bolted joint under different stiffness

5.4. Summary

A method to obtain the mechanical impedance of time variant system with Hilbert Transform as the processing tool was explained in this chapter. The Hilbert Transform, as one of signal processing tool, transforms a signal in the same domain (time domain) and generates the imaginary part of the signal. An analytic signal can be created with a combination of the real imaginary part of the signal. The mechanical impedance is obtained by dividing the analytic signal of force with the analytic signal of velocity as shown in Equation (5-9). The mechanical impedance which is obtained is in the time domain and not the frequency domain. The frequency domain has disappeared as the mechanical impedance is solved at a particular frequency (ω_f). Since the results of the mechanical impedance taken from the sample calculation are oscillating, it is necessary to take the average value of the results. Furthermore, the mechanical impedance is used to derive the system properties of the bolted joints. For a simple mass, spring and damping system, the real part of mechanical impedance represents the damping of the system while the imaginary part represents the mass and stiffness of the system. The relationships were shown in Equations (5-10) and (5-11).

The behaviour of bolted joints under vibration can be modelled on this simple mass, spring and damping system. The system properties of the bolted joints can be identified from measuring the mechanical impedance of bolted joints and substituting it into Equations (5-10) and (5-13). A DC motor with a calibrated transduction matrix is employed to perform this task. The motor applies a single frequency sinusoidal excitation to the bolted joint and the response is reflected in the motor shaft. For the purposes of measuring the mechanical impedance, the excitation is the torque and the response is the rotational speed. The torque and rotation speed are obtained from the measured electrical input of motor with the help of the transduction matrix. Hilbert Transform is applied to the torque and rotation speed signal to obtain the mechanical impedance and the system properties are derived from the mechanical impedance. In this experiment, bolted joints with different tightness, surface condition, and excitation frequency are

measured. The results show that the damping and stiffness of bolted joint are affected by the preload of the bolted joint and surface condition. The hysteresis curve shows that the simple mass, spring and damping system only fit perfectly for excitation at frequencies above 1.0 Hz. Another system model is needed for bolted joint excited at frequencies below 1.0 Hz as the system is affected by dry friction.

After obtaining the system properties of bolted joint, the loosening mechanism of the bolted joint under transverse vibration can be studied. The response of the bolted joint is calculated by substituting the system properties and the excitation frequency into Equation (5-27). Based on the response, the cause of loosening at bolted joints can be investigated. The results show that the change in the system properties of the bolted joint can be attributed to the rotation of the bolt. Due to this change, especially in the stiffness, the oscillation of the bolted joint increases and cause the amplitude of oscillation to be higher until the total loosening occurs. This phenomenon explains why loosening occurs at a low rate at the outset and gradually increases in rate.

CHAPTER 6
CONCLUSIONS AND RECCOMENDATIONS

This chapter summarizes the completed works, major findings from the research and relevant suggestions.

6.1. Conclusions

6.1.1. Transduction matrix of DC motor

In this thesis, the transduction matrix of a DC motor and its applications were investigated. A transduction matrix is a two by two matrix consisting of four frequency response functions between the electrical inputs (voltage and current) and mechanical outputs (torque and rotational speed) of an electric motor. Each element of the matrix relates one input with one of output in the frequency domain that is independent from the other elements. The value of each element reflects the system properties of the electric motor. As a DC motor is supplied with electrical power at DC power (constant values), the transduction matrix of a DC motor is simplified as a matrix consisting of four (4) constant values (0 Hz frequency).

The values of the transduction matrix of a DC motor can be obtained by theoretical and experimental methods. The theoretical method is based on an equivalent electric circuit model of a DC motor. The values of the matrix are obtained by applying two boundary conditions to the circuit model. On the other hand, for the experimental method, the values of the matrix are obtained from a pair of electrical input and mechanical output of a DC motor under different load conditions based on Equation (3-39). It is assumed that the transduction matrix obtained relates the electrical input to the DC motor with its mechanical output linearly within its operating range. Since the relationship is linear, the mechanical output of the DC motor can be calculated from its electrical input. A comparison of the theoretical (Equation 3-41) and experimental matrixes (Equation 3-45) shows that the experimental matrix has less mean error. Thus, with the

experimentally obtained transduction matrix, the DC motor can be used as a device to actuate and measure a mechanical system, such as a bolted joint, by measuring and controlling the electrical input supplied to it.

6.1.2. Tightness indicator of bolted joint

Bolts and nuts are used to clamp two components (e.g. plates and mechanical parts) together. To clamp the two components, the bolt or the nut is turned to stretch the bolt and generate a clamping force in the components. The existence of the clamping force ensures that the joint is kept intact. The magnitude of the clamping force also indicates the tightness of bolted joint.

Besides clamping force, there are several other tightness indicators that are mentioned in the literature. These indicators are used as they have a linear relationship with the clamping force. Amongst these indicators, torque is the most commonly used as it is relatively easy to measure. However, the relationship between torque and clamping force is affected by the friction condition of the bolt. That the relationship is so affected is confirmed by the results of an experiment where the value of the clamping force between a set of normal bolt and a set of lubricated bolt are compared. With the same value of tightening torque, the clamping force generated by the lubricated bolt is higher than the clamping force generated from the normal bolt.

This thesis proposed a new tightness indicator based on the total energy input during the tightening process. The total energy input is calculated by integrating, with respect to time, the torque applied to the bolted joint multiplied by the rotational speed during tightening (Eqn. 3-20). This calculation is made possible with the use of the transduction matrix, which allows the torque and rotational speed during the tightening of the bolted joint to be concurrently obtained from the electrical input of the DC motor, and hence for the total energy input during the tightening process to be measured. It was found that the total energy input is a better indicator of clamping force than torque. It is able to distinguish different

preloads in the two different cases of the lubricated and normal bolts which have the same value of tightening torque. This is because the total energy input, which consists of the potential energy stored in the bolt and which is linearly related to the clamping force, is independent of coefficient of friction.

6.1.3. Time variant mechanical impedance measurement with Hilbert Transform as the signal processing tool

Mechanical impedance is a form of frequency response function. It is obtained by dividing the excitation over response of the system in the frequency domain. The excitation is the torque applied while the response is the rotational speed. It describes the resistance of the system to a motion applied to it, which is a property of the system. In the case of a tightened bolted joint, the mechanical impedance describes the resistance of a tightened bolted joint to an external disturbance.

The Hilbert Transform is a signal processing tool that transforms a signal in the same domain (time domain) and generates the imaginary part of the signal. An analytic signal can be created by combining the real and imaginary part of the signal. The mechanical impedance of the time variant system can be obtained with the help of the Hilbert Transform as shown in Equation (5-9). The mechanical impedance is obtained in the time domain and not in frequency domain. The frequency of obtained mechanical impedance is limited to a particular frequency, which is the excitation frequency (ω_f). Following this concept, the mechanical impedance of a tightened bolted joint can be measured with a calibrated DC motor with a known transduction matrix. To obtain the mechanical impedance at a particular frequency, the tightened bolted joint is excited with a torque at a fixed constant frequency using the DC motor. Due to the excitation, the tightened bolted joint gives out a response in form of rotational speed. The magnitudes of the torque applied to the tightened bolted joint and the rotational speed response from the torque can be obtained from electrical input of the DC motor with the help of its transduction matrix. The torque and rotation speed that is obtained are assumed to be mechanical signals of the tightened bolted joint. The Hilbert Transform is

applied to the mechanical signals to obtain their real part and imaginary parts in the time domain. The mechanical impedance is calculated by dividing the real and imaginary parts of the torque signal over the rotational speed signal. Since the mechanical impedance is obtained in time domain, it can be monitored over a period of time. However, the mechanical impedance is restricted to a particular frequency only which is the applied constant frequency.

The measured mechanical impedance of the tightened bolted joint shows that its real part and imaginary parts are affected by the clamping force of the joint (preload), the surface condition of the bolt and the excitation frequency (Figures 5-10 to 5-15). The real part increases with an increase in preload at the tightened bolted joint, an increase in surface friction (no lubricant) and a decrease in excitation frequency. An increase in the real part implies an increase in the resistance of the bolted joint to motion applied to it, as the real part and damping are associated. The imaginary part increases with a decrease in preload, a decrease in surface friction (applying lubricant to the surface) and an increase in the excitation frequency. The imaginary part is related to the mass and stiffness of the system. Hence, to better understand the changes of imaginary part, system modelling is carried out for the tightened bolted joint. This model is explained in the next section.

6.1.4. System modelling and identification of a tightened bolted joint

A bolted joint under excitation can be modelled as a simple linear time-variant mechanical system consisting of mass, spring and damping. Mass, spring and damping are properties of a mechanical system which describe the dynamic behaviour of the system. The relationship between mechanical impedance and the system's properties is described in Equations (5-10) and (5-11). The real part of the impedance (resistance) is associated with the damping of the system while the imaginary part of the impedance (reactance) is associated with the mass and spring of the system. The result of system properties of the tightened bolted joint are plotted in Figures 5-16 to 5-19.

Based on the figures, the effective mass is assumed to be constant due to the small change in its value. It can also be seen that the change in effective stiffness depends on the preload and surface friction (Figures 5-18 and 5-19). The stiffness increases with an increase in the preload and surface friction. The increase in preload and friction leads to an increase in system rigidity, thus allowing smaller oscillations to occur in it. Similarly, the damping increases with an increase in surface friction and preload. The surface friction and preload increases the resistance of the tightened bolted joint. Hence it dissipates more energy to prevent loosening. The damping decreases with an increase in excitation frequency. This decrease in damping may be explained by the effect of structural damping where the damping is inversely proportional to the excitation frequency.

The simple mass, spring and damping model is only applicable for bolted joint under an excitation frequency above 1.0 Hz as shown in the Hysteresis curve (Figures 5-23 to 5-25). The hysteresis curve constructed from the model almost match with the hysteresis curved constructed from the measured data. However, another system model is needed for bolted joints excited at frequencies below 1.0 Hz as the hysteresis curve does not match.

6.1.5. Transverse vibration leading to self loosening of the bolted joint

Transverse vibrations of a bolted joint can lead to self-loosening of the joint. The transverse force applied to the bolted joint causes its top plate to slide relatively to its bottom plate and bends the bolt. The bolt's bending generates a bending moment at the bolted joint and affects its axial force. Due to the linear relationship between friction force and axial force, a change in the axial force affects the frictional force. Thus, a certain region of the bolted joint has a smaller frictional force and permits a sliding motion. The sliding motion, especially at threaded part of the bolt, rotates the bolt in the loosening direction with a certain value of torque. The transformation of the transverse force applied on the bolted joint to a loosening torque is mathematically derived in Appendix B. From the derivation, it

can be seen that a sinusoidal transverse force applied on a bolted joint is transformed to a loosening torque in the form of absolute value of sinusoidal ($|\sin\theta|$). The factors that affect the amplitude of the loosening torque are the preload, the transverse force, the coefficient of friction, the grip length and the thread type of the bolted joint. The preload and coefficient of friction reduce the amplitude of the loosening torque. The transverse force and grip increase the amplitude of the loosening torque. A fine thread has a smaller thread angle than a coarse thread and thus reduces the amplitude of the loosening torque.

A bolted joint, as a mechanical system, responds to excitation in the form of motion based on the system's properties. The response of a bolted joint to the loosening torque due to the transverse force is calculated from the convolution integral of its impulse response. The impulse response of the system can be calculated by substituting the system properties obtained and the excitation frequency into Equation (5-26). It can be concluded from the calculated result that a change in the system properties of the bolted joint can be attributed to the rotation of the bolt. Due to a change in stiffness, the oscillation of the bolted joint oscillates more and the amplitude of oscillations increases until total loosening occurs. This phenomenon explains why loosening occurs at a low rate at the outset and gradually increases in rate.

The factors which affect the response of a bolted joint to excitation are the excitation amplitude, the damping and stiffness of the bolted joint. A higher excitation amplitude leads to a greater response and the bolted joint loosens more quickly. On the other hand, greater damping leads to a lower response. However, the degree of damping does not affect speed of loosening of a bolted joint as shown in Figure 5-37. The stiffness affects both the response and speed of loosening the bolted joint. A stiffer bolted joint has a lower response and loosens more slowly. Both the stiffness and damping of the bolted joint, as explained in chapter 5, are affected by the preload of the bolted joint, its friction condition and the excitation frequency applied to it. Thus, the designer of the bolted joint should

take into consideration the amplitude and frequency of the excitations common to the applications that the bolt designed for, to decide the preload and friction condition of the bolt. The purpose of considering is to allow the designer to provide adequate stiffness and damping in his design to minimize the self-loosening effect of the bolted joint.

6.2. Future research direction and recommendation

6.2.1. Solution to change surface friction condition of a bolt

The surface friction of the bolt affects the relationship between the torque experienced by the bolt and the clamping force that the bolt exerts. The rougher the surface, the greater the torque that is needed to achieve the same magnitude of clamping force. On the other hand, surface friction helps the bolted joint resist external disturbances. Therefore, surface friction needs to be kept as low as possible during the tightening process but as high as possible after the tightening process. Hence, a solution whereby the friction condition of a bolt surface can be changed is necessary. This solution must be able to reduce the surface friction of a bolt during tightening and increase its surface friction after tightening.

6.2.2. System modelling of a bolted joint

By knowing the system properties of the bolted joint, its dynamic behaviours can be predicted. The response of a tightened bolted joint to an external disturbance can be calculated based on its system properties. This system modelling helps to ensure the proper installation of a tightened bolted joint. The selection of the bolt's material and the requisite tightness can be made from its required system properties.

In this thesis, the bolted joint was modelled as a simple mass, damping and spring system. The value of the mass, damping and stiffness are identified from the measured mechanical impedance of the bolted joint. However, it is found out that

the simple mass, damping and spring is not sufficient to model bolted joint with excitation frequency below 1 Hz. Thus, a new model need to be developed.

6.2.3. Sensorless control of electrical motor

In this thesis, it was shown that a transduction matrix is capable of relating the electrical input of an electrical motor to its mechanical output. The availability of the transduction matrix reduces the need for mechanical sensors (such as encoders, torque meters and tachometers) to measure the mechanical output of the motor. This application help in minimizing Brushless DC motor where the encoder is still needed to measure the shaft position to control the motor rotation. With the help of transduction matrix, the shaft position and the output torque of the motor can be predicted from its electrical input. The controller will able to know the shaft position without the usage of encoder. Thus, it will lead to development for sensorless control of Brushless DC motor. With this sensorless control, it helps in extending the lifetime and miniaturizing of the motor as the mechanical sensor (encoder) is subjected to wear and tear.

REFERENCES

1. Dille, J.C. *How A Bolt Works.* [cited 2012 5 May 2012]; Available from: http://home.jtan.com/~joe/KIAT/kiat_1.htm.
2. Bickford, J.H., *Introduction to the design and behavior of bolted joints*, in *Mechanical engineering*. 2008, CRC Press: Boca Raton.
3. Motosh, N., *Development of design charts for bolts preloaded up to the plastic range.* TRANS. ASME, SER. B. J. ENGNG. IND., 1976. **98**(3 , Aug. 1976): p. 849-851.
4. Junker, G.H., *New criteria for self-loosening of fasteners under vibration.* SAE Transactions, 1969. **78**: p. 314-335.
5. Housari, B.A. and S.A. Nassar. *Effect of coating and lubrication on the vibration-induced loosening of threaded fasteners.* 2006. Chicago, IL.
6. Housari, B.A. and S.A. Nassar, *Effect of thread and bearing friction coefficients on the vibration-induced loosening of threaded fasteners.* Journal of Vibration and Acoustics, Transactions of the ASME, 2007. **129**(4): p. 484-494.
7. Nassar, S.A. and B.A. Housari, *Effect of thread pitch and initial tension on the self-loosening of threaded fasteners.* Journal of Pressure Vessel Technology, Transactions of the ASME, 2006. **128**(4): p. 590-598.
8. Nassar, S.A. and B.A. Housari, *Study of the effect of hole clearance and thread fit on the self-loosening of threaded fasteners.* Journal of Mechanical Design, Transactions of the ASME, 2007. **129**(6): p. 586-594.
9. Ibrahim, R.A. and C.L. Pettit, *Uncertainties and dynamic problems of bolted joints and other fasteners.* Journal of Sound and Vibration, 2005. **279**(3-5): p. 857-936.
10. Ling, S.-F. and Y. Xie, *Mechanical impedance detection utilizing sensing capability of piezoceramic inertial actuator.* Proceedings of the International Modal Analysis Conference - IMAC, 2000. **2**: p. 1901-1905.
11. Donald, E., *Fatigue-indicating fasteners("bleeding bolts"): a new dimension in qualtiy control.* Fastener Technology.
12. Yokoyama T., I.S.a.S.S., *Analytical Modelling of the Mechanical Behavior of Bolted Joint Subjected to Transverse Loading.* Journal of Solid Mechanics and Materials Engineering, 2010. **4**.
13. Fisher, J.H.A.S.a.J.W., *Bolt tension control with a direct tension indicator.* AISC Engineering Journal, 1973. **10**: p. 1-5.
14. Cornford, A.S., *Bolt preload- how can you be sure it's right.* Machine Design, March 6, 1979. **47**(5): p. 78-82.
15. Nassar, S.A., G.C. Barber, and D. Zuo, *Bearing friction torque in bolted joints.* Tribology Transactions, 2005. **48**(1): p. 69-75.
16. Nassar, S.A., et al., *An experimental study of bearing and thread friction in fasteners.* Journal of Tribology, 2005. **127**(2): p. 263-272.
17. Shigley, J.E. and C.R. Mischke, Mechanical Engineering Design, 1989.
18. Nassar, S.A., et al., *Effect of tightening speed on the torque-tension and wear pattern in bolted connections.* Journal of Pressure Vessel Technology, Transactions of the ASME, 2007. **129**(3): p. 426-440.

19. Nassar, S.A. and T.S. Sun, *Surface roughness effect on the torque-tension relationship in threaded fasteners.* Proceedings of the Institution of Mechanical Engineers, Part J: Journal of Engineering Tribology, 2007. **221**(2): p. 95-103.
20. Nassar, S.A. and T.S. Sun. *Effect of surface roughness and joint material on the torque-tension relationship in threaded fasteners*. 2005. Long Beach, CA.
21. Nassar, S.A. and Y. Xianjie, *Novel formulation of the tightening and breakaway torque components in threaded fasteners.* Journal of Pressure Vessel Technology, Transactions of the ASME, 2007. **129**(4): p. 653-663.
22. Zou, Q., et al., *Effect of lubrication on friction and torque-tension relationship in threaded fasteners.* Tribology Transactions, 2007. **50**(1): p. 127-136.
23. Park, G., H.H. Cudney, and D.J. Inman, *Feasibility of using impedance-based damage assessment for pipeline structures.* Earthquake Engineering and Structural Dynamics, 2001. **30**(10): p. 1463-1474.
24. Park, G., D.E. Muntges, and D.J. Inman, *Self-repairing joints employing shape-memory alloy actuators.* JOM, 2003. **55**(12): p. 33-37.
25. Park, G., et al., *Overview of piezoelectric impedance-based health monitoring and path forward.* Shock and Vibration Digest, 2003. **35**(6): p. 451-463.
26. Sun, F.P., et al., *Truss structure integrity identification using PZT sensor-actuator.* Journal of Intelligent Material Systems and Structures, 1995. **6**(1): p. 134-139.
27. Mascarenas, D.D.L., G. Park, and C.R. Farrar. *Monitoring of bolt preload using piezoelectric active devices*. 2005. San Diego, CA.
28. Ritdumrongkul, S., et al., *Quantitative health monitoring of bolted joints using a piezoceramic actuator-sensor.* Smart Materials and Structures, 2004. **13**(1): p. 20-29.
29. Bickford, J.H., *Introduction to the design and behavior of bolted joints*, in *Mechanical engineering*. 2008, CRC Press: Boca Raton. p. Chapter 7: Torque Control of Preload pp. 11.
30. Sakai, T., *Investigations of Bolt Loosening Mechanisms - 1. On the Bolts of Transversely Loaded Joints.* Bull JSME, 1978. **21**(159): p. 1385-1390.
31. Hess, D.P., *Vibration- and shock-induced loosening.* Handbook of Bolts and Bolted Joints, 1998: p. 757-824.
32. Hess, D.P. and S.V. Sudhirkashyap, *Dynamic analysis of threaded fasteners subjected to axial vibration.* Journal of Sound and Vibration, 1996. **193**(5): p. 1079-1090.
33. Hess, D.P. and K. Davis, *Threaded components under axial harmonic vibration, Part 1: Experiments.* Journal of Vibration and Acoustics, Transactions of the ASME, 1996. **118**(3): p. 417-422.
34. Hess, D.P., *Threaded components under axial harmonic vibration, Part 2: Kinematic analysis.* Journal of Vibration and Acoustics, Transactions of the ASME, 1996. **118**(3): p. 423-429.
35. Basava, S. and D.P. Hess, *Bolted joint clamping force variation due to axial vibration.* Journal of Sound and Vibration, 1998. **210**(2): p. 255-265.

36. Zadoks, R.I. and X. Yu, *An investigation of the self-loosening behavior of bolts under transverse vibration.* Journal of Sound and Vibration, 1997. **208**(2): p. 189-209.
37. Yamamoto, A. and S. Kasei, *Solution for Self-Loosening Mechanism of Threaded Fasteners under Transverse Vibration.* Bulletin of the Japan Society of Precision Engineering, 1984. **18**(3): p. 261-266.
38. Nassar, S.A. and B.A. Housari. *Self-loosening of threaded fasteners due to cyclic transverse loads.* 2005. Denver, CO.
39. Jiang, Y., et al., *An experimental study of self-loosening of bolted joints.* Journal of Mechanical Design, Transactions of the ASME, 2004. **126**(5): p. 925-931.
40. Vibration Loosening of Bolts and Threaded Fasteners, 1999.
41. Bishop, R.E.D., *The analysis and synthesis of vibrating systems.* Journal of the Royal Aeronautical Society, 1954. **58**: p. 703-719.
42. Tsai, J.S. and Y.F. Chou, *The identification of dynamic characteristics of a single bolt joint.* Journal of Sound and Vibration, 1988. **125**(3): p. 487-502.
43. Hanss, M., S. Oexl, and L. Gaul, *Identification of a bolted-joint model with fuzzy parameters loaded normal to the contact interface.* Mechanics Research Communications, 2002. **29**(2-3): p. 177-187.
44. Hanss, M., *The transformation method for the simulation and analysis of systems with uncertain parameters.* Fuzzy Sets and Systems, 2002. **130**(3): p. 277-289.
45. Hanss, M., S. Oexl, and L. Gaul, *Simulation and analysis of structural joint models with uncertainties.* Proc. of the International Conference on Structural Dynamics Modeling - Test, Analysis, Correlation and Validation, 2002: p. 165-174.
46. Hanss, M. and K. Willner, *Fuzzy arithmetical approach to the solution of finite element problems with uncertain parameters.* Mechanics Research Communications, 2000. **27**(3): p. 257-272.
47. Hanss, M. and K. Willner, *On using fuzzy arithmetic to solve problems with uncertain model parameters.* Proc. of the Euromech 405 Colloquium, 1999: p. 85-92.
48. Hanss, M., K. Willner, and S. Guidati, *On applying fuzzy arithmetic to finite element problems.* Proc. 17th Internat. Conf. of the North Amer. Fuzzy Informat. Process. Soc. - NAFIPS '98, 1998: p. 365-369.
49. Oldfield, M., H. Ouyang, and J.E. Mottershead, *Simplified models of bolted joints under harmonic loading.* Computers and Structures, 2005. **84**(1-2): p. 25-33.
50. Oldfield, M., H. Ouyang, and J.E. Mottershead, *Experimental study and analytical modelling of a bolted joint subjected to harmonic excitation.* Proceedings of the 29th International Conference on Noise and Vibration Engineering, 2004.
51. Gaul, L. and R. Nitsche, *The role of friction in mechanical joints.* Applied Mechanics Reviews, 2001. **54**(2): p. 93-105.
52. Vakakis, A.F. and D.J. Ewins, *Effects of weak nonlinearities on modal analysis.* Proc. 10 Int. Modal Analysis Conf.th, 1992: p. 72-78.

53. Bouc, R., *Forced vibration of mechanical systems with hysteresis.* Proceedings of the 4th Conference on Non-Linear Oscillation, 1967: p. 315-315.
54. Wen, Y.-K., *METHOD FOR RANDOM VIBRATION OF HYSTERETIC SYSTEMS.* ASCE J Eng Mech Div, 1976. **102**(2): p. 249-263.
55. Laboratory, T.C.U.V.E. *Automotive Electronics*. 3 March 2012]; Available from: http://www.cvel.clemson.edu/auto/actuators/motors-dc-brushed.html.
56. Ling, S.F., X. Hou, and Y. Xie, *Decoupling loading effect in simultaneous sensing and actuating for dynamic measurement.* Sensors and Actuators, A: Physical, 2005. **120**(1): p. 257-265.
57. Czajkowsky, C.J., *Investigations of corrosion and stress corrosion cracking in bolting materials on light water reactors.* International Journal of Pressure Vessels and Piping, 1986. **26**: p. 87-96.
58. Ewins, D.J., *Modal Testing: Theory and Practice*. 1984. 27.
59. Piersol, J.S.B.a.A.G., *Random Data*. 2000.

APPENDIX A

EQUIPMENT LISTS

i. Maxon DC Brushed motor RE 40: *Figure A-1*

Model	:	Maxon
Power	:	150 Watt
Nominal Voltage	:	24 Volt
No load speed	:	7580 rpm
No load cuurent	:	137 mA
Nominal speed (continuous running)	:	6930 rpm
Nominal torque (max Continous torque)	:	94.9 mNm
Nominal current	:	5.77 A
Stall torque	:	2280 mNm
Starting current	:	75.7 A
Efficiency	:	91%
Terminal Resistance (R)	:	0.317 Ω
Terminal Inductance (L)	:	0.0823 mH
Torque constant (k_T)	:	30.2 mNm/A
Speed constant (k_E)	:	317 rpm/V

ii. Planetary Gearhead GP52C 40: *Figure A-1*

Reduction	:	353 :1
Reduction absolute	:	29561/81
Number of stage	:	4
Max efficiency	:	68%

Based on the electric motor and gear combination, the torque constant and speed constant of the motor are:

- $k_T = (30.2\times10^{-3})(353)(0.68) = 7.2488 \ \ Nm/A$
- $k_E = \frac{1}{317}\times353\times\frac{60}{2\pi} = 10.634 \ \ V/rad$

iii. High Voltage Differential Probe (Tektronix P5205) & TEKPROBE Power Supply (Tektronix 1103): *Figure A-2*

Maximum Operating Voltage	:	±1.3 kV (DC + peak AC)
Attenuation Range	:	50X, 500X
Rise Time	:	3.5 ns
Bandwidth Limit	:	5 MHz
AC Noise	:	50 Hz
Propagation Delay	:	17 ns

iv. Current Probe (Tektronix A6303) & Current Probe Amplifier (Tektronix AM 503B): *Figure A-3*

Maximum Operating Current	:	20 Amperes
Bandwidth	:	DC to 50 MHz, -3 dB
Rise Time	:	≤7 ns
Gain Accuracy	:	≤3%
Signal Delay	:	Approximately 30 ns

v. Torque Detector (Ono Sokki SS 100) & Torque Converter (Ono Sokki TS-2600): *Figure A-4*

Torque Range	:	50 Nm / 5 kgf·m
Maximum Speed	:	8000 rpm
Time Constant	:	63 ms

vi. Dynamic Signal Analyzer (Dynamic Signal Acquisition Module NI 4462): *Figure A-5*

Analog Input	:	4
Sampling Rate per Channel	:	204.8 kS/s
Dynamic Range	:	118 dB
Maximum Signal Bandwidth	:	92 kHz
Input Range	:	±316 mV to 42.4 V

vii. Donut Load Cell (LEPS CLC_DT 4060901) and Amplifier: *Figure A-6*

Capacity	:	35000 Newton/3.5 Tonne
Output current range	:	4-20 mA
Force/Ampere conversion	:	2.125 kN/mA

Figure A-1: Maxon Brushed DC motor and gearhead

Figure A-2: High Voltage Differential Probe & Power Supply

Figure A-3: Current Probe & Current Probe Amplifier

Figure A-4: Torque Detector & Torque Converter

Figure A-5: Dynamic Signal Analyzer

Figure A-6: Donut Load Cell and Amplifier

APPENDIX B

MECHANICAL IMPEDANCE CALCULATION

A single degree of freedom time variant dynamic mechanical system is modelled as a spring mass and damping system with the following:

- Mass (m) = 1.3 kg
- Damping ($c(t)$) = $1.8243 - \frac{t}{100}$ Ns/m
- Stiffness ($k(t)$) = $25 - \frac{t}{5}$ N/m
- Natural frequency of the system (ω_n), which is calculated with the formula

$$\omega_n(t) = \sqrt{\frac{k(t)}{m}}$$

- Damping coefficient (ζ), which is calculated with the formula:

$$\zeta(t) = \frac{c(t)}{2\sqrt{k(t)m}}$$

The system is excited with a single frequency continuous force (F_{real}):

$$F_{real}(t) = 3\cos(\omega_f t) \ N$$

Where $\omega_f = 0.2\pi$ and the response of the system is calculated with the following equation

$$v_{real}(t) = \left(\frac{-3\omega_f}{k(t)\left(1 - \left(\frac{\omega_f}{\omega_n(t)}\right)^2\right)^2 + \left(\frac{2\xi(t)\omega_f}{\omega_n(t)}\right)^2} \right) \sin\left(\omega_f t - \varphi(t)\right)$$

where

$$\varphi(t) = \tan^{-1}\left(\frac{\frac{2\varsigma(t)\omega_f}{\omega_n(t)}}{1-\left(\frac{\omega_f}{\omega_n(t)}\right)^2}\right)$$

The Hilbert Transform is applied to both F_{real} and v_{real} to form F_{imag} and v_{imag}. Both the real and imaginary part of the excitation and response of the system are plotted in Figures B-1 and B-2.

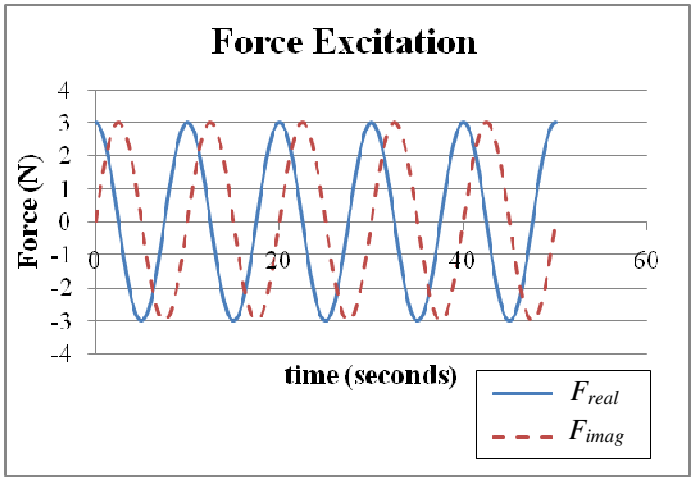

Figure B-1 The force excitation given to the system

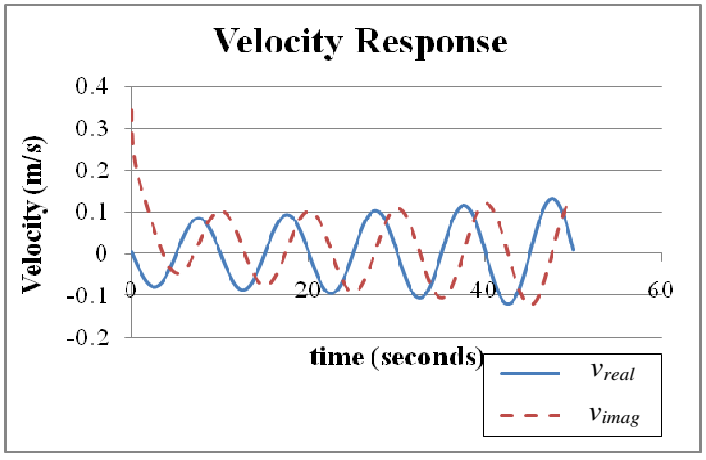

Figure B-2 The velocity response of system due to force excitation

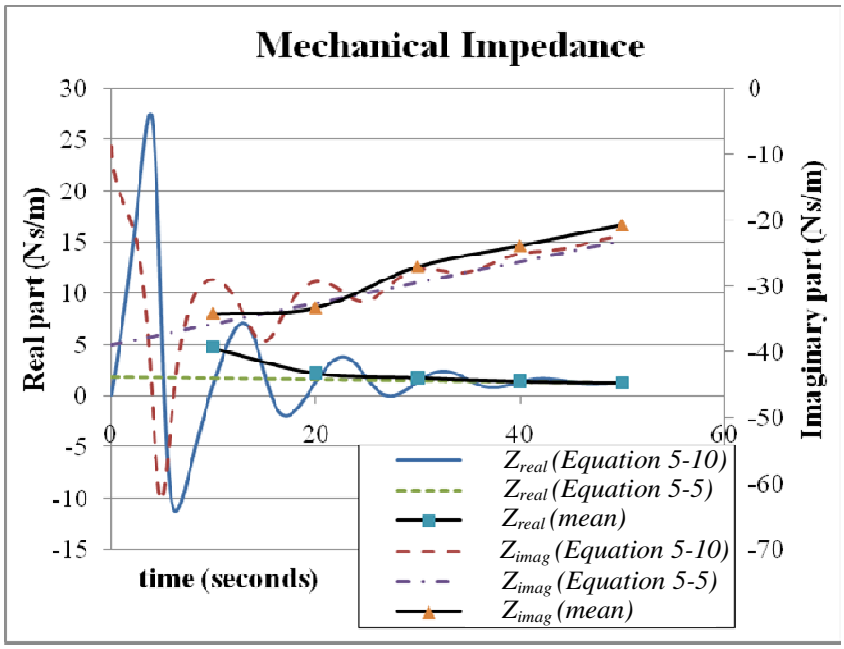

Figure B-3 Mechanical impedance of time variant system

The Mechanical impedance of the system is calculated using Equations (5-5) and (5-11) and the results are plotted in Figure B-3. Figure B-3 shows that the mechanical impedance obtained by Equation (5-10) is oscillating. By calculating the mean value of the mechanical impedance (Equation (5-10)) for every cycle of oscillation, it can be seen that an almost similar pattern with mechanical impedance is obtained using Equation (5-5). Thus, Equation (5-10) can be used to obtain the mechanical impedance of the time variant system. However, the mean value needs to be implemented for every cycle to obtain the mechanical impedance.

APPENDIX C
LOOSENING TORQUE DUE TO TRANSVERSE VIBRATION

This appendix derives a mathematical formula of how an excitation torque is generated from transverse vibration. When transverse vibration is applied to bolted joint, the joined part will slide with relative to each other due to friction force between the two joined parts is overcome. This slide joint makes the bolt head or the nut to slide and generate a bending moment (M_b) at the bolt. Due to the bending moment, an uneven distribution of axial force at the bolt is generated. This uneven distribution of force affects friction at the bolted joint and permits motion at threaded part. The motion normally moves the bolt to loosening direction.

To model the bolted joint under transverse vibration, a model of a typical bolted joint is shown in Fig. B-1. The bolted joint consists of two plates joined by bolt and nut. The upper plate is tightened to a fixed plate with a certain value of preload (P). A transverse force ($F_s \sin(\omega_f t)$) is applied at the upper plate and slides the plate at x-direction due to zero friction force between the plates. Because of the upper plate and bolt head are in contact, the transverse force applied at the upper plate is transmitted to bottom surface of the bolt head. The transmitted force bends the bolt and generates a bending moment (M_B).

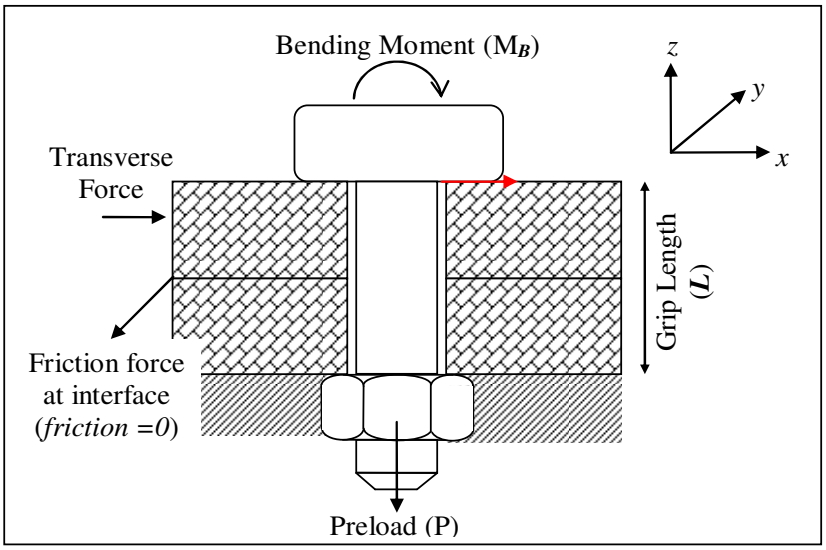

Figure C-1 Model bolted joint

In Figure C-2 free body diagram of the bolt is shown. The bolt is divided into 2 segments which are bolt head and bolt thread. At the bolt head, forces and moment act on it are preload forces (P) in negative z-axis, transverse force (F_s) at bottom surface of the bolt head in x-axis and bending moment (M_B) about y-axis. These forces and moment act at bolt thread as well. Due to the forces and moment, torque is generated at bolt head and bolt thread which the formulas are derived below.

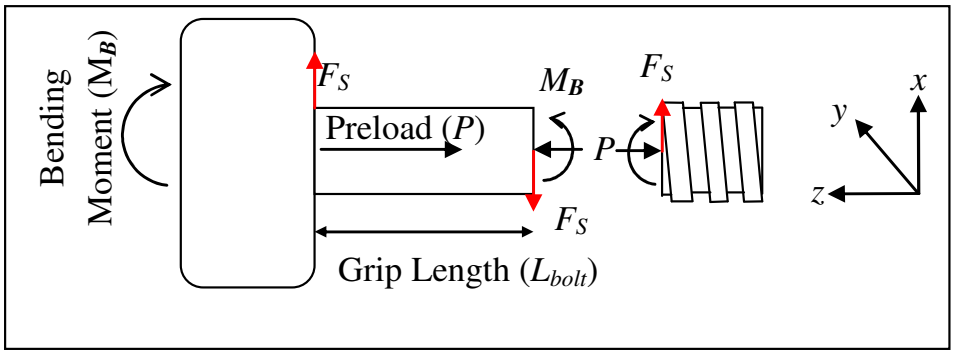

Figure C-2 Free body diagram of bolt

C-1 Torque generated at bolt head of bolted joint

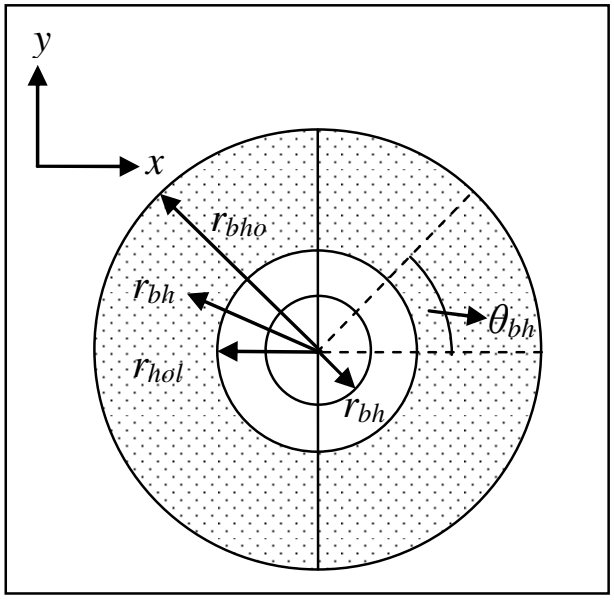

Figure C-3 Bottom surface of bolt head

Bolt head is in a shape of a ring divided into small area by angle $d\theta_{bh}$ (Figure C-3). Outer radius of ring is equal to radius of bolt head (r_{bho}) and inner radius of ring is equal to radius of hole at the plate (r_{hole}). Force and moment act on bolt head are differentiated into differential force act on the small area. Those differential forces are as follow:

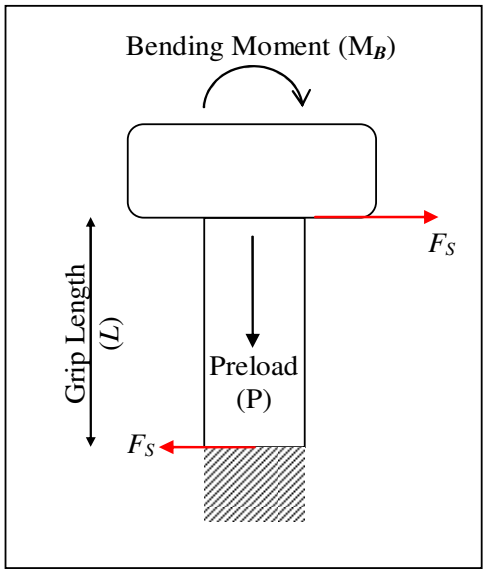

Figure C-4 Free body diagram of bolt head

a) Differential force due to preload

Preload (P) is a force result from bolt elongation. At the bolt head preload acts on negative z-direction. The preload force is distributed evenly over the area of the ring. For a small area of ring with small angle $d\theta_{bh}$, differential force due to preload is calculated as:

$$dF_{bh-P} = -\frac{P}{2\pi}\hat{z} \tag{C-1}$$

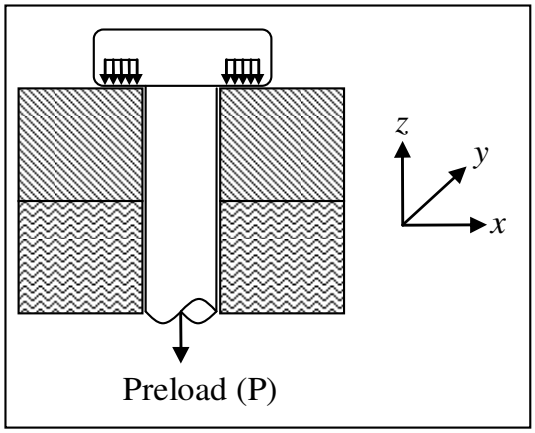

Figure C-5 Preload at bolted joint

b) Differential force due to transverse force given to upper plate

Transverse force ($F_s \sin(\omega_f t)$) given to upper plate is directly transmitted to bottom surface of bolt head that is in contact with upper plate. The force is assumed to be evenly distributed over the area of the ring. The differential force is calculated as:

$$dF_{bh-s} = \frac{F_s \sin \omega_f t}{2\pi} \hat{x} \qquad \text{(C-2)}$$

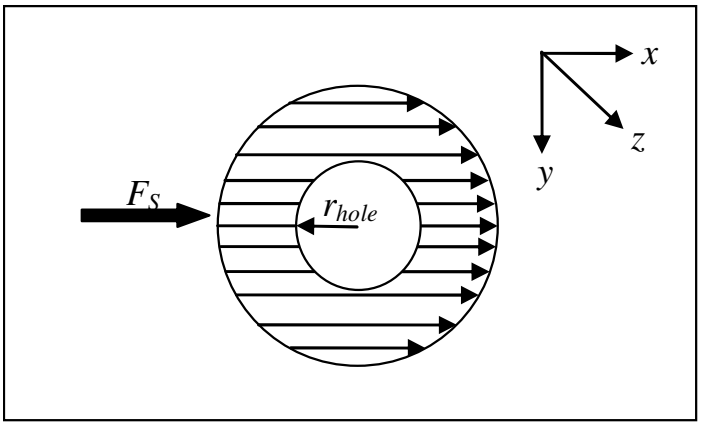

Figure C-6 Transverse force at bolted joint

c) Differential force due to bending moment

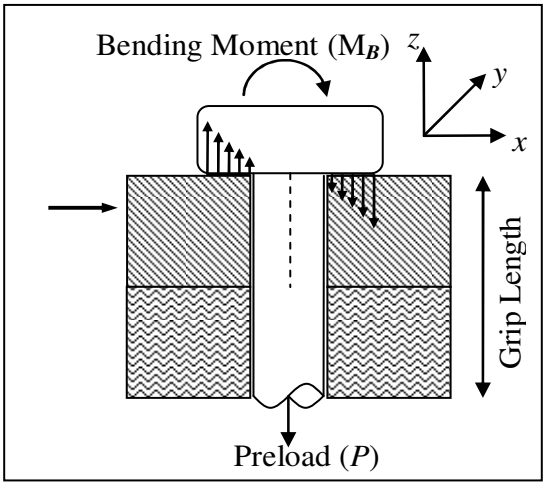

Figure C-7 Bending Moment generated due to transverse force

As bottom part of the bolt is restricted to move, the transverse force transmitted at the bolt head bends the bolt and generated a bending moment. The bending moment is formulated as:

$$M_b = F_s L_{bolt} \hat{y} \tag{C-3}$$

Due to the moment, an uneven pressure distribution is generated at bolt head (Figure C-7). This pressure distribution is calculated using equation of bending moment which is:

$$\frac{F_{axial}}{A_{bh}} = -\frac{Mx}{I_{ring}} \hat{z} \tag{C-4}$$

With area moment of inertia for a ring shape object is:

$$I_{ring} = \frac{\pi \left({r_{bho}}^4 - {r_{hole}}^4 \right)}{4} \tag{C-5}$$

In obtaining the differential force due to bending moment, Eqn. C-3 is derived to become:

$$F_{axial} = \left(-\frac{Mx}{I_{ring}} \hat{z} \right) A_{bh}$$

$$\int_0^{2\pi} dF_{bh-Mb} d\theta_{bh} = \int_0^{2\pi} \int_{r_{bhi}}^{r_{bho}} \left(-\frac{Mx}{I_{ring}} \right) x dx d\theta_{bh} \hat{z}$$

$$dF_{bh-Mb} = \int_{r_{bhi}}^{r_{bho}} \left(-\frac{Mx^2}{I_{ring}} \right) dx \hat{z}$$

$$dF_{bh-Mb} = -\frac{4F_s \sin\left(\omega_f t\right) L_{bolt} \left({r_{bho}}^3 - {r_{bhi}}^3 \right) \left(\cos\theta_{bh} \right)^3}{3\pi \left({r_{bho}}^4 - {r_{bhi}}^4 \right)} \hat{z} \tag{C-6}$$

d) Differential force due to friction force at bottom surface of bolt head

Friction force is generated at bottom surface of the bolt head to oppose the movement of bolt head. The friction force is calculated as product of coefficient friction and normal force. The normal force is force that act in

normal direction of the surface (*x*-*y* surface). The force is summation of the differential force due to preload and bending moment. Mathematically, differential force due to friction is calculated as:

$$dF_{bh-fric} = \mu_{bh} \left| dF_{bh-Mb} + dF_{bh-P} \right| \frac{\left| F_s \sin\left(\omega_f t\right) \right|}{F_s \sin\left(\omega_f t\right)} \hat{x} \tag{C-7}$$

Where the direction of force is opposed the direction of motion.

Based on forces and moment above, the summation of differential force that act on surface of bolt head is calculated as:

$$dF_{bh} = \begin{bmatrix} \left(dF_{bh-Fs} - dF_{bh-fric}\right) & \hat{x} \\ 0 & \hat{y} \\ \left(dF_{bh-P} + dF_{bh-Mb}\right) & \hat{z} \end{bmatrix} \tag{C-8}$$

This differential force generates a differential torque at z-axis and it is calculated as:

$$dT_{bh} = \left(r_{bhm} \left(dF_{bh} \bullet \hat{x} \sin\frac{\theta_{bh}}{2} \right) \right) \hat{z} \tag{C-9}$$

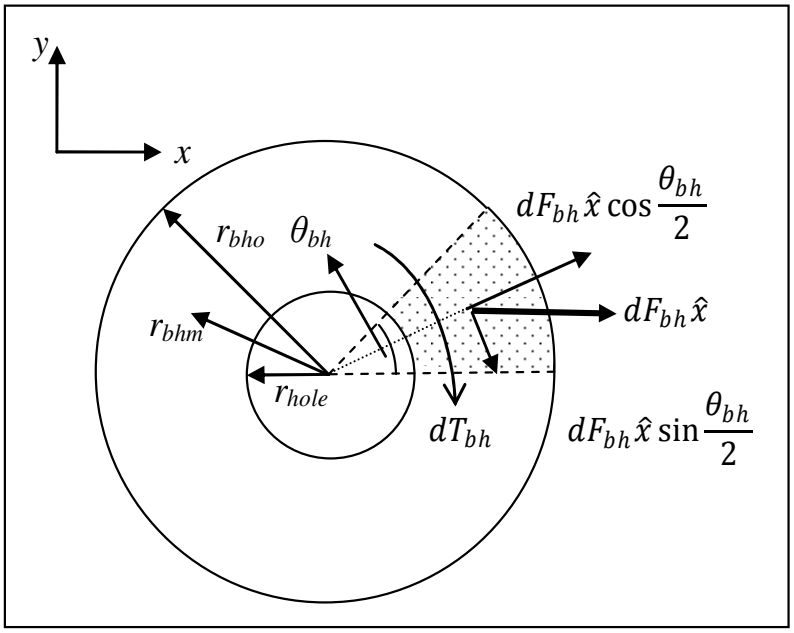

Figure C-8 Force act on bottom surface of bolt head

The total torque at bolt head is calculated as integral of the differential torque over 1 revolution (2π) of bolt head which is:

$$T_{bh} = \left(\int_0^{2\pi} dT_{bh} d\theta_{bh} \right) \hat{z} = \left(\int_0^{2\pi} r_{bhm} \left(dF_{bh} \bullet \hat{x} \sin \frac{\theta_{bh}}{2} \right) d\theta_{bh} \right) \hat{z} \qquad \text{(C-10)}$$

With torque at positive z-direction turn the bolt at loosening direction (counter clockwise).

C-2 Torque generated at bolt thread of bolted joint

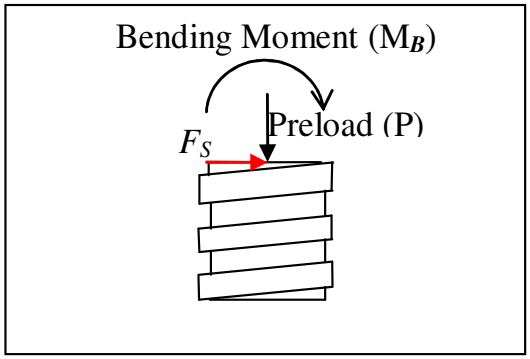

Figure C-9 Free body diagram of bolt thread

Bending moment, preload and transverse force acting at the bolt head act at the bolt thread as well (Figure C-9).Those force and moment generate a motion at bolt thread. This motion is being opposed by friction force at surface of the bolt thread. In calculating the friction force, transformation matrix is needed to transform the direction of force and moment from global coordinate into local coordinate at thread surface. The transformation is done by three transformations where the global coordinate x-y-z is rotate by angle θ_{bt}, lead angle (β) and thread profile angle (2α) to become local coordinate u_2-v_2-w_2. The transformation matrix is explained as follow:

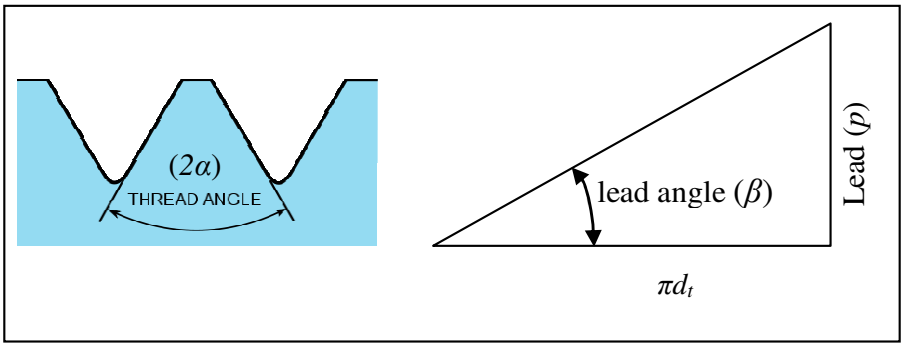

Figure C-10 Thread profile and lead angle of bolt

a) Transformation due to angle θ_{bt}

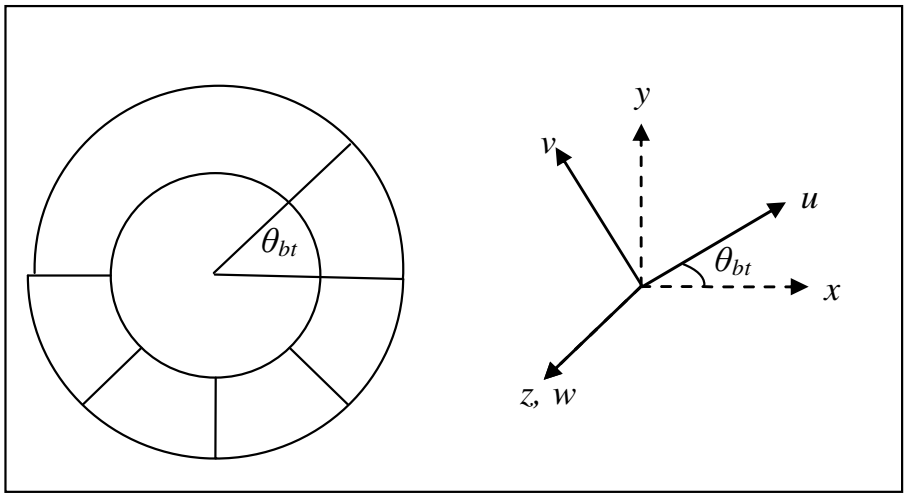

Figure C-11 Bolt thread divided into small section

Bolt thread is divided into small section based on angle $d\theta_{bt}$. The local coordinate *u*-*v*-*w* is attached to the section. The relationship between *u*-*v*-*w* coordinate with *x*-*y*-*z* coordinate is define by transduction matrix:

$$\begin{bmatrix} u \\ v \\ w \end{bmatrix} = [\mathbf{T}_{x,u}] \begin{bmatrix} x \\ y \\ z \end{bmatrix}$$

$$\begin{bmatrix} u \\ v \\ w \end{bmatrix} = \begin{bmatrix} \cos\theta_{bt} & \sin\theta_{bt} & 0 \\ -\sin\theta_{bt} & \cos\theta_{bt} & 0 \\ 0 & 0 & 1 \end{bmatrix} \begin{bmatrix} x \\ y \\ z \end{bmatrix} \quad \text{(C-11)}$$

b) Transformation due to thread angle (α)

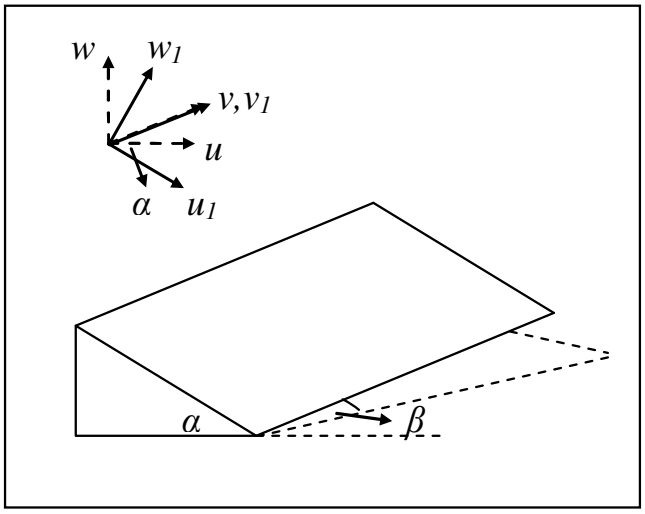

Figure C-12 Thread angle of threaded part

Thread angle is the angle between the thread. Due to this angle, the local coordinate u-v-w at section of bolt thread is rotated for α degree at v-axis and form u_1-v_1-w_1-coordinate. The transformation matrix is:

$$\begin{bmatrix} u_1 \\ v_1 \\ w_1 \end{bmatrix} = [T_{uu_1}] \begin{bmatrix} u \\ v \\ w \end{bmatrix}$$

$$\begin{bmatrix} u_1 \\ v_1 \\ w_1 \end{bmatrix} = \begin{bmatrix} \cos\alpha & 0 & -\sin\alpha \\ 0 & 1 & 0 \\ \sin\alpha & 0 & \cos\alpha \end{bmatrix} \begin{bmatrix} u \\ v \\ w \end{bmatrix} \quad \text{(C-12)}$$

c) Transformation due to lead angle (β)

Lead angle is increment angle at thread of bolt for 1 rotation. Due to this lead angle, the u_1-v_1-w_1-coordinate is rotate upwards with u_1 as axis of rotation for β angle and form u_2-v_2-w_2 coordinate. The matrix for this axis transformation is written:

$$\begin{bmatrix} u_2 \\ v_2 \\ w_2 \end{bmatrix} = [T_{u_1u_2}] \begin{bmatrix} u_1 \\ v_1 \\ w_1 \end{bmatrix}$$

$$\begin{bmatrix} u_2 \\ v_2 \\ w_2 \end{bmatrix} = \begin{bmatrix} 1 & 0 & 0 \\ 0 & \cos\beta & \sin\beta \\ 0 & -\sin\beta & \cos\beta \end{bmatrix} \begin{bmatrix} u_1 \\ v_1 \\ w_1 \end{bmatrix} \quad \text{(C-13)}$$

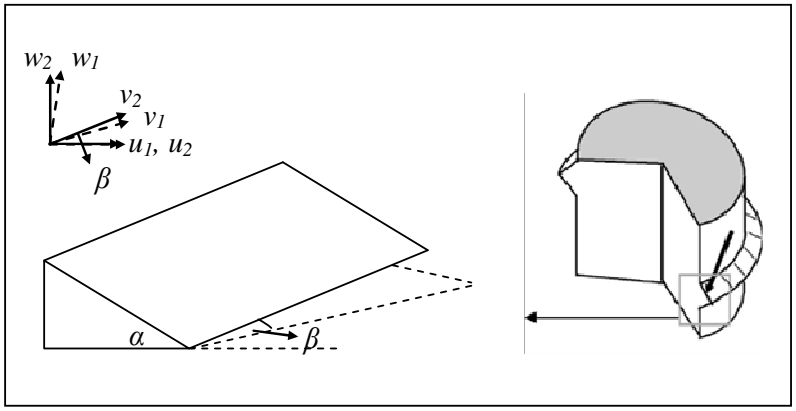

Figure C-13 Lead angle of threaded part

By combining transformation matrix at equation (C-11), (C-12) and (C-13) the transformation of *x-y-z* coordinate into u_2-v_2-w_2 coordinate is obtained as:

$$\begin{bmatrix} u_2 \\ v_2 \\ w_2 \end{bmatrix} = \left[T_{u_1,u_2}\right]\left[T_{u,u_1}\right]\left[T_{x,u}\right]\begin{bmatrix} x \\ y \\ z \end{bmatrix} \quad \text{(C-14)}$$

where:

a) u_2 is the axis point to the radial direction of bolt

b) v_2 is the axis along bolt thread

c) w_2 is the axis that normal to thread surface

With the transformation matrix at equation (C-14), differential friction force act on each section of thread surface can be obtained. The normal force from thread surface is differential force acting at in w_2 directions. It is obtained by transforming directions of differential forces act on the bolt thread from global coordinate *x-y-z* into local coordinate u_2-v_2-w_2. Those differential forces are:

a) Differential force due to preload at bolt thread

At bolt thread, preload acts on z-axis. The differential force due to the preload is calculated as:

$$dF_{bt-P} = -\frac{P}{2\pi}\hat{z}$$

with transformation matrix in Eqn. C-14 the force act at u_2-v_2-w_2 coordinate is:

$$dF_{bt-P} = -\frac{P}{2\pi}\begin{bmatrix} -\sin\alpha & \hat{u}_2 \\ \sin\beta\cos\alpha & \hat{v}_2 \\ \cos\alpha\cos\beta & \hat{w}_2 \end{bmatrix} \tag{C-15}$$

b) Differential force due to transverse force at bolt thread

The transverse force transmitted to bolt thread is acted on x-axis. The differential force acting on small section of bolt thread is calculated as:

$$dF_{bt-Fs} = \frac{F_s \sin\omega_f t}{2\pi}\hat{x}$$

The differential force acting on the u_2-v_2-w_2 coordinate is calculated as:

$$dF_{bt-Fs} = \frac{F_s \sin\omega_f t}{2\pi}\begin{bmatrix} \cos\alpha\cos\theta_{bt} & \hat{u}_2 \\ \sin\alpha\sin\beta\cos\theta_{bt} - \cos\beta\sin\theta_{bt} & \hat{v}_2 \\ \sin\alpha\cos\beta\cos\theta_{bt} + \sin\beta\sin\theta_{bt} & \hat{w}_2 \end{bmatrix} \tag{C-16}$$

c) Differential force due to bending moment

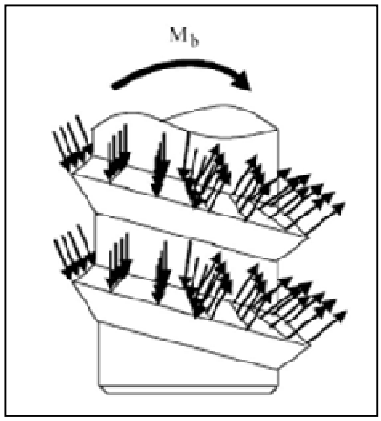

Figure C-14 Pressure distribution due to bending moment at bolt thread

The bending moment acting at bolt thread generates a differential force at z-axis (Figure C-13). This differential force is calculated based on Eqn. (C-6) where:

$$dF_{bt-Mb} = -\int_{r_{bti}}^{r_{bto}} \frac{Mx}{I_{ring}} x dx \hat{z} = -\frac{4F_s \sin\omega_f t L_{bolt}\left(r_{bto}{}^3 - r_{bti}{}^3\right)}{3\pi\left(r_{bto}{}^4 - r_{bti}{}^4\right)}(\cos\varphi)^3 \hat{z}$$

$$dF_{bt-Mb} = -\frac{4F_s \sin\omega_f t L_{bolt}\left(r_{bto}{}^3 - r_{bti}{}^3\right)}{3\pi\left(r_{bto}{}^4 - r_{bti}{}^4\right)}(\cos\varphi)^3 \begin{bmatrix} -\sin\alpha & \hat{u}_2 \\ \sin\beta\cos\alpha & \hat{v}_2 \\ \cos\alpha\cos\beta & \hat{w}_2 \end{bmatrix} \quad \text{(C-17)}$$

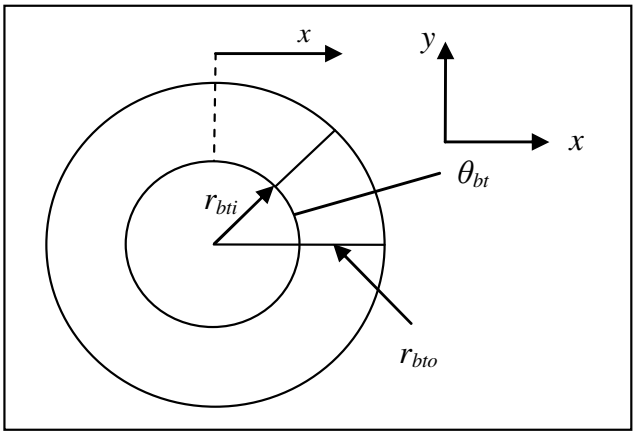

Figure C-15 Cut section of bolt thread

By summation of three differential forces above, normal force acting on thread surface can be obtained. The summation of the three differential forces above is calculated as:

$$dP = dF_{bt-P} + dF_{bt-Fs} + dF_{bt-Mb}$$

$$dP \bullet \begin{bmatrix} \hat{u}_2 \\ \hat{v}_2 \\ \hat{w}_2 \end{bmatrix} = -\left(\frac{4F_s \sin\omega_f t L_{bolt} \left({r_{bto}}^3 - {r_{bti}}^3 \right)}{3\pi \left({r_{bto}}^4 - {r_{bti}}^4 \right)} \left(\cos\theta_{bt} \right)^3 + \frac{P}{2\pi} \right) \bullet \begin{bmatrix} -\sin\alpha & \hat{u}_2 \\ \sin\beta\cos\alpha & \hat{v}_2 \\ \cos\alpha\cos\beta & \hat{w}_2 \end{bmatrix} \quad \text{(C-18)}$$
$$+ \frac{F_s \sin\omega_f t}{2\pi} \bullet \begin{bmatrix} \cos\alpha\cos\theta_{bt} & \hat{u}_2 \\ \sin\alpha\sin\beta\cos\theta_{bt} - \cos\beta\sin\theta_{bt} & \hat{v}_2 \\ \sin\alpha\cos\beta\cos\theta_{bt} - \sin\beta\sin\theta_{bt} & \hat{w}_2 \end{bmatrix}$$

From the force above, normal force acting on thread surface is obtained as force acting at w_2 direction. By obtaining normal force at thread surface, differential friction force at each section of bolt thread is calculated as:

$$dF_{bt-friction} = \mu_{bt} \left| dP \bullet \hat{w}_2 \right| \begin{bmatrix} \dfrac{\left(dP \bullet \hat{u}_2 \right)}{\sqrt{\left(dP \bullet \hat{u}_2 \right)^2 + \left(dP \bullet \hat{v}_2 \right)^2}} & \hat{u}_2 \\ \dfrac{\left(dP \bullet \hat{v}_2 \right)}{\sqrt{\left(dP \bullet \hat{u}_2 \right)^2 + \left(dP \bullet \hat{v}_2 \right)^2}} & \hat{v}_2 \\ 0 & \hat{w}_2 \end{bmatrix} \quad \text{(C-19)}$$

And differential force acts at each section of bolt thread can be calculated as summation of the differential force due to preload, transverse force and bending moment, minus off differential friction force which is:

$$dF_{bt} \bullet \begin{bmatrix} \hat{u}_2 \\ \hat{v}_2 \\ \hat{w}_2 \end{bmatrix} = \left(dF_{bt-P} + dF_{bt-Fs} + dF_{bt-Mb} - dF_{bt-friction} \right) \bullet \begin{bmatrix} \hat{u}_2 \\ \hat{v}_2 \\ \hat{w}_2 \end{bmatrix} \quad \text{(C-20)}$$

The force above is transformed back from u_2-v_2-w_2 coordinate into u-v-w coordinate to calculate torque generated at bolt thread. The transformation is done with inverse matrix of equation (C-14) which are:

$$dF_{bt} \bullet \begin{bmatrix} \hat{u} \\ \hat{v} \\ \hat{w} \end{bmatrix} = \left[T_{u,u_1} \right]^{-1} \left[T_{u_1,u_2} \right]^{-1} dF_{bt} \bullet \begin{bmatrix} \hat{u}_2 \\ \hat{v}_2 \\ \hat{w}_2 \end{bmatrix}$$

$$dF_{bt} \bullet \begin{bmatrix} \hat{u} \\ \hat{v} \\ \hat{w} \end{bmatrix} = \begin{bmatrix} \cos\alpha & \sin\alpha\sin\beta & \sin\alpha\cos\beta \\ 0 & \cos\beta & -\sin\beta \\ -\sin\alpha & \sin\beta\cos\alpha & \cos\alpha\cos\beta \end{bmatrix} dF_{bt} \bullet \begin{bmatrix} \hat{u}_2 \\ \hat{v}_2 \\ \hat{w}_2 \end{bmatrix} \tag{C-21}$$

And differential torque generated at bolt thread in *z*-axis is calculated as:

$$dT_{bt} = \left(r_{btm} dF_{bt} \bullet \hat{v} \right) \hat{z} \tag{C-22}$$

Where for 1 revolution of thread, the torque is calculated as:

$$T_{bt} = \left(\int_0^{2\pi} dT_{bt} d\theta_{bt} \right) \hat{z} \tag{C-23}$$

and for *n*-thread engagement, the torque is equal to:

$$T_{btn} = \left(n \int_0^{2\pi} dT_{bt} d\theta_{bt} \right) \hat{z} \tag{C-24}$$

Based on Eqn. (C-10) and Eqn. (C-24), torque generated at bolted joint is obtained as summation of both the equation where:

$$T_{bolt} = \left(\int_0^{2\pi} r_{bh} \left(dF_{bht} \hat{x} \sin d\theta_{bh} \right) d\theta_{bh} + n \int_0^{2\pi} dT_{bt} d\theta_{bt} \right) \hat{z} \tag{C-25}$$

with the torque rotate at positive z-axis (counter clockwise) is turning the bolt to loosening direction.

C-3 Numerical analysis of total torque at the bolted joint

In previous section, a torque formulation has been derived from transverse force given to the bolted joint. To calculate the value of the torque, the formula obtained from previous section is discretized. The bolt head and bolt thread are assumed to be a shape of ring divided into a large number of sections (N). The small angle forms at each section are formulated as:

$$d\theta_{bh} = \frac{2\pi}{N} \tag{C-26}$$

$$d\theta_{bt} = \frac{2\pi}{N} \tag{C-27}$$

By substituting the angle in Eqn. (C-26) and Eqn. (C-27) into the differential force formula derived from previous section, the differential force formula in discrete mode is as follow:

a) Differential force and torque at bolt head

By substituting small angle of bolt head in equation (C-26) into differential force at equation (C-1), (C-2) and (C-6), the differential force at bolt head become:

$$dF_{bh} \bullet \hat{z} = -\left(\frac{P}{2\pi} + \frac{4F_s \sin\left(\omega_f t\right) L_{bolt} \left({r_{bho}}^3 - {r_{bhi}}^3 \right) \left(\cos n\frac{2\pi}{N} \right)^3}{3\pi \left({r_{bho}}^4 - {r_{bhi}}^4 \right)} \right) \tag{C-28}$$

$$dF_{bh} \bullet \hat{x} = \frac{F_s \sin \omega_f t}{2\pi} - \mu_{bh} \left| dF_{bh} \bullet \hat{z} \right| \frac{F_s \sin \omega_f t}{\left| F_s \sin \omega_f t \right|} \tag{C-29}$$

And differential torque generated at each section is calculated as:

$$dT_{bh} = r_{bhm} \times \left(dF_{bh} \bullet \hat{x} \sin n\frac{\pi}{N} \right) \tag{C-30}$$

with torque at bolt head is:

$$T_{bh} = \sum_{n=0}^{N} r_{bh} \left(dF_{bh} \bullet \hat{x} \sin n\frac{\pi}{N} \right) \frac{2\pi}{N} \tag{C-31}$$

Where n= 0 to N

b) Differential force and torque at bolt thread

Force at bolt thread in discrete mode is obtained by substituting angle at equation (C-27) into differential force formula at equation (C-18) and (C-19) where:

$$dP \bullet \begin{bmatrix} \hat{u}_2 \\ \hat{v}_2 \\ \hat{w}_2 \end{bmatrix} = -\left(\frac{4F_s \sin \omega_f t L_{bolt} \left({r_{bto}}^3 - {r_{bti}}^3 \right)}{3\pi \left({r_{bto}}^4 - {r_{bti}}^4 \right)} \left(\cos n \frac{2\pi}{N} \right)^3 + \frac{P}{2\pi} \right) \bullet \begin{bmatrix} -\sin\alpha & \hat{u}_2 \\ \sin\beta\cos\alpha & \hat{v}_2 \\ \cos\alpha\cos\beta & \hat{w}_2 \end{bmatrix}$$

$$+ \frac{F_s \sin \omega_f t}{2\pi} \bullet \begin{bmatrix} \cos\alpha\cos n\frac{2\pi}{N} & \hat{u}_2 \\ \sin\alpha\sin\beta\cos n\frac{2\pi}{N} - \cos\beta\sin n\frac{2\pi}{N} & \hat{v}_2 \\ \sin\alpha\cos\beta\cos n\frac{2\pi}{N} - \sin\beta\sin n\frac{2\pi}{N} & \hat{w}_2 \end{bmatrix} \quad \text{(C-32)}$$

$$dF_{bt-friction} = \mu_{bt} \left| dP \bullet \hat{w}_2 \right| \begin{bmatrix} \dfrac{\left(dP \bullet \hat{u}_2 \right)}{\sqrt{\left(dP \bullet \hat{u}_2 \right)^2 + \left(dP \bullet \hat{v}_2 \right)^2}} & \hat{u}_2 \\ \dfrac{\left(dP \bullet \hat{v}_2 \right)}{\sqrt{\left(dP \bullet \hat{u}_2 \right)^2 + \left(dP \bullet \hat{v}_2 \right)^2}} & \hat{v}_2 \\ 0 & \hat{w}_2 \end{bmatrix} \quad \text{(C-33)}$$

and total differential force generated at bolt thread is obtained as:

$$dF_{bt} \bullet \begin{bmatrix} \hat{u} \\ \hat{v} \\ \hat{w} \end{bmatrix} = \begin{bmatrix} \cos\alpha & \sin\alpha\sin\beta & \sin\alpha\cos\beta \\ 0 & \cos\beta & -\sin\beta \\ -\sin\alpha & \sin\beta\cos\alpha & \cos\alpha\cos\beta \end{bmatrix} \left(\left(dP - dF_{bt-friction} \right) \bullet \begin{bmatrix} \hat{u}_2 \\ \hat{v}_2 \\ \hat{w}_2 \end{bmatrix} \right) \quad \text{(C-34)}$$

With torque generated at bolt thread is obtained as:

$$T_{bt} = n_t \sum_{n=0}^{N} \left(r_{btm} dF_{bt} \bullet \hat{v} \right) \frac{2\pi}{N} \quad \text{(C-35)}$$

From equation (C-31) and (C-35), total excitation torque at the bolted joint is calculated as:

$$T_{bolt} = \sum_{n=0}^{N} r_{bh} \left(dF_{bh} \bullet \hat{x} \sin n \frac{\pi}{N} \right) \left(\frac{2\pi}{N} \right) + n_t \sum_{n=0}^{N} \left(r_{btm} dF_{bt} \bullet \hat{v} \right) \frac{2\pi}{N} \quad \text{(C-36)}$$

In calculating torque at bolted joint due to transverse vibration, a bolted joint is assumed to be tightened at preload of 8,000 Newton. Transverse force given to the bolted joint is a sinusoidal force with value of 6,000 Newton (6,000 *sin 2πt N*).

The joint use a M8 bolt with the length of 70 mm. Major dimension at the bolt are as follow:

Symbol	Remarks	Value
r_{bh}	Mean radius of bolt head	5.25 mm
r_{bho}	Outer radius of bolt head	6.5 mm
r_{bhi}	Inner radius of bolt head	4 mm
α	Thread angle of bolt	30°
β	Lead angle of bolt	2.8473°
r_{bto}	Outer radius of thread	3.97 mm
r_{bti}	Inner radius of thread	3.29 mm
r_{btm}	Mean radius of bolt thread	3.63 mm
L_{bolt}	Grip length	55 mm

Table C-1 Dimension at bolt

Coefficient friction at bolt is chosen to be 0.27 (coefficient friction of Steel- Steel with thick oxide film). Number of thread at nut that engaged with the bolt are 3 thread (n_t=3). Both bolt head and bolt thread of the bolt is divided into 36,000 section (N=36,000). By substituting the value to equation (C-31) and equation (C-35), torque at bolt head and bolt thread are obtained and plotted in Figure C-15 and Figure C-16.

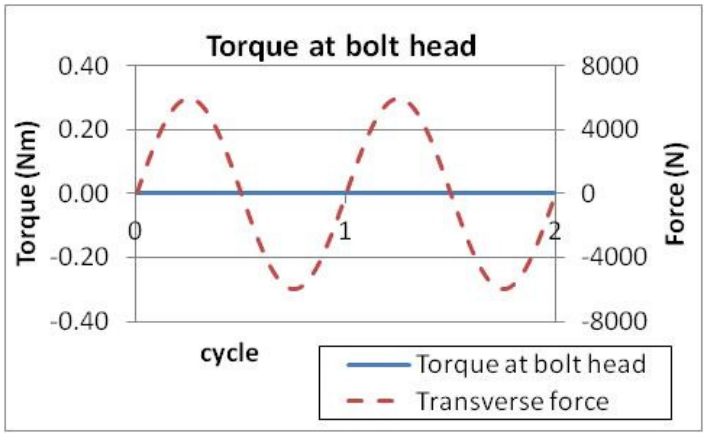

Figure C-16 Excitation torque at bolt head

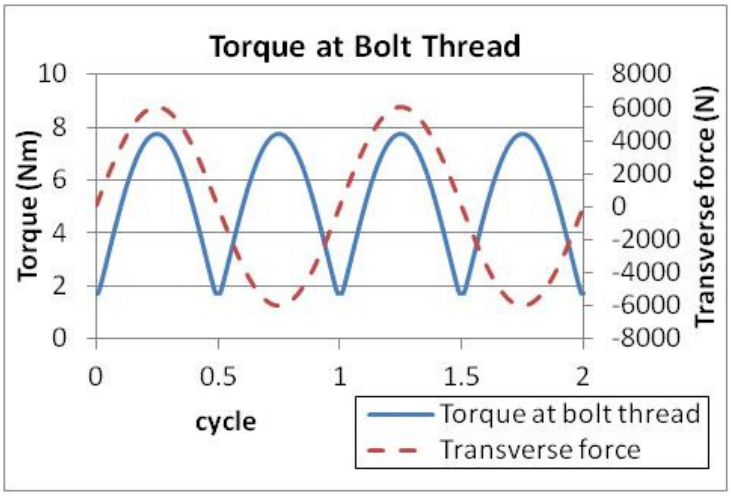

Figure C-17 Excitation torque at bolt thread

From figure above, it shows torque at bolt head due transverse force given is zero. Transverse force given to bolt head only slide the bolt head however it does not generate torque to loosen bolt. At the bolt thread, the torque is generated at positive value. The torque is in the form of a continuous shock spectrum ($|A \sin \omega_f t|$). Hence, it can be conclude that cause of self-loosening of bolt is happened only at thread part of the bolted joint.

C-4. Flow chart of loosening progress

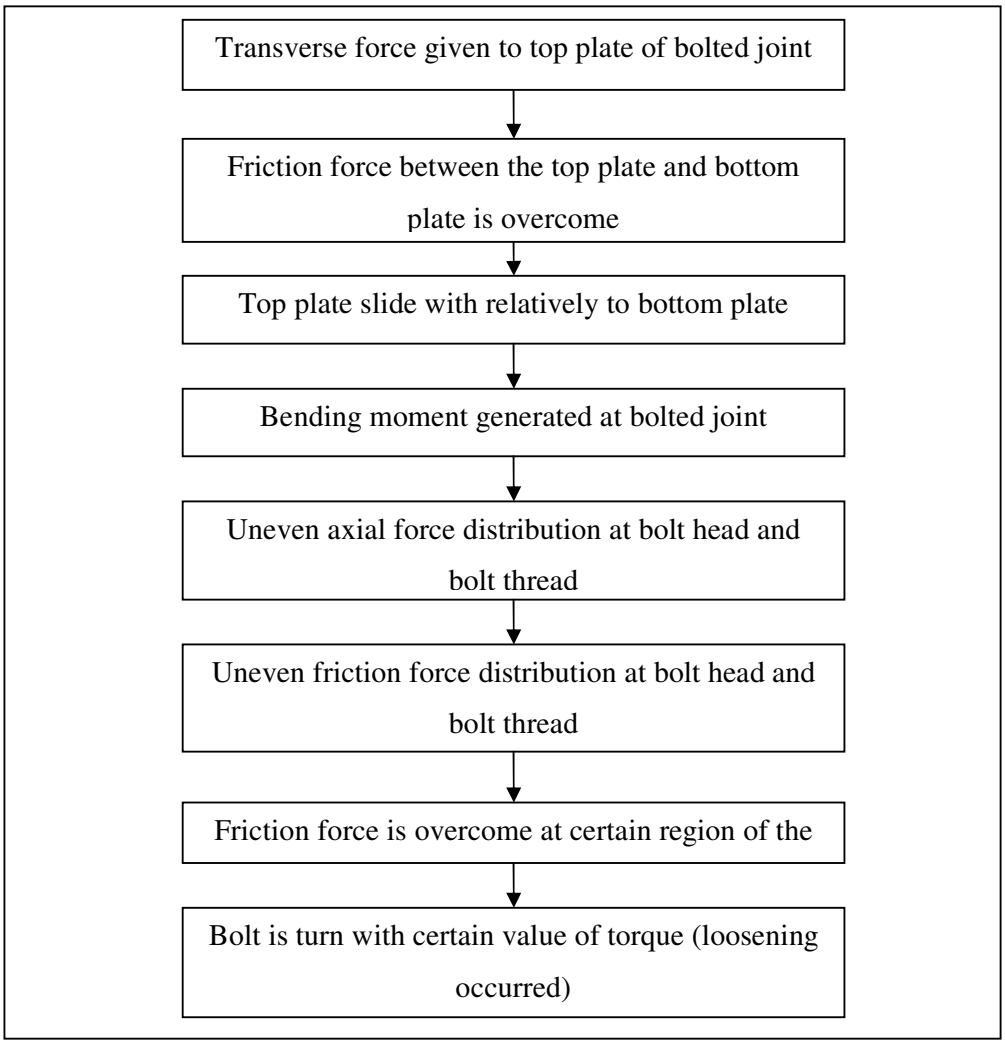

Figure C-18 Flow chart loosening mechanism of bolted joint

The loosening mechanism of bolted joint due to transverse force given to the bolted joint is shown at flow chart in Figure C-17. The transverse force given to the top plate of bolted joint overcomes friction force between the top and bottom plate. This permits sliding movement of the top plate with relative to the bottom plate. As the top plate is sliding, it bends the bolt and generates a bending moment. The bending moment affect distribution of axial force at the bolt and indirectly affect distribution of friction force at the surface of the bolt. At some region of the

bolt, the friction force is overcome and it permits the movement of the bolt. The movement turn the bolt to loosening direction. The torque generated to loosen the bolt is calculated with the equation which its derivation is shown in Figure C-18 and Figure C-19.

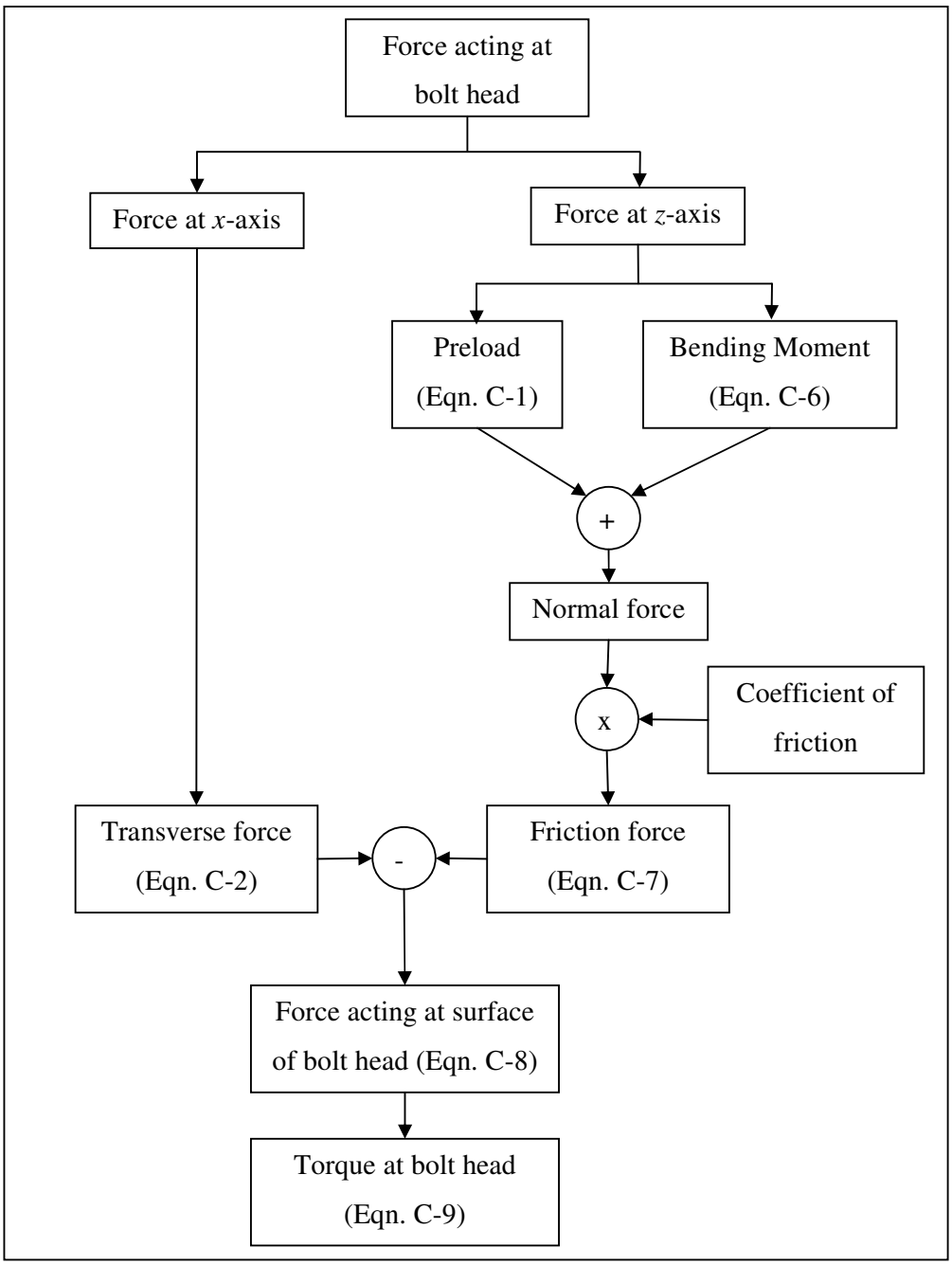

Figure C-19 Flow chart of torque generated at bolt head

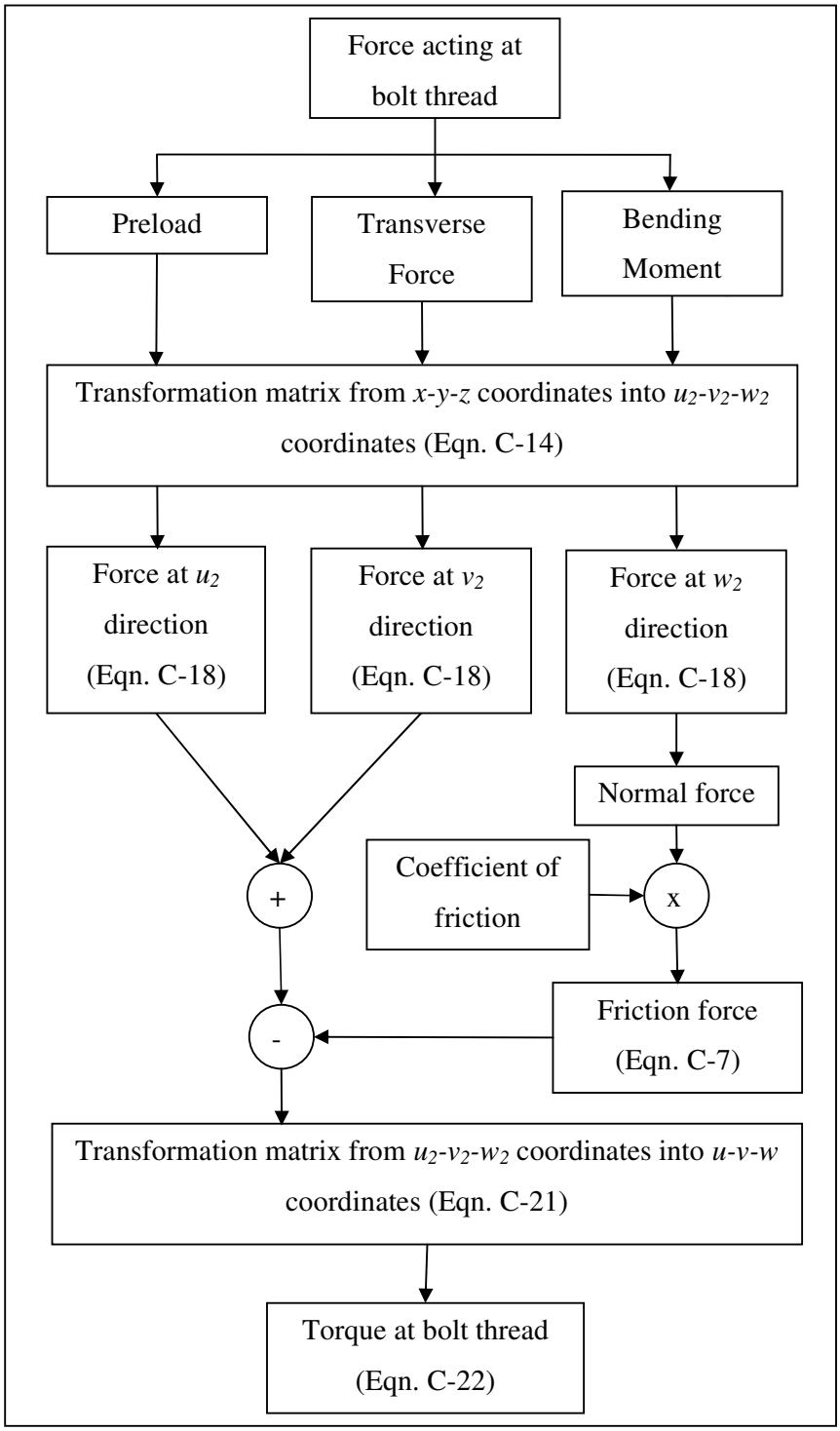

Figure C-20 Flow chart of torque generated at bolt thread

C-5 Factor affect amplitude of the excitation torque

From the mathematical formula shows that excitation torque is affected by preload of bolted joint, coefficient friction of bolt surface, transverse force applied to it, grip length of the bolt and type of thread. The effects of those factors are as follow:

a) Preload of the bolted joint

Preload is the indicator for the existence of joint force between the jointed parts. The higher value of preload indicates the more tighten of the joint. Figure below shows the effect of preload to the excitation torque. By increasing the value of preload at bolt joint, it decreases the value in excitation torque. It implies that higher value of preload is needed in order to prevent the loosening due to vibration.

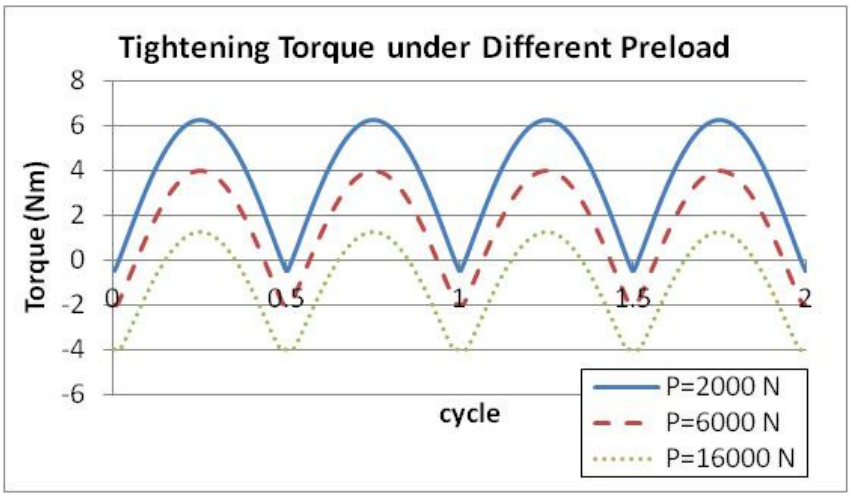

Figure C-21 Variation of excitation torque under different preload

b) Coefficient of friction of bolt surface

Based on derivation of the formula of excitation torque, the torque is generated at thread surface. Variation of coefficient of friction at thread surface affects the value of excitation torque. The effect is shown at figure below. The higher value of the coefficient friction of thread surface shows the lower amplitude of excitation torque. It shows that higher coefficient of friction is better in

preventing loosening of the bolted joint. However higher coefficient of friction of the bolt need a higher tightening torque to tighten the bolt.

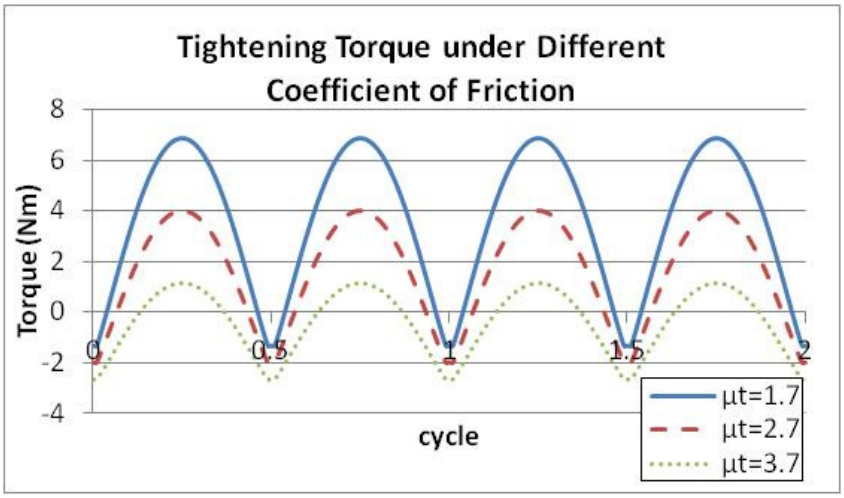

Figure C-22 Variation of excitation torque under different coefficient of friction

c) Transverse force given to bolted joint

Transverse vibration generates a torque at thread part of bolted joint. Due to this torque, the bolt is loosened. The amplitude of the transverse vibration affects the amplitude of the torque. Figure below shows that the higher transverse force applies to the bolted joint, the higher the torque generated to loosen the bolt. It is advisable for the bolted joint to avoid high amplitude of vibration.

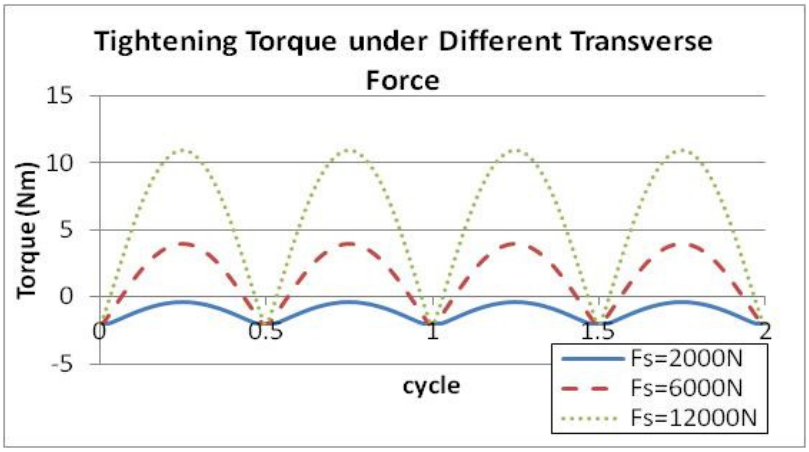

Figure C-23 Variation of excitation torque under different transverse force

d) Grip length (L_{bolt})

Grip length is the height of the jointed part that is supposed to hold/grip by the bolt. Based on Eqn. B-3, the grip length affect the value of bending moment generate at bolt joint. The bending moment affect the distribution of axial load at the bolt and it indirectly affects value of excitation torque.

Figure below show effects of grip length to the excitation torque. The higher the grip length of bolted joint, it generates higher value of excitation torque. It shows that in tightening a bolted joint, it is advisable to have a grip length as small as possible to avoid loosening.

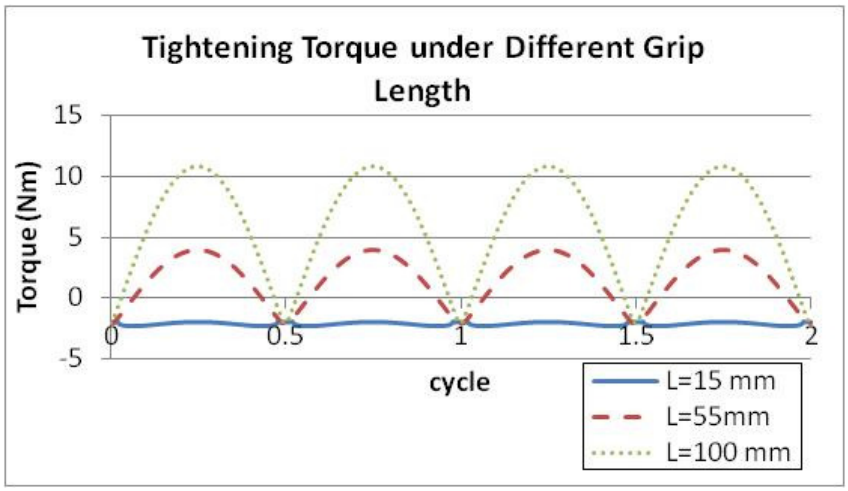

Figure C-24 Variation of excitation torque under different grip length

e) Thread type

Normally there are two type of thread which is coarse thread and fine thread. The difference between these two types of threads is the dimension of the pitch of the bolt. Coarse thread has a larger pitch compare to the fine thread. The effect of this larger pitch is increment in lead angle of the bolt and the thread become steeper. The steeper thread makes bolt have a higher tendency to loosen. This is shown with a higher torque that is generated at coarse thread compare to the fine thread (Figure C-24).

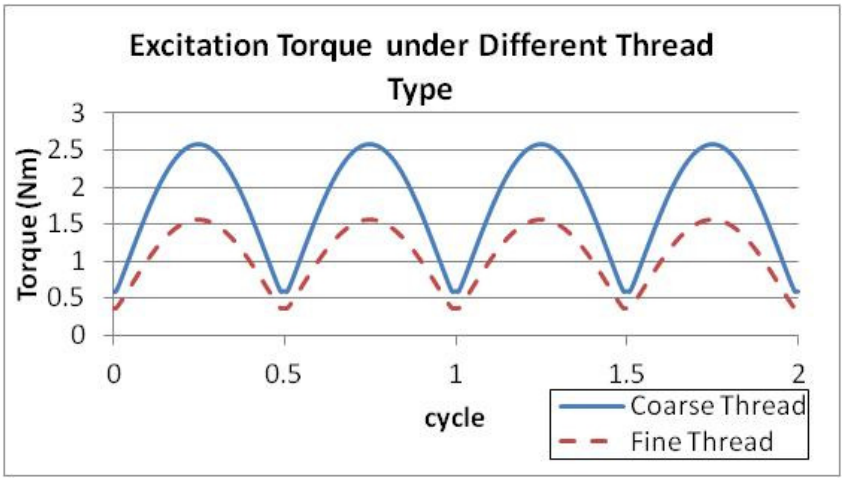

Figure C-25 Variation of excitation under different type of thread

APPENDIX D

MATLAB CODE TO CALCULATE BOLTED JOINT RESPONSE

```
%% clear
clear all

%% Initialize the coefficient
m= 1.3; %mass
k= 25; %stiffness
c=4; %damping
wn=sqrt(k/m);  %natural frequency
phi=c/(2*sqrt(k*m)); %damping ratio
wd=wn*sqrt(1-phi^2); %damped natural frequency
Fa=10; %excitation force
wf=2*pi/5; %excitation frequency

%% Response calculation

A=Fa/k(1)/sqrt((1-(wf/wn)^2)^2+(2*phi*wf/wn)^2); %amplitude
response
z=atan((2*phi*wf/wn)/(1-(wf/wn)^2));    %phase angle
% Initalize calculation
        t=1*0.001;
        F1(1)=Fa*cos(wf*t);
        x1(1)=A*cos(wf*t-z);
        v1(1)=-wf*A*sin(wf*t-z);
        a1(1)=-wf^2*A*cos(wf*t-z);
        A=-(D*cos(wf*ta)+E*sin(wf*ta));
        B=(-wf*E*cos(wf*ta)+wf*D*sin(wf*ta)+A*phi*wn)/wd;
% Loop calculation up to n=20000 point
for i=2:1:20000
        t=i*0.001;
        F1(i)=Fa*cos(wf*t);
        c=4+x1(i-1)/0.4257; %update damping value
        k=25-x1(i-1)/0.4257*5; %update stiffness value
        wn=sqrt(k(i)/m);
        phi=c/(2*sqrt(k(i)*m));
        A=Fa/k(i)/sqrt((1-(wf/wn)^2)^2+(2*phi*wf/wn)^2);
        x1(i)=A*cos(wf*t-z);
        v1(i)=-wf*A*sin(wf*t-z);
        a1(i)=-wf^2*A*cos(wf*t-z);

end
```